REPUBLIC OF TÜRKİYE
HARRAN UNIVERSITY
INSTITUTE OF GRADUATE EDUCATION

DOCTORATE THESIS

SURVEY AND MAPPING OF SOIL FERTILITY STATUS OF SOME ARABLE LANDS IN DUHOK PROVINCE, IRAQ

MOYASSAR ABDULLAH SALIH SALIH

DEPARTMENT OF SOIL SCIENCE AND PLANT NUTRITION

Şanlıurfa
2025

REPUBLIC OF TÜRKİYE
HARRAN UNIVERSITY
INSTITUTE OF GRADUATE EDUCATION

DOCTORATE THESIS

SURVEY AND MAPPING OF SOIL FERTILITY STATUS OF SOME ARABLE LANDS IN DUHOK PROVINCE, IRAQ

MOYASSAR ABDULLAH SALIH SALIH

DEPARTMENT OF SOIL SCIENCE AND PLANT NUTRITION
Thesis Supervisor: Prof. Dr. Ali VOLKAN BİLGİLİ

Şanlıurfa
2025

ACKNOWLEDGEMENT

I would like to express my profound gratitude to my esteemed supervisors, Prof. Dr. Ali Volkan BILGILI and Dr. Shukri Ibraheem Khan ALREKANI, whose invaluable academic guidance, continuous support, and exceptional patience have been instrumental throughout the course of my doctoral research. Their insightful feedback, constructive advice, and unwavering encouragement played a decisive role in shaping and completing this thesis. My sincere appreciation is also extended to Dr. Süreyya Betül RUFAİOĞLU and Amjed Mohammed İSMAEL for their significant contributions to data processing, statistical analysis, manuscript preparation, and research development. Their collaboration greatly enhanced the scientific quality and rigor of this work. I would further like to express my deep thanks to Mr. Ahmed Jameel, the General Director of Duhok Agriculture, for his valuable support, cooperation, and the facilitation he provided during the fieldwork and data collection stages, which contributed meaningfully to the successful implementation of this research. I am equally grateful to the distinguished faculty members and the administrative and technical staff at Harran University for their respectful attitude, academic support, and kind assistance throughout my academic journey. My deepest appreciation goes to my family especially my late father, mother, and sister, whose memory has remained a constant source of strength and inspiration. I dedicate this work to their enduring legacy. I am profoundly grateful to my wife and children for their unconditional love, patience, and encouragement, which sustained me through the most challenging stages of this journey. Finally, I would like to thank my friends for their continual moral support and motivation throughout my studies.

İÇİNDEKİLER

ABSTRACT

DOCTORATE THESIS

SURVEY AND MAPPING OF SOIL FERTILITY STATUS OF SOME ARABLE LANDS IN DUHOK PROVINCE, IRAQ

MOYASSAR ABDULLAH SALIH SALIH

HARRAN UNIVERSITY
INSTITUTE OF GRADUATE EDUCATION
DEPARTMENT OF SOIL SCIENCE AND PLANT NUTRITION

Thesis Supervisor: Prof. Dr. Ali VOLKAN BİLGİLİ
Year:2025, Page : 102

Soil fertility evaluation is crucial for long-term agricultural management and land-use planning, particularly in dry and semi-arid countries. The fertility condition of agricultural soils in Bardarash and Semel districts, Duhok Province, northern Iraq, is assessed using an integrated method that includes field sampling, laboratory analysis, geostatistics, and machine learning. A total of 105 composite soil samples (52 from Bardarash and 53 from Semel) were analyzed for 19 key physicochemical attributes, including soil texture, bulk density, pH, electrical conductivity, organic matter (OM), calcium carbonate ($CaCO_3$), cation exchange capacity (CEC), and available macro and micronutrients. To create the Soil Fertility Index (SFI), two different weighting schemes were used: Analytical Hierarchy Process (AHP) and Principal Component Analysis (PCA) for Bardarash and integrated with fuzzy logic for Semel. The normalized soil characteristics were weighted and aggregated to provide SFI values, which were then modeled using several prediction algorithms. SFI prediction in Bardarash was achieved using regression-based machine learning models with field spectroradiometer data as input factors. Semel, on the other hand, used machine learning techniques using remote sensing-derived indicators like as NDVI and soil indices as predictors to perform SFI classification. Gradient boosting regression (GBR) had the strongest predictive reliability in Bardarash, whereas classification-based techniques produced robust findings in Semel. Model performance was tested using R^2, MAE, MSE, and RMSE metrics. Soil fertility is mostly limited by OM depletion, poor phosphate availability, excessive $CaCO_3$ concentration, and insufficient CEC, according to the investigation. Additionally, spatial mapping revealed that approximately 58% of the soils in Semel and about 70% in Bardarash were classified as having low to very low fertility levels. In order to promote precision agriculture and sustainable land management practices in northern Iraq, these findings emphasize the significance of combining multivariate weighting approaches with geospatial machine learning and remote sensing to create precise, site-specific soil fertility maps.

KEYWORDS: Iraq, PCA, NDVI, Toprak verimlilik indeksi, Machine learning (Ml), Fuzzylogic

ABSTRACT

DOKTORA TEZİ

IRAK'ıN DUHOK İLINDE SEçILI TARıM ALANLARıNıN TOPRAK VERIMLILIK DURUMUNUN İNCELENMESI VE MEKâNSAL HARITALANDıRıLMASı

MOYASSAR ABDULLAH SALIH SALIH

HARRAN ÜNİVERSİTESİ
LİSANSÜSTÜ EĞİTİM ENSTİTÜSÜ
TOPRAK BİLİMİ VE BİTKİ BESLEME BÖLÜMÜ

Tez Danışmanı:Prof. Dr. Ali VOLKAN BİLGİLİ
Yıl:2025, Sayfa : 102

Toprak verimliliğinin değerlendirilmesi, özellikle kurak ve yarı kurak ülkelerde uzun vadeli tarımsal yönetim ve arazi kullanım planlaması için kritik öneme sahiptir. Irak'ın kuzeyindeki Duhok iline bağlı Bardarash ve Semel ilçelerindeki tarım topraklarının verimlilik durumu; arazi örneklemesi, laboratuvar analizleri, jeoistatistik ve makine öğrenmesini içeren bütünleşik bir yöntemle değerlendirilmiştir. Toplam 105 kompozit toprak örneği (52 Bardarash'tan, 53 Semel'den) alınmış ve 19 temel fizikokimyasal özellik (toprak tekstürü, hacim ağırlığı, pH, elektriksel iletkenlik, organik madde (OM), kalsiyum karbonat ($CaCO_3$), katyon değişim kapasitesi (KDK) ve mevcut makro ile mikro besin elementleri) analiz edilmiştir. Toprak Verimlilik İndeksi (SFI) oluşturmak için iki farklı ağırlıklandırma yöntemi uygulanmıştır: Bardarash için Analitik Hiyerarşi Prosesi (AHP) ve Temel Bileşen Analizi (PCA), Semel için ise bulanık mantık ile bütünleştirilmiş yöntem. Normalize edilmiş toprak özellikleri ağırlıklandırılarak toplanmış ve SFI değerleri elde edilmiştir. Bu değerler daha sonra çeşitli tahmin algoritmaları ile modellenmiştir. Bardarash'ta SFI tahmini, alan spektro-radyometre verilerinin giriş faktörü olarak kullanıldığı regresyon tabanlı makine öğrenmesi modelleri ile yapılmıştır. Semel'de ise NDVI ve toprak indisleri gibi uzaktan algılama kaynaklı göstergeleri kullanarak makine öğrenmesi ile sınıflandırma uygulanmıştır. Bardarash'ta Gradient Boosting Regression (GBR) en güçlü tahmin doğruluğunu sağlamış, Semel'de ise sınıflandırma tabanlı teknikler güvenilir sonuçlar vermiştir. Modellerin performansı R^2, MAE, MSE ve RMSE ölçütleriyle test edilmiştir. Araştırmaya göre toprak verimliliği büyük ölçüde OM eksikliği, düşük fosfat bulunurluğu, yüksek $CaCO_3$ konsantrasyonu ve yetersiz CEC nedeniyle sınırlanmaktadır. Ayrıca, mekânsal haritalama, Semel'deki toprakların yaklaşık %58'inin ve Bardarash'taki toprakların yaklaşık %70'inin düşük ile çok düşük verimlilik düzeylerine sahip olarak sınıflandırıldığını ortaya koymuştur. Bu bulgular, Irak'ın kuzeyinde hassas tarım ve sürdürülebilir arazi yönetimi uygulamalarını teşvik etmek için, çok değişkenli ağırlıklandırma yaklaşımlarının jeo-uzamsal makine öğrenmesi ve uzaktan algılama ile bütünleştirilerek kesin ve saha-özel toprak verimlilik haritalarının üretilmesinin önemini vurgulamaktadır.

ANAHTAR KELİMELER: Irak, PCA, NDVI, Soil fertility index , Makine öğrenmesi, Bulanık mantık

ŞEKİLLER DİZİNİ

ÇİZELGELER DİZİNİ

SYMBOLS

	GPS : Küresel Konumlama Sistemi
	greater than
CEC	Cation exchange capacity
cmol kg-1	Centimoles per kilogram
cmol kg-1	Centimoles per kilogram
CV	Varsyasyon Katsayısı
DAP	Diamonyum Fosfat
DD	Degree of Dependence
DD	Degree of Dependence
DTPA	Dietilentriaminpentaasetik asit
DTPA	Dietilentriaminpentaasetik asit
Ec	İletkenlik Bandı Enerji Seviyesi
FAO	Food and Agriculture Organization of the United Nations (Birleşmiş Milletler Gıda ve Tarım Örgütü)
FC	Field Capacity
GBR	Gradient Boosting Regression
GIS	Geographic Information System
kPa	kilopascal
MAE	Mean Absolute Error
Mg m-3	Milligram per cubic meter
Mg m-3	Milligram per cubic meter
mic.	micronaire
mS m-1	milliSiemens per meter
mS m-1	milliSiemens per meter
MSE	Mean Squared Error
NIR	Near-Infrared
OK	Ordinary Kriging
PCA	Temel Bileşenler Analizi (Principal Component Analysis)
PSD	Particle Size Distribution
PWP	Permanent Wilting Point
RF	Random Forest
RMSE	Root Mean Square Error
SD	Standart Deviation
SOC	Soil Organic Carbon
SOM	Soil Organic Matter

SOM	Soil Organic Matter
SP	Saturation Percentage
SVM	Support Vector Machine
USDA	United States Department of Agriculture
USDA	United States Department of Agriculture
UV	Ultraviolet
WHC	Water Holding Capacity
µg	Mikrogram
°C	Celsius degree

ABBREVIATIONS

CEC	Cation exchange capacity
CV	Coefficient of Variation
DAP	Diammonium Phosphate
DD	Degree of Dependence
DTPA	Diethylenetriaminepentaacetic acid
EC	Electrical Conductivity
FAO	Food and Agriculture Organization of the United Nations
FC	Field Capacity
GBR	Gradient Boosting Regression
GIS	Geographic Information System
GPS	Global Positioning System
GPS	Global Positioning System
MAE	Mean Absolute Error
MSE	Mean Squared Error
NIR	Near-Infrared
OK	Ordinary Kriging
PCA	Principal Component Analysis
PSD	Particle Size Distribution
PWP	Permanent Wilting Point
RF	Random Forest
RMSE	Root Mean Square Error
SD	Standard Deviation
SOC	Soil Organic Carbon
SOM	Soil Organic Matter
SP	Saturation Percentage
USDA	United States Department of Agriculture
UV-Vis	Ultraviolet Vissible
WHC	Water holding capacity

1. INTRODUCTION

1.1. Background

Soil is a dynamic and diverse natural system made up of minerals, organic matter (OM), water, air, and biota. It regulates biogeochemical cycles and facilitates agricultural production through its interactions (Joshi et al., 2009; Flores-Magdaleno et al., 2011). The sustainable maintenance of soil fertility is a critical objective as the global food demand increases, with the world population anticipated to reach 9 billion by 2050 (FAO, 2017). This resource is essential for food security and rural livelihoods. In arid and semi-arid regions with low tolerance to degradation, agricultural systems and long-term production are being jeopardized by nutrient depletion and inadequate land management.

Bekele and Hudnall (2006) assert that soil fertility surveys and maps provide indispensable information for the evaluation of crop suitability, site-specific nutrient management, and the development of evidence-based policy. A variety of interacting physical, chemical, and biological properties determine soil fertility, which is the soil's capacity to generate critical nutrients in the proportions and balance necessary for crops under favorable environmental conditions. The spatial variability of nutrient availability and uptake is influenced by both intrinsic soil-forming factors and extrinsic management practices, such as texture, bulk density, pH, electrical conductivity (EC), organic matter (OM), calcium carbonate (CaCO3), and cation exchange capacity (CEC) (Cambardella and Karlen, 1999; Dhanve et al., 2018). Uniform fertilizer recommendations are impeded by the high level of geographical variability, but it also motivates the development of precision techniques that adjust inputs to specific soil conditions (Goovaerts, 1998).

In order to synthesis complicated information and provide spatially explicit fertility products for decision support, modern soil fertility evaluation increasingly makes use of multivariate statistics, geostatistics, remote sensing, and machine learning (Kumawat and Gehlot, 2020; Musarhad et al., 2023). The ability to convert laboratory diagnosis into geographical maps and management recommendations is enhanced by these integrated digital technologies. The lack of region-specific calibration, the variability of weighting schemes for multi-indicator fertility indices, and the inconsistent availability of ground spectral and remote sensing data, however, continue to limit their use and make it uneven across regions (Tematio et al., 2011; Tsozué et al., 2019).

This thesis covers gaps in the context of northern Iraq (Duhok Province) by integrating traditional laboratory investigations with modern weighting methods, field spectroscopy, remote sensing indices, and machine learning. A total of 105 composite soil samples (52 from Bardarash and 53 from Semel) were examined for 19 physicochemical properties in order to create a Soil Fertility Index. To account for regional differences in indicator importance, two complementary weighting frameworks were used: Principal Component Analysis (PCA) to generate objective statistical weights for Bardarash, and an Analytical Hierarchy Process (AHP) integrated with fuzzy logic to incorporate expert judgement and handle uncertainty for Semel. Normalized indicator values were multiplied by their appropriate weights to calculate site Soil Fertility Index (SFI) scores. Spatial modeling and prediction combined ordinary kriging (OK) with machine learning approaches such as Random Forest (RF) and Gradient Boosting Regression (GBR), with input predictors tailored to each region: field spectroradiometer measurements were used for regression-based SFI prediction in Bardarash, whereas Normalized Difference Vegetation Index (NDVI) and remote sensing-derived soil indices were used as predictors for classification-based SFI mapping in Semel.

This study develops robust, site-adapted fertility maps and decision-relevant diagnostics for precision nutrient management by explicitly combining dual weighting methods, ground spectroscopy, remote sensing indices, geostatistics, and current machine learning. An integrated framework is especially important in dry and semi-arid agroecosystems in northern Iraq, where insufficient baseline knowledge and considerable spatial variability impede efficient soil management.

1.2. Scope of the study

The main tasks for this study include;

Soil samples in all key agricultural locations, the number of locations for soil sampling per 4 km2 will depend on the soil variability within the study areas.

Determine levels of the major plant nutrient elements (N, P, K, Ca, Mg) and essential plant micronutrients (Fe, Cu, Zn, Mn, B, etc.), OM, pH, EC, CaCO3 and CEC.

Classify the soils in selected locations into good soil fertility and degraded soils (in cultivated and non-cultivated areas).

Develop a comprehensive soil fertility map for more than 100 villages under the study area in Bardarash and Semel districts in Duhok.

Draw recommendations on how to improve soil fertility in degraded areas and on how to maintain soil fertility in non-degraded areas.

Determine the level of appropriateness of type of fertilizer materials already in use by smallholder famers including their application methods/rates in Bardarash and Semel.

Identify the major risks associated with environmental hazards for each of the fertilizer materials already in use and recommend risk mitigation measures.

Document best practices in sustainable soil fertility management already adopted in the study areas.

Identify the appropriate conservation agricultural practices for each village.

1.3. Study objectives

The main objective of this research is to use an integrated framework that integrates laboratory investigations, geostatistics, machine learning, and remote sensing to evaluate, map, and predict the fertility condition of arable soils in the Bardarash and Semel districts of Duhok Province, northern Iraq. In order to accomplish this goal, the study aims to accomplish the following particular goals:

Evaluate the overall fertility status of the study area through comprehensive laboratory analysis of key soil physical and chemical properties.

Develop high-resolution soil fertility maps using Geographic Information Systems (GIS) and digital soil mapping techniques to support precision agriculture and sustainable land management.

Quantify and model the spatial variability of soil fertility parameters using geostatistical methods based on OK.

Apply advanced machine learning algorithms such as RF and GBR, and

Support Vector Machine (SVM) to predict the SFI, assessing the predictive capability of Visible and Near-Infrared (VNIR) spectroradiometry, remote sensing indices (e.g., NDVI, soil indices), and laboratory-based soil analyses.

Formulate region-specific recommendations for soil fertility improvement and sustainable management tailored to the agroecological and socioeconomic conditions of the study area.

This study, conducted in Bardarash and Semel districts of Duhok Province, represents the first systematic soil fertility state survey and mapping effort in Iraq. The results are expected to serve as a reference framework for extending similar assessments across the country, thereby contributing to national strategies for sustainable agriculture and food security.

2. PREVIOUS STUDIES

2.1. Literature review

The assessment of soil fertility is the fundamental decision-making instrument for the effective planning of a certain land use system (Worku and Hunduma, 2020). From an agricultural standpoint, soil value has historically been assessed based on its productivity, which is defined as the soil's ability to yield a plant or series of plants under specific management approaches (Pierce, 1994). Soil productivity encompasses two dimensions: the intrinsic productivity of the soil and its reaction to regulated inputs (Hillel and Hatfield, 2005). The ongoing cultivation and persistent extraction of nutrients by plants, with minimal or no replenishment, may heighten the likelihood of future nutrient-related plant stress and yield reduction (Dobermann et al., 2022). Both excessive and insufficient use of chemical fertilizers adversely affects crop output, while excessive use contributes to heightened environmental contamination (Savci, 2012).

2.1.1. Fertility status of soil

The appropriate application of fertilizer is essential for the sustainability of farms and the preservation of the environment, as it is one of the most expensive commodities in agriculture (Rawal et al., 2018). In contrast, the environment is polluted and these limited, costly resources are wasted when fertilizers are applied in an excessive or imbalanced manner (Kumawat and Gehlot, 2020). The current nutrient status of the soils is not taken into account by farmers when applying high or very low fertilizer dosages, as they are unable to implement the developed norms due to a lack of knowledge and institutional incapacity (Rawal et al. (2018). In recent years, the response (production) efficiency of chemical fertilizer nutrients has significantly decreased under intensive agriculture due to the low efficiency of other inputs and the imbalanced and inadequate use of fertilizers (Meena et al., 2006). Consequently, in order to make an informed decision regarding the type and quantity of fertilizer to be applied, producers must be cognizant of the nature and severity of the nutrient issues (Rashid and Ryan, 2004). The fertilizer recommendation can be determined by the profitability and fertility status of the soil. Soil testing is a valuable tool for recommending the appropriate quantities and types of fertilizer and other amendments to enhance and profitably produce crops, as it provides information about the physico-chemical characteristics of the soil. The primary factor in the preservation of soil fertility is the understanding of the physico-chemical properties of the soil.

2.1.2. Soil physical properties

The physical properties of soil are those that govern the movement of water, solutes, oxygen, and heat within the soil. It is the process of determining the soil's adaptability to cultivation and the extent of biological activity that can be sustained. Texture, structure, color, depth, temperature, bulk density, and soil moisture content (SMC) are the primary physical soil properties (Sanchez, 1977). The physical properties of any soil are subject to change as a result of changes in its soil fertility management, including the intensity of cultivation, crop rotation, crop residue management, farmyard manure application, and the nature of the land under cultivation. This results in a decrease in soil permeability and an increased susceptibility to runoff and erosion losses. Mulugeta and Wondwosen (2019) assert that the fertility and productivity of soils are significantly influenced by the soil's physical properties, which include soil aeration and moisture-holding capacity. The concepts of some of the primary physical properties of soil will be discussed below, as we previously mentioned.

2.1.3. Soil texture

One of the soil's most critical attributes is its texture. It influences numerous soil functions and physical properties, including infiltration, drainage, aeration, soil organic carbon (SOC) content, pH buffering, and porosity (Akpa et al., 2014). It is classified into various textural classes, including sandy, loamy, and clay soils, as well as several intermediate classes, based on the relative proportions of soil components. The large pore spaces between particles and low surface area of sand particles create favorable conditions for root growth, soil aeration, and the drainage of surplus water, despite their limited capacity to retain water, retain nutrients, and provide a low SOC. In contrast, the Clay particles have a significantly greater capacity to retain water and nutrients due to the numerous medium and small pores. However, soil aeration is restricted (Jones and Jacobsen, 2005).

Loamy soils, such as sandy or silty loam, are generally the most optimal for cropping due to their intermediate properties (Verchot et al., 2007). The clay and silt content of soils affects their ability to retain organic carbon (Hassink, 1997; Bationo et al., 2007). The elevated surface areas and small pores of soils that are primarily composed of clay prevent water from draining freely. Fine-textured soils are capable of retaining nutrients due to their high surface area, which provides nutrients with numerous binding sites. The second reason is that clays are frequently composed of

minerals with high net negative charges on their surfaces (Jones and Jacobsen, 2005). The proportions of clay and sand particles have been employed to develop pedotransfer functions that estimate challenging soil properties, including bulk density, hydraulic conductivity, and water holding capacity (Minasny and Hartemink, 2011). The suitability of the soil for a specific use and management, waste disposal, and water management is determined by its texture (Thompson et al., 2012).

Soil texture is employed in soil taxonomy to differentiate soil orders (e.g., Vertisols or Alfisols) and is employed up to the family level of particle-size classes (Soil Survey Staff, 2010). Moreover, soil texture is employed to diagnose certain critical epipedons, particularly those associated with the argillic, natric, and kandic horizons (Bockheim and Hartemink, 2013). Despite the significance, there is a scarcity of information on soil texture, particularly the particle-size fractions at the resolution necessary for environmental modeling (Scull et al., 2005). Quantitative and continuous soil attributes are necessary in modeling, as opposed to taxonomic soil classes (Gessler et al., 1996). Nevertheless, the majority of soil maps are generated as discrete class surface maps, which fail to account for the continuous variability of soil attributes across space and depth (Adhikari et al., 2013).

2.1.4. Soil color

The color is one of the most valuable characteristics for distinguishing and identifying soils. It is frequently the most significant and readily apparent characteristic of the soil. Consequently, its accurate determination is crucial in numerous soil studies (Torrent and Barrón, 1993). Mineral composition, element concentration, OM, and SMC all contribute to soil color. The surface pigment, which is typically a reflection of the processes that are at play during soil formation, may also be indicative of other factors, such as excess salinity or erosion (Shields et al., 1966).

Soil pigments are employed to infer pedogenic processes in soils. OM, Fe, and Mn are the primary pigmenting agents in soils, with Mn being less prevalent. The matrix color is the prevalent color by volume when a soil horizon contains more than one color. (Owens and Rutledge, 2005). The Munsell Soil Color Charts are the most well-known to pedologists, and they are typically used to visually compare a soil sample with the fragments of standard color charts in the field (Munsell, 1975).

In general, soil color is influenced by two factors: the type of iron compounds and humus (organic material). The soil is given a dark brown, almost black, appearance by the humus. Iron is a significant factor in the color of soil, particularly in weathered forms (Table 2.1). The color and appearance of soil are also influenced by a variety of minerals and ions, including calcium, aluminum, carbonates, and gypsums.

Table 2.1. . The typical oxidation states of iron (Fe) in soils and the corresponding colors they impart (Kalev and Toor, 2018).

Form	Color
Iron (III) oxide (Fe_2O_3)	Red
Iron (II) oxide (FeO)	Gray
Iron (III) hydroxide (Fe $(OH)_3$)	Yellow

Soil is composed of two or more strata with unique characteristics and properties, which are referred to as horizons, and is formed in a surface-downward sequence. The accumulation of OM is represented by the uppermost stratum, which is known as the O horizon. The A horizon, which is directly beneath it, is typically characterized by a dark hue due to its humus enrichment.

2.1.5. Bulk density

The bulk density is the ratio of the mass of oven-dried soil to its bulk volume, which encompasses the volume of the particles and the cavities (pore space) between the particles. An indicator of limited soil porosity and soil compaction is a high bulk density. It may result in the restriction of root growth and the inefficient movement of oxygen and water through the soil (Hillel, 2012; McKenzie et al., 2004; Soane, 1990). It is susceptible to the effects of farming systems and can provide information on critical soil processes and productivity that are crucial for plant growth, including soil infiltration rooting depth/restrictions, plant nutrient availability, soil microorganism activity, water holding capacity (WHC) for plants, soil water movement, and aeration (Arvidsson, 1999; Chaudhari et al., 2013).

Arshad et al. (1997) also employ bulk density to express soil physical, chemical, and biological measurements on a volumetric basis for the purpose of assessing soil quality and comparing management systems. An increase in moisture

content results in a decrease in air-filled pores, as the pore space can be filled with either water or air, and there is an inverse relationship between these two parameters (Shand, 2007).

Bulk density of soil varies widely with soil texture and structure (Hunt and Gilkes, 1992). Bulk density values of fine texture soils (clay) commonly ranged from 1.0 to 1.6 Mg m-3, while those of coarse texture soils (sand) ranged from about 1.3 to 1.8 Mg m-3. Organic soils have a low bulk density; it may range between 0.4 - 0.8 Mg m-3 according to what was stated in Rekani et al. (2022).

2.1.6. Soil moisture content (SMC)

Soil moisture content (SMC) has quite a significant influence on the agricultural, geological, and hydrological behavior of the soil mass (Mittelbach et al., 2012; Jackson et al., 2008; Clevers et al., 2008). The Mechanical properties of the soil, such as cracking, swelling, shrinkage, and density, are dependent on the soil moisture content (Schwartz et al., 2008). Additionally, it is essential for the preservation of biodiversity, the stabilization of natural ecosystems, and the promotion of plant development (Alwis and Grattan, 2013).

According to Das and Sobhan (1990), the application of sufficient and opportune moisture for irrigation is crucial for crop production, contingent upon the soil-moisture-plant environment. Consequently, the assessment of soil moisture content is of paramount importance in the agricultural sector. In conclusion, the moisture content of soil has a substantial impact on its physical, chemical, mineralogical, mechanical, geotechnical, hydrological, and biological characteristics. Given this, previous researchers have devised a variety of methods for determining soil moisture, including thermogravimetric neutron scattering, soil resistivity, and dielectric techniques such as capacitance, frequency domain reflectometry, and time domain reflectometry (Fityus, et al., 2011; Gaskin and Miller, 1996).

2.2. Chemical properties of soil

2.2.1. Organic matter (OM)

The majority of soils are composed of minerals; however, their topsoil contains OM, which is defined as the accumulation of plant and animal residues at different phases of decomposition, cells and tissues of soil organisms, and well-decomposed substances (Brady, 1984). Despite its low content, it is of significant

significance to numerous aspects of plant growth and soil fertility. It contributes to the biological, chemical, and physical properties of the soil. The average composition of SOM is 47% C, 44% O, 7% H, 2% N, and very minor amounts of other elements. The resistant material lignin comprises 10–40% of SOM, while the remaining portion is composed of N compounds (Shand, 2007). Carbohydrates comprise more than half of SOM.

Soil fertility is significantly influenced by the comprehensive complex of organic matter, soil organisms, and soil flora. It performs a variety of functions in the soil, such as nutrient storage by increasing the CEC of the soil, providing chelates, and increasing the solubility of specific nutrients in the soil solution. SOM is composed of the fully-decomposed fine humus fraction, small plant roots, and members of the flora and fauna domains. Humus, a dark, complex mixture of organic substances modified from original organic tissue, is synthesized by various soil organisms and is resistant to further microbial decomposition, accounting for approximately 35-50% of total SOM (Prasad and Power, 1997).

SOM serves a function that surpasses its proportion of the soil volume. It is a virtual reservoir of nutrients, directly contributes to cation exchange and water retention, releases nutrients into the soil solution, and generates acids that influence the fixation and release of other nutrients. Additionally, it enhances soil structure by increasing soil water-holding capacity, infiltration, microbial activities, and aeration to facilitate successful cultivation (Grossl and Inskeep, 1991). The C:N ratio is a general indicator of the quality of SOM, with a range of 10–15:1 for fertile soils. Organic manures or green manures are incorporated into the soil's organic reservoir upon their addition (Roy et al., 2006).

2.2.2. Soil reaction (pH)

One of the most critical parameters obtained from soil testing is the soil reaction, which is expressed as pH. This parameter is a critical indicator of soil health. It has a significant impact on the incidence of soil-borne diseases, nutrient availability, microbial activity, plant growth, soil structure, and the effectiveness of pesticides. Soils are classified as acidic, neutral, or alkaline according to their pH values, which range from 0 to 14 (Shand, 2007). Generally, the optimal pH range for most crops is between 6.0 and 7.5, as this range optimizes nutrient availability. Numerous factors, such as climate, land management practices, mineral weathering, ammonium-based fertilizers, and organic matter decomposition, influence soil pH.

Acidification is frequently the consequence of intensive cultivation, leaching, and the continuous application of acid-forming fertilizers, while sodium dominance frequently leads to soils that are exceedingly alkaline. Reduced crop productivity can result from the restriction of essential nutrients' solubility due to excessive acidity or alkalinity.

The pH of soil can be adjusted by implementing a variety of amendments. Agricultural lime is the most effective and extensively used method for acidic soils, with application rates dependant on the soil's buffering capacity and crop requirements (McCauley et al., 2009). In contrast, materials such as gypsum, elemental sulfur, or iron pyrites may be employed in alkaline soils, although their effects are frequently transitory and economically not viable (Roy et al., 2006). In general, plants are more susceptible to alkalinity, which is primarily influenced by Na+, than to acidity, which is primarily influenced by H+. Their adaptation is closely associated with nutrient availability rather than pH alone.

2.2.3. Cation exchange capacity (CEC)

The capacity of a soil or any other substance with a negatively charged exchange complex to retain cations in exchangeable form is referred to as the CEC (Shand, 2007). It is a critical attribute of soil fertility. The CEC is a metric that reflects the soil's capacity to retain and supply nutrients, specifically the positively charged nutrient ions known as cations (Bolt et al., 1976). It is a metric that quantifies the soil's net negative charge. Expressed in cmol+ kg-1 or me/100 g of soil. The CEC is contingent upon the quantity and composition of clay minerals and organic matter in the soil. The CEC of clay soils is greater than that of barren soils. In the same vein, soils that are abundant in OM exhibit a higher CEC than soils that are deficient in OM (Desalegn Eshetu, 2021).

Differing cations are retained at the exchange sites due to their adsorption affinity or bonding strength (Schroeder, 1984). This determines the ease or difficulty with which these can be dislodged from the exchange site by cations in the solution. A CEC exceeding approximately 15 meq 100g-1 has a relatively high capacity to retain nutrient cations, such as Ca2+, Mg2+, K+, NH4+, Cu+2, Fe+2, Mn+2, and Ni+2. Table 2.2 illustrates some typical CEC values for a variety of soil textures.

Table 2.2. Cation Exchange Capacities (CEC) for a range of soil textures (Brady,

1984).

Soil Texture	CEC Range (meq $100g^{-1}$)
Sand	2 - 4
Sandy loam	2 - 17
Loam	8 - 16
Silt loam	9 - 26
Clay	5 - 58

(H+) and (Al3+) are classified as acidic cations due to their tendency to decrease soil pH. Conversely, (K+), (Ca2+), and (Mg2+) are classified as basic cations and do not have a direct impact on soil pH. In general, the vigor with which various cations are held on the exchange complex is arranged in the following order: Al3+ > Ca2+ > Mg2+ > K+, H+, NH4+ > Na+. The ideal ratio of cations on the exchange complex for average mineral soils is 75:15:5-3 of Ca:Mg:K. One that is held on a negatively charged surface and displaced by another cation is referred to as an exchangeable cation.

In general, the chemical activity of the soil is contingent upon its CEC. The most fertile soils are those with a high degree of base saturation, provided that the exchange complex is not dominated by a single cation (e.g., Na in sodic soils). In the surface horizons of mineral soils, the CEC is substantially influenced by the high OM and clay contents. However, in the subsoil, particularly where the Bt horizon is present, the clay fractions contribute more CEC than the OM due to the decline of OM with profile depth (Foth, 1991; Brady and Weil, 2008).

The highest CEC value was observed in soils under forest land, while the lowest was observed under cultivated land, as noted by Bewket and Stroosnijder (2003). Soil erosion and OM depletion are the primary causes of the significantly reduced CEC of the cultivated lands. Consequently, it is imperative to investigate and assess the chemical properties of soil in order to prevent the depletion and degradation of soil nutrients and to ensure the sustainability of production.

2.2.4. Electrical conductivity (EC)

The measurement of EC is the most frequently employed method for

assessing soil salinity (Rhoades and Miyamoto, 1990; Shirokova et al., 2000). The results are typically expressed in mS m^{-1} and adjusted to 25 °C, and the experiment is typically conducted in saturated paste or near field capacity (Rhoades et al., 1999). Salinity, water content, bulk density, texture, organic matter, and CEC are all factors that affect soil EC (Corwin and Lesch, 2005a; Lukas et al., 2009). In order to characterize soil properties that influence crop yield, such as salinity, nutrients (e.g., NO_3^-), compaction, and organic matter, spatial EC surveys have become essential (Friedman, 2005). Nevertheless, the correlation between EC and crop yield is frequently erratic as a result of soil heterogeneity, temporal yield variability, and climatic conditions (Corwin and Lesch, 2003). In instances where correlations are present, EC maps are advantageous for the identification of soil properties that restrict yield and for the development of soil sampling strategies (Corwin et al., 2003; Corwin and Lesch, 2005b).

2.2.5. Calcium carbonate (CaCO3)

CaCO3 forms significantly impact the majority of the physical, chemical, and biological properties of soil that are inherited. It is a naturally occurring component of numerous soils, primarily in the form of sparingly soluble alkaline earth carbonate, such as dolomite and calcite. In the majority of chemical and mineralogical properties, the soils of arid and semi-arid regions are closely related to their bed minerals. In these regions, limestone rock is the predominant substrate. Despite excessive leaching, a substantial quantity of CaCO3 will persist within soil horizons, potentially exceeding 30% (Umer et al., 2020). The majority of carbonate minerals in Iraqi soils are calcite, which comprises 90% of the total soil carbonates (Al-Kasyi, 1989). The American soil classification system classifies the soil in arid and semi-arid regions as calcisols, with a significant secondary deposition of calcium carbonate as a consequence of precipitation from the soil solution caused by evaporation in arid conditions (Portal, 2016). The identification of total carbonate, such as CaCO3, in soil is of considerable interest due to its high utility in the diagnosis of soil status in terms of structure, texture, biological activity, or nutrient content. Calcareous soils are typically alkaline due to the presence of CaCO3. Ca+2 in soil is derived from the weathering and degradation of bedrocks in the lithosphere or from the surface (Dijkstra et al., 2003). The soils contain an excessive quantity of soluble calcium, which results in a strong tendency for the available phosphate forms, such as orthophosphate HPO4 and H2PO4, to be fixed as apatite Ca5(PO4)3(OH, F, Cl).

2.2.6. Nitrogen (N)

N is one of the most abundant and critical mineral constituents in plants. Plants absorb it in the fourth highest quantity, following C, O, and H (Tisdale et al., 1985). Fertilizer N additions and the mineralization of organic N from OM, crop residues, and organic detritus are among the numerous sources of available N in soils (Keeney, 1982; Meisinger, 1984). The quantity of N in surface soils is typically between 0.02 and 0.25% and is closely correlated with the amount of OM, which accounts for approximately 5% (Bear, 1977). 8 to 120 kg of N ha-1 are released in a plant-available form if 1 to 3% of this organic N is mineralized annually (Bremner, 1965). Soil is naturally supplemented with nitrogen through rainfall and the fixation of nitrogen by soil microorganisms and legumes. The soil is typically supplemented with nitrogen through the application of fertilizer, manure, or other organic materials (Lamb et al., 2014).

Although the majority of plant species are capable of utilizing either NH4 or NO3, a small number of them exhibit a preference for NH4. NO3 is typically the predominant form of available nitrogen in the plant root zone, as NH4 is converted to NO3 in the majority of soils (Bear, 1977). The quantity of organic nitrogen that soil microbes convert to a form that is readily available is contingent upon environmental factors such as soil oxygen levels, rainfall, and temperature (Bundy and Meisinger, 1994).

Under-fertilization, leaching, poor nodulation in legumes, and denitrification caused by waterlogged soils are the most prevalent causes of nitrogen deficiency. Additionally, soil drainage, soil texture, CaCO3 content, and slope steepness affect the transport and transformation processes of nitrogen, which can restrict its availability to crops or increase the potential for loss (Lamb et al., 2014). The soils' insufficient N supply necessitate substantial fertilizer additives to accommodate the nitrogen requirements of high-yielding non-leguminous crops, including maize, rice, sorghum, and finger millet (Foth, 1991).

2.2.7. Phosphorus (P)

Phosphorus (P) is an essential nutrient for plants, second only to nitrogen in fertilizer utilization, as per Troeh and Thompson (2005). The majority of the total soil P is bonded within organic matter or mineral forms, with less than 5% of it being readily accessible to plants (Johan et al., 2021). The average total soil P concentration is 0.02–0.2% (Desalegn Eshetu, 2021). P is distinguished by its

restricted mobility in soils, where it is present as $H_2PO_4^-$ in acidic conditions and HPO_4^{2-} in alkaline conditions. In surface soils, the organic fraction, which is predominantly associated with humus, may account for 25–65% of the total P (Brady, 1984). Conversely, the inorganic fraction is frequently fixed in low-solubility Fe, Al, or Ca compounds (Schulte and Kelling, 1996). Mineralization of organic matter releases plant-available inorganic P, a process that is facilitated in warm, well-aerated soils. Conversely, soluble fertilizer P is swiftly converted to less-available forms. Soil pH, clay mineralogy, ionic interactions, organic matter content, and soil–phosphate contact time further regulate the availability of P.

2.2.8. Potassium (K)

Potassium (K) is the seventh most abundant element in the Earth's crust, with an average concentration of 2.6% in the lithosphere (Rich, 1968; Gurav et al., 2018; Murashkina et al., 2007). Sparks (2000) reports that it is typically the most abundant of the major and secondary nutrients in soils (Reitemeier, 1951), with concentrations in the top 20 cm ranging from 3000 to 100,000 kg ha^{-1}. Soil K is available to plants in four forms, each of which has an increasing availability: solution 1-10 ppm, exchangeable 40-600 ppm, nonexchangeable 50-750 ppm, and mineral 5000-25,000 ppm (Tisdale and Nelson, 1966). Clay minerals, soil moisture, texture, and fertilization rate significantly influence plant-available K, despite its abundance (Samadi, 2006; Simonsson et al., 2007).

K is a macronutrient that is third in fertilizer use, following N and P (Mikkelsen and Bruulsema, 2005). It is also instrumental in improving the tolerance of crops to environmental stresses (Zorb et al., 2014). It is crucial for the physiological processes of protein synthesis, membrane permeability, photosynthesis, enzyme activation, osmoregulation, translocation of photosynthates, and cell turgor. Additionally, it reduces the uptake of toxic ions in saline or flooded soils (Marschner, 2011; Mengel and Kirkby, 2001; Lakudzala, 2013; Hasanuzzaman et al., 2018). Additionally, it is essential for the maintenance of cell turgor.

2.2.9. Calcium (Ca)

For more than a century, Ca has been acknowledged as an essential nutrient and occupies a distinctive position among plant nutrient elements. Although higher plants frequently contain 1-50 mg g^{-1} of Ca in dried matter, the optimal Ca concentration in plants is approximately 0.2-1% (Rekani et al., 2022). Ca is typically ten times more concentrated than potassium in soil solutions, rendering it a

significant source of nutrient uptake. Nevertheless, the absorption of Ca^{2+} can be impeded by the application of fertilizers containing K^{+}, NH_4^{+}, and Mg^{2+}, as is frequently observed in horticultural and agricultural practices (Mengel and Kirkby, 1987).

The levels of soil calcium are highly variable, ranging from less than 0.01% calcium oxide in corrosive laterites and wetlands to extremely high levels in chalky soils (Burstrom, 1968). Ca is essential for the preservation of membrane stability and cell integrity in a physiological context. Ca ions stabilize the plasmalemma by binding to the phosphate and carboxylate groups of phospholipids and proteins at membrane surfaces. Although other cations may displace Ca, none can entirely replace its stabilizing function (Legge et al., 1982; Marschner, 2011). Ca deficiency symptoms initially manifest in juvenile leaves and tissues as a result of its immobility in plants. Brown chlorotic patches along leaf margins, leaf distortion and crinkling, and impaired root tip development are among the characteristic symptoms. Ca deficiency results in wilting and, in severe cases, plant mortality (Rekani et al., 2022).

2.2.10. Magnesium (Mg)

Magnesium (Mg) is present in both primary and secondary minerals and constitutes approximately 2% of the Earth's mantle. However, 90–98% of the Mg in soil is immobilized within mineral crystal lattices and thereby unavailable to plants (Grimme, 1991; Maguire and Cowan, 2002; Gransee and Führs, 2013). The total Mg content of soil typically varies between 0.05 and 0.5%, contingent upon the source material and the extent of weathering. Common minerals that contain magnesium include amphibole, dolomite, biotite, chlorite, olivine, pyroxene, serpentine, montmorillonite, and vermiculite (Schulte, 2004a). In general, soil magnesium is classified into four fractions: readily exchangeable, slowly exchangeable (acid-soluble), organically complexed, and structural forms (Mayland and Wilkinson, 1989). Approximately 10% of the total soil magnesium is available to plants, with the majority of it being released from secondary clay minerals like mica and chlorite (Salmon, 1963).

2.2.11. Micronutrients

Micronutrients are elements that are essential for plant nutrition, despite their minuscule quantities, and are required by plants. The main micronutrients in this study are Fe, Mn, Zn, Cu, and B, which collectively account for less than 1% of plant

dry matter. Their accessibility is contingent upon OM, pH, texture, and progenitor material. In contrast, the primary processes that regulate micronutrient dynamics are sorption, desorption, precipitation, dissolution, mineralization, and plant assimilation, while OM increases availability by releasing chelating agents (Foth and Ellis, 1997; Brady and Weil, 2008).

2.2.11.1. Iron (Fe)

It is the fourth most abundant element in the Earth's crust, primarily found in silicate minerals, oxides, and hydroxides that contribute reddish and yellowish hues to sediments (Bould and Hewitt, 1963). The total soil Fe content typically ranges from 1-5% (20,000-100,000 kg ha^{-1} in the plow layer), but less than 0.1% is plant-available (Schulte, 2004b; Jones and Jacobsen, 2009). Ferrous (Fe^{2+}) and ferric (Fe^{3+}) forms of Fe are present in soils, and their dominance is determined by soil pH and aeration. Deficiencies that are prevalent in calcareous soils are a result of the sudden decrease in soluble Fe concentrations that occurs as pH increases, particularly between 7.4 and 8.5. The availability of Fe is further diminished by inadequate aeration as a result of inundation or compaction (Greenland and Mott, 1978; Schwertmann, 1979; Sharma and Mathpal, 2020). Organic matter enhances the availability of Fe by producing stable complexes, which in turn decreases its precipitation as ferric hydroxide. In plants, deficiency symptoms manifest initially on young leaves, resulting in interveinal chlorosis, which is frequently confounded with Mn deficiency due to Fe's immobility. In severe cases, successive new leaves become progressively paler.

2.2.11.2. Manganese (Mn)

In the soil solution, manganese is primarily present as Mn^{2+} in soils. However, it is also present as exchangeable Mn, Mn oxides, organic complexes, and as a component of ferro-magnesian silicate minerals. In certain soils, concentrations can exceed 3000 ppm; however, plants are unable to utilize a significant portion of this (Schulte, 1992). According to Enakiev et al. (2018) and Krauskopf (1972), its availability is significantly impacted by soil pH, organic matter, precipitation, and aeration. Deficiencies are prevalent in soils with a pH greater than 6.5, while toxicities are more prevalent below pH 5.5.

2.2.11.3. Copper (Cu)

Copper is primarily found in mineral lattices in soils, with lesser fractions

occurring as Cu^{2+} adsorbed to clays or bound to organic matter (Mengel et al., 2001). The average concentration of total Cu is 30 ppm, with a range of 2-100 ppm. Liming reduces Cu availability by increasing sorption, which is primarily regulated by soil pH and organic matter (Reed and Martens, 1996). Sandy soils are more susceptible to Cu deficiency, and the requirements of different crops vary. Beet, lettuce, onion, sunflower, and tomato are among the most demanding (Schulte and Kelling, 2004a).

2.2.11.4. Zinc (Zn)

Zinc is a trace element with total soil contents ranging from 10-300 ppm, while the lithosphere average is approximately 80 ppm (Goldschmidt, 1954; Swaine and Mitchell, 1960). Soluble ions (Zn^{2+}, $ZnOH^{+}$), exchangeable forms on clay and OM, and secondary minerals are all examples of plant-available zinc (Kiekens, 1995). Parent material, pH, organic matter (OM), soil compaction, and moisture all influence availability (Alloway, 2008). Zn deficiency is a globally prevalent micronutrient issue that results in yield losses in numerous crops. However, excess exchangeable Zn (>100 ppm) has the potential to be toxic (Yang et al., 2020; Alsafran et al., 2022).

2.2.11.5. Boron (B)

Boron is indispensable for the development of plants (Shelp, 1993). Soil B is primarily present as borate anions (BO_3^{3-}) in solution, which are mobile and readily leached, with a range of 2-100 $\mu g\ g^{-1}$ (Warington, 1923). Its availability is contingent upon the pH, OM content, and soil texture, with the highest adsorption occurring at pH 8-9 (Shorrocks, 1997; Roy et al., 2006). Toxicity (>5 ppm) can occur in saline or B-rich irrigated soils, while deficiency is prevalent in sandy and calcareous soils. B management is difficult due to the narrow margin between deficiency and toxicity (Alloway, 2008).

2.2.12. Machine learning in estimation of soil properties

The integration of machine learning (ML) algorithms and GIS has significantly advanced soil fertility research, facilitating the analysis of multidimensional datasets and the identification of intricate relationships between soil properties and environmental factors. In particular, when trained on satellite imagery, VNIR spectroscopy, and laboratory datasets, methods such as neural networks, decision trees, RF, and GBR have exhibited high predictive performance

for soil properties and fertility indices (Viscarra Rossel et al., 2010; Shahabi et al., 2020; Gökmen et al., 2023). These predictive models have facilitated the production of spatially explicit soil fertility maps, which provide essential insights for precision agriculture and sustainable land management, when combined with GIS (van Zonneveld et al., 2020).

The Analytic Hierarchy Process–Fuzzy (AHP-Fuzzy) weighting methodology has been implemented in numerous studies to further improve the integration of diverse datasets. This methodology enables the distinct prioritization of soil properties and spectral indices, while simultaneously minimizing subjectivity and uncertainty in expert-based weighting systems (Saaty, 1990; Kahraman et al., 2003). Subsequently, the SVM was employed to analyze the weighted datasets. This classifier is renowned for its ability to identify intricate nonlinear relationships and to categorize soils into fertility categories that are beneficial for agricultural planning (Cortes and Vapnik, 1995). Despite the fact that algorithms such as SVM and RF have demonstrated exceptional predictive performance in soil science (Heung et al., 2016; Taghizadeh-Mehrjardi et al., 2020), the black-box" problem which obscures the reasoning behind model predictions and reduces confidence among scientists and land managers remains a significant impediment to their general adoption (Murdoch et al., 2019).

2.2.13. Soil fertility index (SFI)

Soil fertility ensures that plants get the macronutrients and micronutrients they need to grow well. However, low soil fertility results in stunted plant growth, reduced yields, and severe economic losses in agriculture. Excessive quantities of some nutrients, on the other hand, can cause nutritional imbalances, lower productivity, and environmental dangers such as water eutrophication and soil degradation (Lal, 2004). As global agriculture faces mounting pressure to strike a balance between production and sustainability, these constraints underscore the pressing need for more effective, scalable, and economical evaluation techniques (McBratney et al., 2003; Stenberg et al., 2010).

Establishing the SFI in recent years has led to notable advances in soil research. The SFI is a comprehensive method that assesses fertility holistically by integrating many soil metrics, such as physical, chemical, and biological characteristics (Askari and Holden, 2015). By classifying soils into fertility classes, the SFI offers practical advice for putting specific and efficient soil-handling

methods into reality. SFI development techniques are increasingly dependent on cutting-edge technologies, including digital elevation models (DEMs), satellite images, and VNIR spectroscopy. VNIR spectroscopy has become an efficient and inexpensive means to estimate important soil characteristics such as pH, CEC, and OM.

According to Rossel, (2011), it is a compelling substitute for conventional laboratory analyses due to its capacity to produce accurate predictions using spectral reflectance data. Satellite photography also offers a landscape-scale view of soil fertility and gives vital spatial information on vegetation health, soil dynamics, and land use changes. Topographic data, including elevation and slope, which affect soil erosion, water flow, and nutrient distribution, is another way that DEMs enhance this data. By combining these tools, soil fertility may be understood more thoroughly and spatially explicitly.

3. MATERIALS AND METHODS

3.1. Statistical analysis

Statistical analyses included determining the minimum, maximum, mean, standard deviation (St D), coefficient of variation (CV), kurtosis, and skewness. Shape parameters highlighted non-normal data distributions, with high skewness indicating significant deviations from normality (Webster and Oliver, 2007). To assess normality, the Kolmogorov-Smirnov test was used, considering data normally distributed when $p > 0.05$. Ensuring normality and symmetry is crucial, as non-normality can negatively affect geostatistical analyses (Kerry and Oliver, 2007). The Pearson correlation coefficient was calculated to explore relationships between variables, with significant correlations determined at $p < 0.05$. All statistical analyses were conducted using SPSS software (version 9.3).

3.2. Description of study area

3.2.1. Location

The agricultural lands in the Bardarash and Semel districts of Duhok, Iraq, were the subject of this study. The study area is situated between latitudes 36°18′12.64″ and 37°20′33.55″ N, and longitudes 42°20′25.36″ and 44°17′40.50″ E, with elevations spanning from 430 to 2,500 meters above sea level. The entire area of Duhok Province is approximately 11,066 km2 (Table 3.1; Figure 3.1).

The landscape of the study area is predominantly semi-flat, interspersed with hills and mountainous terrain. These elevated areas were excluded from the analysis due to their limited suitability for agricultural activities. Bardarash is situated in the southern part of the province, while Semel lies to the southwest. These two districts were selected for their substantial contribution to agricultural production and their well-established reputation as the province’s primary food-producing zones.

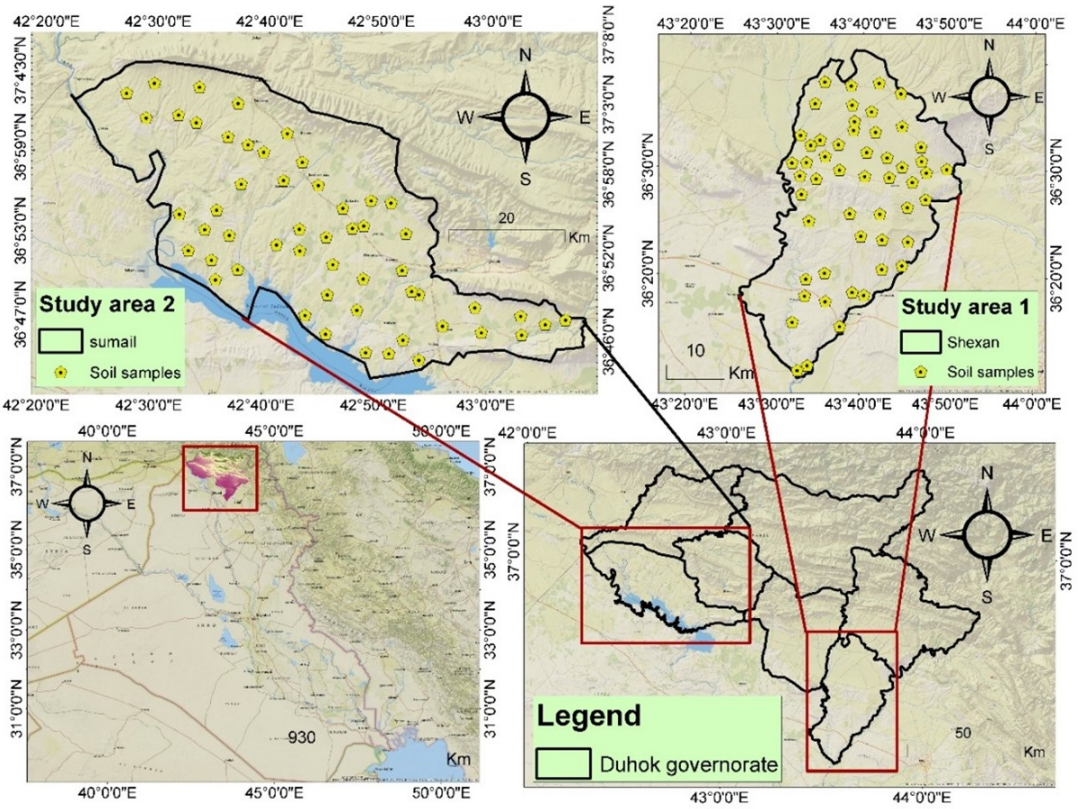

Figure 3.1. Location of the study area (Bardarash and Semel districts).

Table 3.1. GPS Coordinates of the Soil Sample Locations.

No.	District	Sub District	Village	Longitudes	Latitudes	Altitude
1	Bardarash	Kalak	Kavrasor	379001	4019028	339
2	Bardarash	Kalak	Asky kalak	376813	4013153	254
3	Bardarash	Kalak	Wardak	371227	4006402	274
4	Bardarash	Kalak	Tylaban	369489	4005572	233
5	Bardarash	Kalak	Tal alaswad	368626	4013885	255
6	Bardarash	Kalak	Bahre-Sherakan	370774	4018408	268
7	Bardarash	Kalak	Mangubah-Khazer	374347	4017477	297

8	Bardarash	Kalak	Aj kala Bchok	370965	4021316	300
9	Bardarash	Kalak	Aj kala Mazn	374244	4022348	338
10	Bardarash	Kalak	Bshirian	381007	4018553	272
11	Bardarash	Daratoo	Henjirok Bot	384092	4023021	319
12	Bardarash	Daratoo	Bani Nan 1	387596	4023617	285
13	Bardarash	Daratoo	Bani Nan 2	388615	4027726	341
14	Bardarash	Daratoo	Korav	384197	4028102	485
15	Bardarash	Daratoo	Grdapan 1	380500	4028720	420
16	Bardarash	Daratoo	Grdapan 2	378587	4032647	381
17	Bardarash	Daratoo	Gomazard	383779	4032542	444
18	Bardarash	Daratoo	Morelan	388527	4033645	419
19	Bardarash	Daratoo	Dalare	391707	4035021	386
20	Bardarash	Daratoo	Daratu 1	391833	4039667	334
21	Bardarash	Rovia	Chamma	395382	4040255	303
22	Bardarash	Rovia	Barda Sur	390873	4044095	406
23	Bardarash	Daratoo	Daratu 2	391019	4041651	355
24	Bardarash	Daratoo	Daratu 3	389384	4038042	374
25	Bardarash	Daratoo	Daratu 4	387645	4040609	349

26	Bardarash	Daratoo	Girbdau 1	385065	4042251	367
27	Bardarash	Daratoo	Dugondan small	385421	4038856	404
28	Bardarash	Daratoo	Zanganan	381161	4039042	436
29	Bardarash	Bardarash	Zamzamuk	376811	4040159	400
30	Bardarash	Bardarash	Dreen But	371502	4031381	359
31	Bardarash	Bardarash	Qadsy Mazn	370230	4035985	338
32	Bardarash	Bardarash	Kani lan	368648	4041395	357
33	Bardarash	Rovia	Asmawa	370130	4046152	341
34	Bardarash	Rovia	Dolejan	372627	4051611	372
35	Bardarash	Rovia	Husainya	374297	4055384	377
36	Bardarash	Rovia	Dinaran	378884	4054717	392
37	Bardarash	Rovia	Perchawsh	379046	4051386	405
38	Bardarash	Rovia	Rovia	383707	4055158	438
39	Bardarash	Rovia	Rovia 2	387440	4053377	474
40	Bardarash	Rovia	Big Topzawa	387626	4047645	440
41	Bardarash	Daratoo	Girbdau 2	381528	4043192	380
42	Bardarash	Daratoo	Saly Bag	383033	4046687	401
43	Bardarash	Rovia	Qaranaz	379232	4047011	384

44	Bardarash	Rovia Bardarash	Jojar	382368	4050217	420
45	Bardarash	Rovia Bardarash	Kani Asbhan	379423	4048527	364
46	Bardarash	Bardarash	Amian	373493	4045353	350
47	Bardarash	Bardarash	Mamuzin	376674	4044565	359
48	Bardarash	Bardarash	Khelky	374342	4042508	360
49	Bardarash	Bardarash	Small Bardarash	371852	4044419	335
50	Bardarash	Bardarash	Shewara	371120	4041468	370
51	Bardarash	Bardarash	Shewara 2	369994	4039181	391
52	Bardarash	Bardarash	Bardarash	372774	4038652	455
53	Semel	Semel	Kani Gulan	331891	4073416	600
54	Semel	Semel	Salihy	329227	4072832	545
55	Semel	Semel	Tall Khashsf	326085	4071438	495
56	Semel	Semel	Sina	325975	4073927	540
57	Semel	Semel	Rakava kavn	320759	4071753	496
58	Semel	Semel	Kalha badre	319896	4075074	478
59	Semel	Semel	Alouka	312476	4076808	

3.2.2. Climate

Climate plays a crucial role in soil formation and in determining the

suitability of land for agricultural purposes. Among the most influential climatic factors affecting the physical, chemical, mineralogical, and morphological characteristics of soils are temperature and precipitation. Climatic data related to rainfall and temperature for the study area, covering the period from 2015 to 2024, were obtained from the General Directorate of Meteorology and Seismic Monitoring in Duhok.

The study area falls within a subtropical, continental, semi-arid climate zone, characterized by hot, dry summers and cooler winters. Atmospheric pressure tends to be low during summer and high during winter, and the region is considered to lie within the semi-guaranteed rainfall zone. The average annual precipitation recorded during this period was 564.86 mm in Semel and 506.59 mm in Bardarash, with the majority of rainfall occurring between November and April. In terms of temperature, the region experiences high summer temperatures, particularly during June, July, and August. The average summer temperature was 20.20 °C in Semel and 20.08 °C in Bardarash.

3.2.3. Land use and vegetation

Based on field investigations and information obtained from the relevant agricultural departments, five major cropping systems were identified within the surveyed districts, from which soil samples were collected. These cropping systems were not monocultures but rather diversified systems. The wheat-based cropping system was the most extensive and dominant, cultivated primarily as a rainfed winter crop. In contrast, irrigated summer crops included vegetables and fruits such as rice, corn, sesame, tomatoes, potatoes, watermelons, cucumbers, and other vegetables. Grain legumes, such as pigeon peas, cowpeas, and other leguminous crops, formed another important group. Additionally, some areas were interspersed with fruit trees, olive trees, forest species, and patches of natural grasslands.

3.2.4. Land management and activities

The economic activities of the local communities in the study area are primarily based on crop production, within a mixed farming system that also includes animal husbandry. This subsistence-oriented system combines crop and livestock production, forming an integrated agroecosystem. The most commonly applied nutrients in crop production are nitrogen (N) and phosphorus (P), typically supplied in the form of Urea and Diammonium Phosphate (DAP). For several decades, farmers have followed a blanket fertilizer recommendation, applying standard rates

of DAP and Urea across all major crop types without site-specific calibration.

However, for certain crops (particularly potato production) there has been no localized research-based recommendation regarding optimal fertilizer application rates in the study area. This may lead to inefficient nutrient use, environmental risks, or suboptimal yields.

3.2.5. Soil sampling

A preliminary survey was conducted to determine the locations from which samples would be taken. After excluding areas unsuitable for agriculture, valleys, mountains, and inhabited lands the samples were randomly distributed across the remaining area based on the shape and extent of the land surface, obstacles to sample taking, and other factors. A total of 105 soil samples (0-30 cm) across seven sub-districts: Bardarash, Kalak, Daratoo, Rovia, Semel, Batel, and Fayda (Table 3.2) were collected, and each of these 105 samples was as follows: A sample was taken from the previously specified location, then four other samples were taken around this sample from the four directions, at a distance of about 1 km in each direction. Then these five samples were mixed together to form a composite sample that is more accurate and representative of the location. Net samples were air-dried, sieved (2 mm), The prepared samples were stored in polyethylene bags, which were then placed in sealed plastic containers for transport and analysis.

Table 3.2. Sampling of soils from the subdistrict's perspective.

Districts	Sub districts	Field samples collected
Bardarash	Bardarash	11
	Daratoo	18
	Kalak	10
	Rovia	13
Semel	Semel	25
	Batel	22
	Fayda	6
Total		105

The geographic coordinates of each sampling location were recorded using a hand-held GPS unit (GARMIN 76s). Additional information about each site (such as land use, vegetation cover, and sampling conditions) was documented on a field card, which was stored along with the corresponding soil sample.

During sampling, care was taken to avoid contaminated or atypical spots, including areas with dead plants, furrows, old manure piles, wet zones, areas near trees, and compost pits. In addition, separate undisturbed soil core samples were collected using a sharp-edged steel cylinder, manually inserted into the soil, for the purpose of bulk density determination.

3.2.6. Soil laboratory analysis

The major part of the soil physical and chemical analysis was carried out at the Soil Research Laboratory of Mosul University. Standard laboratory procedures were followed in the analysis of the selected physicochemical properties considered according to what was stated in (Rekani et al., 2022).

3.2.7. Soil physical properties

3.2.7.1. Soil texture

It was analyzed by the Bouyoucous hydrometer method (Bouyoucous, 1962; Day, 1965; FAO, 1980), after oxidation of OM using hydrogen peroxide (H2O2), dispersion of soil particles using Calgon [sodium carbonate (Na2CO3) and sodium hexametaphosphate (NaPO3)6] and get rid of soil solution foam using amyl alcohol.

3.2.7.2. Soil Color

The soil color for dry and wet soil was identified using the Munsell chart sample.

3.2.7.3. Bulk density (ρb)

The bulk density of the soil was estimated from undisturbed soil samples which were collected by using a core sampler following the procedures used by Blake (1965).

3.2.7.4. Soil moisture (SMC)

It was determined using the gravimetric method, in which soil samples were

oven-dried at (105 °C for 24 h) until a constant weight was obtained (Gardner, 1986).

3.2.8. Soil chemical properties

3.2.8.1. Organic matter (OM)

The (OM) content was estimated by oxidation method of Walkley and Black using 1N of potassium dichromate (K2Cr2O7) according to Allison (1965).

3.2.8.2. Soil reaction (pH)

Soil pH was measured in soil suspension 1:1 (soil:water) with using pH-meter model HI8417-HI8519 Microprocessor, Bench-top pH-Meter, HANNA, instruments, after shaking for 30 minutes according to Rowell (2014).

3.2.8.3. Electrical conductivity (EC)

EC of soil was measured in soil suspension 1:1 (soil:water) by EC-meter model HI8417-HI8519 Microprocessor, Bench-top pH-Meter, HANNA, instruments, after shaking for 30 minutes according to Rowell (2014).

3.2.8.4. Cation exchange capacity (CEC)

The (CEC) was estimated using sodium acetate at a pH of 8.2 and the displaced sodium was estimated by 1M of ammonium acetate using the Flame photometer according to the method described in Black (1965).

3.2.8.5. Calcium carbonate (CaCO3)

The (CaCO3) was determined by titration method as described in Page and Keeney (1982) using 1N of HCl with 1N of NaOH.

3.2.8.6. Available N

Available N was extracted from the soil using 2M potassium chloride (2M KCL), and it was determined by the Kejldhal method according to (Ryan et al., 2001).

3.2.8.7. Available P

Available P was extracted by 0.5M of sodium bicarbonate modified at pH 8.5, measured via modified method by (Olsen et al., 1954).

3.2.8.8. Available K

Available K was extracted by the neutral ammonium acetate solution, and measured by Flame Photometer (Sherwood Model 410) according to the method mentioned by (Keeney, 1982).

3.2.8.9. Calcium (Ca) and Magnesium (Mg)

Ca and Mg was estimated using EDTA - 2Na according to the method presented by (Keeney, 1982).

3.2.8.10. Micronutrients

Zn, Fe, Mn, Cu and B was extracted by 0.005M of diethylene triamine Penta acetic acid (DTPA) and measured via atomic absorption spectrometer (AAS) according to Lindsay and Norvell (1978).

3.3. Spectral and remote sensing analysis

For the Bardarash district, soil samples previously air-dried and oven-dried at (105 °C for 24 h), were spectrally measured using an ASD FieldSpec Pro/Pro III spectroradiometer (Analytical Spectral Devices, Inc., Boulder, CO, USA) over the 350-2500 nm wavelength range. The instrument generates 2,151 spectral channels, which correspond to absolute reflectance measurements on a 0-1 scale, as per Gangannavar et al. (2023). The sampling interval is approximately 1.4 nm in the 350-1000 nm range and 2 nm in the 1000–2500 nm range. The spectrum resolution in the VNIR is approximately 3 nm, while in the SWIR region it is 8-10 nm. The illumination source was a stabilized quartz tungsten halogen (QTH) lamp. In order to guarantee optically dense measurements and prevent interference from container bottoms, soil samples were positioned in opaque containers at a depth of approximately 3 cm.

Spectral measurements were conducted in a dark enclosure with a fixed geometry of 30° incidence angle and 0° viewing angle. The signal to noise ratio was improved by averaging 10-30 scans for each sample (Dor et al., 2024). Dark current readings were recorded to account for sensor drift, and the spectroradiometer was calibrated against a Spectralon® white reference panel before each acquisition. Equation (3.1) was employed to determine the reflectance values, which were determined as the ratio of soil reflectance to the white reference material.

$$R = \frac{SoilReflection}{Whitespektralonreflectance(reference)} \tag{3.1}$$

Raw spectra were exported into ASCII format using ViewSpec Pro software and subsequently resampled to 10-nm intervals, resulting in 216 spectral bands. A convex hull was fitted to the spectral curve, and continuum removal (CR) was performed by dividing the original spectrum by the hull, according to Equation (3.2):

$$SCR = \frac{s}{c} \tag{3.2}$$

where Scr represents the continuum-removed spectrum, S is the original spectrum, and C is the continuum curve. Processing of CR spectra was carried out using ENVI 4.5 software (ITT Visual Information Solutions, USA). This procedure enhances absorption features and facilitates mineral identification (Clark and Roush, 1984). In addition to soil samples, reference reflectance spectra were acquired for pure salt minerals frequently encountered in the study region, including crystalline magnesium chloride hexahydrate (MgCl2·6H2O), anhydrous sodium carbonate (Na2CO3), gypsum (CaSO4·2H2O), calcite (CaCO3), and halite (NaCl). These spectra were further compared with the USGS Spectral Library v7 (Kokaly et al., 2017) to validate and confirm diagnostic mineral absorption features.

For the Semel district, to describe the research region and determine important biophysical characteristics, remote sensing information was obtained from open-access Sentinel-2 satellite photography. European Space Agency (ESA) Copernicus Open Access Hub provided the images for download. To ensure the correctness of spectral indices and account for atmospheric influences, the Sen2Cor processor was used to atmospherically correct the raw Level-1C imagery to Level-2A before analysis. This technique changed top-of-atmosphere reflectance to bottom-of-atmosphere reflectance. Pixels obscured by clouds were located and hidden to protect the integrity of the data.

To evaluate several land surface characteristics, such as plant vigor, soil condition, and water content, a number of spectral indices were computed from the cleaned data. The near-infrared (NIR), red (RED), green (GREEN), blue (BLUE),

and short-wave infrared (SWIR) bands' atmospherically adjusted reflectance values were used to calculate these indices. Table 3.3 contains the formulas for the indices that were employed in this investigation.

Table 3.3. Formulas of the spectral indices used for predicting the SFI.

Index	Equations	References
Bare Soil Index (BSI)	BSI=(SWIR+R)-(NIR+B)/ (SWIR+R)+ (NIR+B)	Qin et al., 2015
Carotenoid Reflectance Index 1 (CRI1)	CRI1=(1/R510)−(1/R550)	Gitelson et al., 2002
Enhanced Vegetation Index (EVI)	EVI=G((NIR−R)/(NIR+C1 * R−C2 * B+L))	Huete et al., 2002
Green Normalized Difference Vegetation Index (GNDVI)	GNDVI=NIR-G /NIR+G	Gitelson et al., 1996
Modified Soil Adjusted Vegetation Index (MSAVI)	MSAVI=(2NIR+1-	Qi et al., 1994
Normalized Difference Vegetation Index (NDVI)	NDVI=NIR-R/NIR+R	Rouse et al., 1974
Normalized Difference Water Index (NDWI)	NDWI=G-NIR/G+NIR	McFeeters, 1996
Soil Adjusted Vegetation Index (SAVI)	SAVI=(NIR−R)(1+L)/NIR+ R+L	Huete, 1988

For EVI, standard constants are: G=2.5, C1=6, C2=7.5, and L=1 For SAVI, the soil brightness correction factor (L) is typically set to 0.5.

3.4. Soil fertility index (SFI)

To assess the fertility status of soils in the districts of Bardarash and Sumel, the Soil Fertility Index (SFI) was developed independently using two different methodological frameworks: an expert-based decision-support approach using the Fuzzy Analytic Hierarchy Process (Fuzzy-AHP) for Sumel, and a statistical weighting approach based on Principal Component Analysis (PCA) for Bardarash. This two-pronged strategy made sure that the assessment of soil fertility included

both expert knowledge under uncertainty and objective data-driven criteria.

3.5. Assigning weights to soil properties

3.5.1. PCA-based weighting in Bardarash district

Principal Component Analysis (PCA), a multivariate statistical method that reduces dimensionality and finds the most important variables within complicated datasets, was used to calculate the weights of specific soil characteristics for the Bardarash district (Jolliffe, 2002; Xu et al., 2021). To ensure comparability across variables obtained on various scales, including pH, EC, organic matter, and nutrients, all soil parameters were standardized using scikit-learn's StandardScaler function prior to analysis (Pedregosa et al., 2011). The sklearn.decomposition package was then used to perform PCA on the standardized dataset. The main components and their explained variance were then determined by extracting the eigenvalues and eigenvectors. The ideal number of components to keep was determined by a variance retention analysis, which was bolstered by a cumulative variance plot that showed the percentage of information retained. Weights were allocated based on the relative contributions of each soil parameter, with parameters exhibiting larger loadings being given more weight in the evaluation of soil fertility. The loadings of each soil parameter on the retained components were also evaluated. The contribution of each variable was represented by vectors in a scatterplot of the first two main components to facilitate comprehension (Demšar et al., 2013). Through the objective selection and weighting of the most important soil fertility indicators for Bardarash, this process made sure that the evaluation accurately represented the main causes of variability in the dataset.

3.5.2. Fuzzy-AHP-based weighting in Semel district

The Fuzzy Analytic Hierarchy Process (Fuzzy-AHP), which combines fuzzy logic and expert judgment to overcome subjectivity and confusion in decision-making, was used to weight the soil attributes for the Semel area (van Laarhoven & Pedrycz, 1983). Fuzzy-AHP enables expert-driven prioritizing, which makes it appropriate for diverse landscapes like Semel, in contrast to PCA, which only uses statistical variance. The fuzzy synthetic extent approach was used in the process (Chang, 1996). Triangular Fuzzy Numbers (TFNs) were used to describe the opinions of a panel of soil specialists who first created a hierarchical structure of soil attributes and conducted pairwise comparisons using a fuzzy linguistic scale (Table 3.4). The relative relevance of each criterion was represented in a flexible and

complex manner by these TFNs. Next, by combining the evaluations from the pairwise comparison matrix, the fuzzy synthetic extent value for each criteria i was determined. This value may be mathematically stated as follows:

$$Si = (\sum_{j=1}^{m} M_{ij}) x (\sum_{i=1}^{n} \sum_{j=1}^{m} M_{ij})^{-1} \quad (3.3)$$

where n is the total number of criteria, m is the number of judgments, and mij is the TFN for criterion i in comparison to criterion j the relative significance of soil attributes was then ascertained by comparing the fuzzy synthetic extent values, and a defuzzification process produced clear (non-fuzzy) weights. This created a solid foundation for evaluating soil fertility in the Sumel district by guaranteeing that professional opinions were translated into trustworthy and defendable numerical weights.

Table 3.4. Linguistic Scale and Corresponding Triangular Fuzzy Numbers (TFNs) for Soil Fertility Parameter Weighting.

Linguistic Scale	Triangular Fuzzy Number (TFN)
Equally Important	(1,1,1)
Slightly Important	(2/3,1,3/2)
Moderately Important	(3/2,2,5/2)
Strongly Important	(5/2,3,7/2)
Very Strongly Important	(7/2,4,9/2)
Extremely Important	(9/2,5,11/2)

This approach provided a thorough weighing system tailored to the specific soil conditions in Sumel by allowing the integration of both quantitative and qualitative factors.

3.6. Data normalization and SFI calculation

After assigning weights, all soil attribute data were normalized to a similar scale before calculating the composite SFI. Normalization was required to avoid the

excessive impact of parameters with broad numeric ranges (for example, EC vs. organic matter). Normalization was performed using min–max transformation (Zhang et al., 2024):

$$Ni = \frac{X_i - X_{min}}{X_{max} - X_{min}} \tag{3.4}$$

where Ni is the normalized value of parameter i, Xi is the observed value, and X min, X max are the minimum and maximum values within the dateset

The Soil Fertility Index was then calculated using the weighted additive model (Andrews et al., 2004; Nganga et al., 2020):

$$SFI = \sum_{l=1}^{n} (W_i x P_i) \tag{3.5}$$

where Wi is the weight assigned to parameter i (derived from PCA for Bardarash and Fuzzy-AHP for Sumel) and Ni is the normalized value. SFI values close to 0 indicated poor fertility, while SFI values close to 1 indicated high fertility.

The PCA-derived weights for the Bardarash district focused on variables that have been shown to statistically explain the greatest variation in soil fertility. The weights obtained by fuzzy-AHP for the Sumel district focused on criteria that experts agreed were crucial in the face of uncertainty.

This combination of methods improved the robustness of the index for both districts by ensuring that the evaluation of soil fertility reflected both context-specific expert knowledge and objective statistical connections.

3.7. Machine learning approaches for soil fertility assessment and land suitability classification in study area

In the Bardarash district, machine learning methodologies were utilized to forecast the Soil Fertility Index (SFI) as a continuous variable. Two ensemble-based techniques, Random Forest (RF) and Gradient Boosting Regression (GBR), were utilized employing spectral parameters (UV, Blue, Green, Red, NIR1, and NIR2)

alongside the associated SFI values derived from laboratory investigation

In Semel district, the combined dataset needed to undergo extensive preprocessing in order to guarantee the best possible model performance before the SVM was used for land suitability classification. There were numerous crucial phases in this procedure. Initially, all gathered information was cleaned to remove any discrepancies or anomalies, including the soil characteristics determined by laboratory examination and the remote sensing indices. Second, a single scale was used to normalize all feature variables. For distance-based machine learning algorithms like SVM, normalization is crucial because it keeps features with higher numerical values from unduly affecting the model's training. Normalization was subsequently applied using the min-max normalization approach to a range between 0 and 1 according to equation 3.3. This preprocessing step was crucial for preparing a high-quality, standardized dataset for subsequent classification (Bishop, 2006).

In the Semel district, the modeling framework emphasized land suitability classification instead of continuous prediction. A Support Vector Machine (SVM) model with a Radial Basis Function (RBF) kernel was constructed to address the intricate, non-linear correlations between soil and remote sensing variables and the suitability classifications (e.g., very appropriate, moderately suitable, less suitable). Data preprocessing entailed normalization via the Min–Max method, as delineated in Equation (3.3).

3.8. Explainable AI (XAI) approaches

Explainable AI (XAI) techniques were applied to the Support Vector Machine (SVM) model in order to enhance the interpretability of the machine learning models and offer insights beyond black-box forecasts. Gaining a better understanding of the relative impact of remote sensing indices and soil parameters on land suitability classification was the aim. Because they work especially well with sophisticated non-linear models like SVM, two model-agnostic techniques were used: SHapley Additive exPlanations (SHAP) and Local Interpretable Model-Agnostic Explanations (LIME). Each attribute is given an importance value for a particular prediction using SHAP, which is based on cooperative game theory.

The method identified both globally significant and locally influential variables by quantifying the contribution of remote sensing indices (e.g., NDVI, SAVI) and soil fertility parameters (e.g., pH, organic matter, texture) to the

classification of individual observations into specific land suitability classes through the calculation of SHAP values. In addition, LIME offered localized interpretability by creating surrogate models based on individual predictions. This involved perturbing input characteristics and fitting a simplified interpretable model to roughly represent the intricate SVM decision surface in that area. This method provided case-specific explanations by highlighting the characteristics that had the biggest impact on how each instance was classified.Together, SHAP and LIME improved the transparency and reliability of the analytical process by facilitating the understanding of the SVM model at both the global (dataset-level) and local (individual prediction-level) levels. More importantly, by identifying the environmental and soil elements most important to land productivity, the use of these XAI techniques supported the development of focused, empirically supported soil fertility management plans by giving agricultural stakeholders useful and actionable insights.

3.9. Assessment of the model

The dataset was initially preprocessed to handle missing values and eliminate outliers in order to guarantee the accuracy of the forecasts. Following cleaning, the data was divided into subgroups for testing (20%) and training (80%). In order to assess the Soil Fertility Index (SFI) and land suitability, machine learning models such as Random Forest (RF), Gradient Boosting Regression (GBR), and Support Vector Machine (SVM) were used in both study districts.

SFI was predicted as a continuous variable in the Bardarash district using regression-based models (RF and GBR). The most significant soil characteristics and spectral bands might be identified according to these models' prediction powers and feature significance metrics. According to Equations (3.6–3.9), the Root Mean Square Error (RMSE), Mean Squared Error (MSE), Mean Absolute Error (MAE), and the Coefficient of Determination (R^2) were used to objectively assess the model's performance. By measuring the models' explanatory strength as well as the size of prediction errors, these indicators made sure that SFI value estimations were solid and trustworthy.

(3.6)

$$RMSE = \sqrt{\sum_{i=1}^{n}(y_i\widehat{y}_i)^2}$$

$$MAE = \sqrt{\sum_{i=1}^{n}(y_i\widehat{y}_i)} \tag{3.7}$$

$$MSE = \frac{1}{N}\sqrt{\sum_{i=1}^{n}(y_i\widehat{y}_i)^2} \tag{3.8}$$

$$R^2 = \frac{\sum_{i=1}^{n} y_i\widehat{y}_i}{\sum_{i=1}^{n}(y_i y_{avg}^2)} \tag{3.9}$$

where yi, y^i, represent the observed, estimated, and mean observed SFI values, respectively, and n denotes the number of observations.

Hyperparameter optimization was conducted using a grid search with cross-validation, focusing particularly on the kernel coefficient (γ) and the regularization parameter (C), to maximize both accuracy and generalization capacity.

To classify land suitability in the Semel district, classification-based modeling was used with a Support Vector Machine (SVM) equipped with a Radial Basis Function (RBF) kernel. Standard classification measures, such as accuracy, precision, recall, F1-score (harmonic mean of precision and recall), and the Kappa coefficient (Cohen, 1960), were used to assess the model's performance. It was especially crucial to include the Kappa coefficient since it provides a more accurate assessment than accuracy alone by taking into consideration the likelihood of chance agreement.

The assessment techniques used in both districts taken together made sure that classification-based models (SVM) and regression-based models (RF and GBR) were thoroughly verified. The thorough validation improved the prediction frameworks

created for the categorization of land suitability and the evaluation of soil fertility in the districts of Bardarash and Semel.

3.10. Geostatistical analysis and mapping

The results of the analyzed soil parameters and soil ferlitity indx (SFI) were included in ordinary kriging (OK) and semivariogram geostatistical methods to generate the spatial degree of dependence and predictive spatial maps using ArcGIS software version 10.5.

3.11. Semivariogram analysis

Semivariogram analysis was used to evaluate the degree of reliance and geographical structure among soil fertility metrics. By measuring the variance of paired sample differences as a function of their separation distance, the empirical semivariogram was calculated. Through model fitting, the important semivariogram parameters nugget (C_0), sill ($C_0 + C$), and range (a) were identified. The sill ($C_0 + C$) indicates the overall variance above which spatial autocorrelation becomes insignificant, but the nugget effect (C_0) represents unexplained variability ascribed to measurement error or microscale heterogeneity. The spatial continuity of soil attributes is defined by the range (a), which shows the distance at which samples become spatially independent.

Following Cambardella et al. (1994), the spatial dependence (SD) ratio was calculated as:

$$SD = 100X\frac{C_o}{C_o + C} \tag{3.10}$$

Where Co is the nugget effect and (Co + C) is the total variance (sill). The resulting DD ratio was classified as less than 25%, which denotes high dependency; between 25 and 75% denotes moderate dependence; and beyond 75% denotes weak dependence.

Spatial dependency is quantitatively classified by this ratio: values <25% indicate high dependence, values 25-75% indicate moderate dependence, while values >75% indicate weak dependence. The parameters that were obtained after calibrating the semivariogram model were used in spatial interpolation to produce

continuous surface maps of soil properties and SFI. Since these maps were created in a GIS setting, the distribution of soil fertility throughout the research areas could be seen and interpreted spatially. In addition to measuring the spatial autocorrelation of soil characteristics, this method made it possible to create accurate fertility maps, which are essential for sustainable agricultural planning and site-specific land management.

3.12. Ordinary kriging (OK) method

In order to produce continuous geographic forecasts of soil fertility characteristics from point-based measurements, OK was utilized. In contrast to deterministic approaches like Inverse Distance Weighting (IDW), OK is a geostatistical method that provides unbiased estimates with minimized prediction variance by taking into account both the distance between observations and the spatial autocorrelation structure of the data, as represented by the semivariogram (Webster and Oliver, 2007; Singh et al., 2010). The semivariance at lag distance h was calculated using:

$$\gamma(h) = \frac{1}{2N(h)} + \sum_{n=1}^{n(h)}((Z(x_i) - Z(x_i + h)^2 \quad (3.11)$$

Where γ(h) represents the semivariance at lag distance h, as defined by Webster and Oliver (2007), (□□□□) is the variable value at position □□□□, and (*h*) is the number of data pairs.

A spherical, exponential, and Gaussian theoretical function was used to describe experimental semivariograms. The coefficient of determination (R2) and residual sum of squares (RSS) were used to determine which model best fit the data. Parameterizing the OK interpolator requires the nugget (C_0), sill ($C_0 + C$), and range (a), all of which were supplied by the fitted model.

OKs performance was evaluated using cross-validation utilizing error measures such Mean Standardized Error (MSE), Mean Error (ME), and Root Mean Square Error (RMSE). Ultimately, a GIS environment was used to create the kriged surfaces of soil fertility indices, resulting in high-resolution maps that enable spatially explicit analysis and decision-making in precision agriculture and land management.

4. FINDINGS

This section introduces and discusses the laboratory and spatial datasets obtained from the examination of the physical and chemical characteristics of the soil in the Bardarash and Semel districts of Duhok Province, northern Iraq. A thorough grasp of the spatial behavior of soil properties is crucial given the complex link between agricultural productivity and soil features. Since descriptive and spatial statistics capture the variety, range, and distribution of soil parameters over the terrain, they offer a more reliable foundation than mere averages. The scientific basis for analyzing soil fertility dynamics and directing sustainable land use and agricultural resource management is established by this thorough assessment.

The findings are arranged in a methodical manner, starting with the evaluation of the physical characteristics of the soil (texture, bulk density, soil moisture, and color), then moving on to the chemical aspects (pH, electrical conductivity, organic matter, calcium carbonate, cation exchange capacity, and the micronutrient and macronutrient availability). An integrated interpretation of soil fertility is made easier by this framework, which emphasizes the chemical and physical elements governing nutrient delivery and soil production in addition to physical limitations on root growth and water availability.

4.1. Semel district

4.1.1. Laboratory and statistical evaluation of soil physical parameters

The descriptive statistics for the physical soil parameters show a moderate to high degree of variation (Table 4.7). The mean values for sand (39.17%), silt (29.89%), and clay (30.95%) content indicate a loamy texture class, which is a fundamental aspect of the research area's soil composition. The coefficient of variation (CV) for silt (24.47%) is greater than for both sand (21.47%) and clay (19.18 %). The average bulk density of 1.39 Mg m-3 is within the usual range for agricultural soils. Similarly, the mean soil moisture content is 17.98%, with a moderate standard deviation that reflects the normal range of water availability throughout the soil profile.

Table 4.1. Descriptive statistics of soil physical properties in Semel district

Soil properties	Min	Max	Mean	StD	Skew	Kurt	CV (%)	P-value

Sand %	23.05	60.55	39.17	8.41	0.49	0.44	21.47	0.62
Silt %	13.50	43.5	29.88	7.31	-0.30	-0.37	24.47	0.53
Clay %	17.95	42.45	30.95	5.93	0.01	-0.58	19.18	0.99
Bulk Density	1.13	1.68	1.39	0.13	0.53	-0.44	9.51	0.19
SMC (%)	12.24	23.59	17.98	2.66	-0.35	-0.23	14.84	0.83

The CV data revealed significant discrepancies in the variability of the analyzed parameters. Sand had the highest fluctuation at 21.47%, followed by silt at 24.47%, clay at 19.18%, soil moisture content at 14.84%, and bulk density at 9.51%. The P-values of the Kolmogorov-Smirnov test suggest that none of the soil parameters deviated substantially from normality. The minimum P-value for SMC was 0.83, which suggests that these characteristics can be treated as normally distributed. The distribution characteristics of diverse soil properties were clarified through evaluations of skewness, kurtosis, and coefficient of variation.

The skewness values of clay, silt, and sand are 0.01, -0.30, and 0.49, respectively. Sand's positive skewness implies a right-tail distribution, with a few exceptionally high values interspersed with the majority of observations. The negative skewness of silt suggests a concentration toward upper levels, whereas the nearly zero skewness of clay suggests a fairly symmetrical distribution.

Soil Physical Parameters Spatial Distribution: Figures 4.14 depict the regional distribution of soil physical parameters, including bulk density, SMC, and soil texture, with a particular emphasis on the percentages of sand, silt, and clay. These discrepancies are indicative of topography. Soils that are well-drained but not as productive are indicated by sand in southern regions. The silt content of these soils is indicative of a balance between water retention and appropriate discharge, rendering them more suitable for agricultural production.

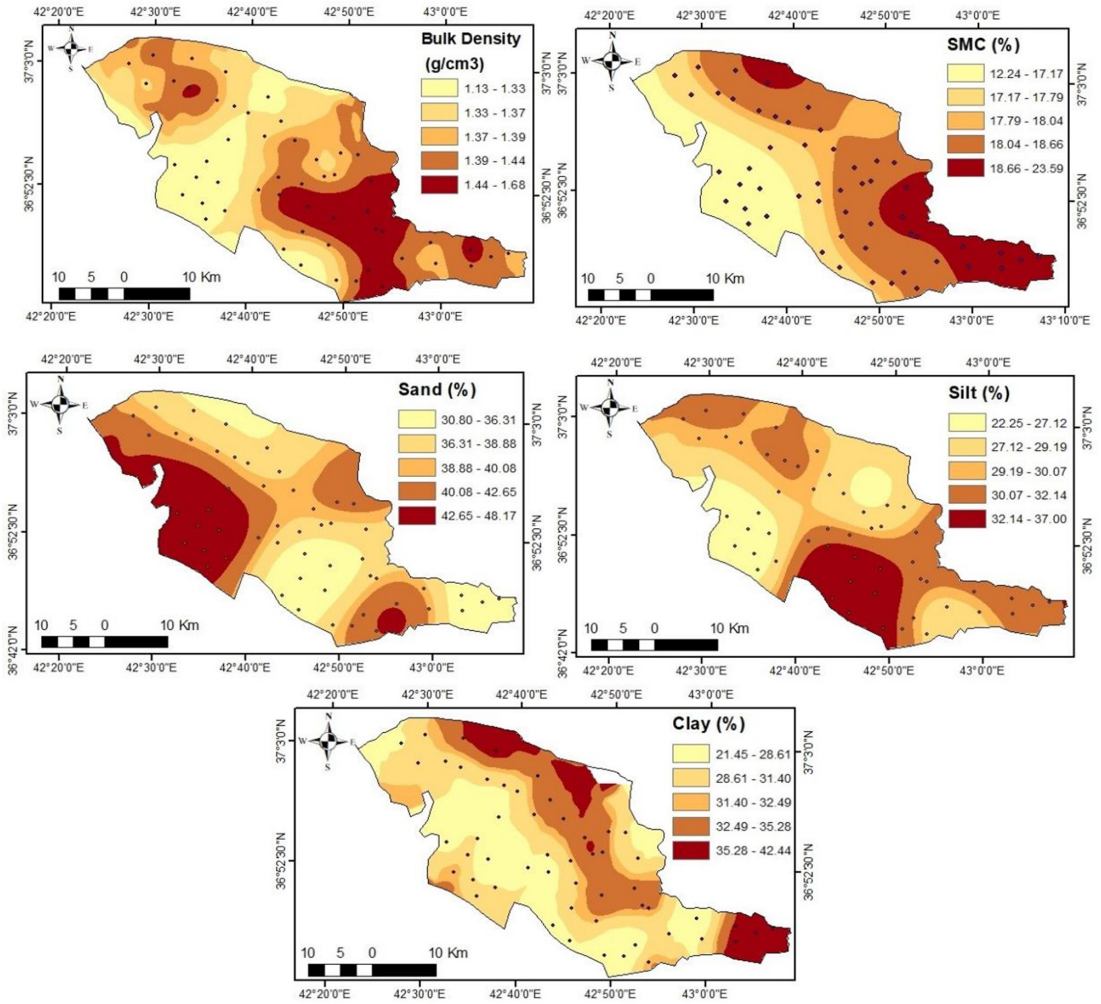

Figure 4.1. Spatial distribution of soil physical properties (bulk density, SMC, and soil particles) in Semel district

In the Semel district, the most frequently recorded colors were pale brown (10YR, 12 samples) and light yellowish brown (10YR, 19 samples) under arid conditions. Brown (10YR) was observed in six samples, pale brown (7.5YR) in two samples, and pink (7.5YR) in one sample. Also observed were occasional colors, including a light brownish gray (10YR, 1 sample) and a very faint brown (10YR, 1 sample). The soils demonstrated a significant transition to darker tints when they were moistened. The coloration of the samples was as follows: dark yellowish brown (10YR) dominated with 23 samples, followed by brown (10YR, 10 samples), dark brown (10YR, 5 samples), and strong brown (7.5YR, 3 samples). Pink (7.5YR, 1 sample) and mild brown (10YR, 6 samples) were additional colors (Figure 4.15).

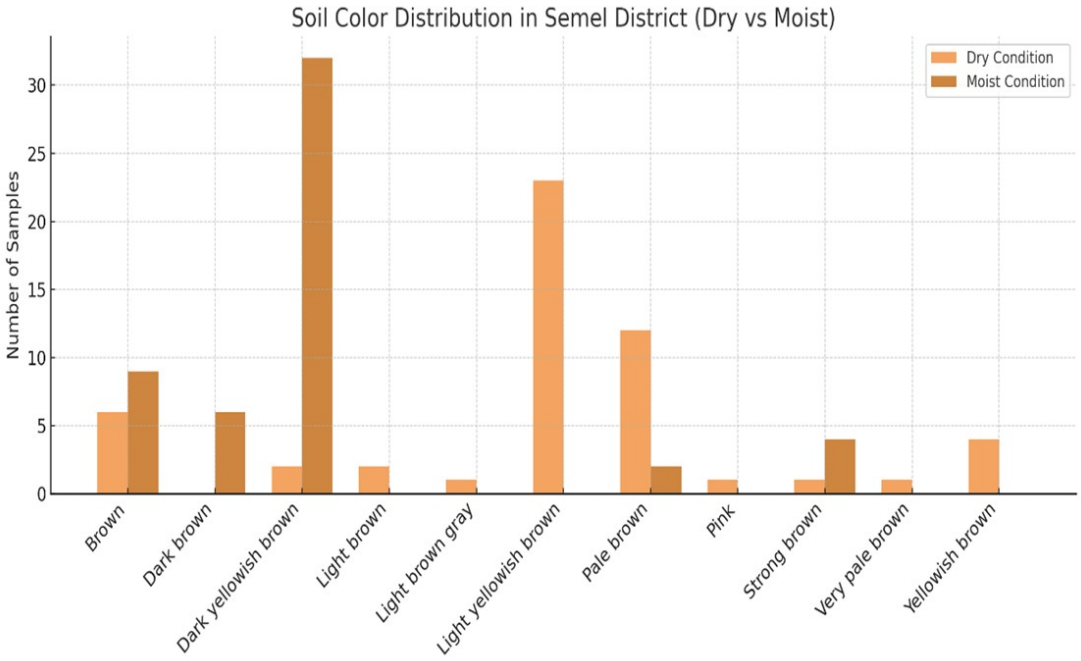

Figure 4.2. Soil color distribution under dry and moist conditions in Semel district

4.1.2. Laboratory and statistical evaluation of soil chemical parameters

The chemical examination of soil characteristics demonstrates significant heterogeneity within the research region. The mean readings show that the soil is somewhat alkaline pH was 7.42 ±0.01, and contains a moderate amount of OM (Table 4.8). The average CEC of 25.48 Cmol+ kg-1, as well as mean values for exchangeable Ca and K, indicate that the soil has a high capacity for nutrient retention and availability (Table 4.8).

Table 4.2. Descriptive statistics of soil chemical properties in Semel district

Soil properties	Min	Max	Mean	StD	Skew	Kurt	CV (%)	P-value
OM (%)	0.89	2.44	1.78	0.42	-0.17	-1.00	23.88	0.61
Soil pH	7.14	7.66	7.42	0.10	-0.30	-0.02	1.47	0.94
EC (dS m^{-1})	0.14	0.57	0.31	0.09	0.78	0.68	31.61	0.47

CEC (Cmol kg^{-1})	16.34	32.95	25.48	3.91	-0.09	-0.40	15.35	0.97
$CaCO_3$ (%))	7.50	35.00	19.14	6.30	0.14	-0.43	32.93	0.94
Avail. N (mg/kg)	10.00	70.00	30.00	0.002	0.07	-0.96	46.30	0.23
Avail. P (ppm)	1.05	11.85	3.01	2.30	1.85	3.27	76.33	0.008
Exch. K (ppm)	124.00	424	268.45	70.10	0.25	-0.47	26.11	0.77
Exch.Ca (ppm)	50.10	160.32	92.82	19.86	0.31	1.37	21.40	0.09
Exch.Mg (ppm)	11.90	27.30	22.16	2.50	-1.70	6.50	11.30	0.07
Exch. Fe (ppm)	0.26	7.18	2.22	1.80	1.07	-0.12	81.06	0.001
Exch. B (ppm)	1.00	9.96	3.35	2.29	1.35	1.08	68.35	0.066
Exch. Cu (ppm)	0.542	5.32	3.42	0.81	-1.28	3.78	23.70	0.19
Exch. Zn (ppm)	1.46	7.11	4.83	1.53	-0.63	-0.58	31.69	0.18
Exch.Mn (ppm)	1.09	9.37	4.04	2.77	0.64	-1.09	68.67	0.06

The soil chemical properties descriptive statistics suggest that there are

numerous prominent fertility constraints. The soils are distinguished by a low level of OM (mean= 1.78%), which is indicative of feeble biological activity and restricted organic inputs. Consequently, the soil structure is subpar, and nutrient cycling is diminished. The deficiency and irregular spatial distribution of available P (mean= 3.01 ppm) were also highlighted, with the highest variability (CV= 76.33%) and a non-normal distribution (P-value= 0.008).

Simultaneously, the soils calcareous nature was evident in the relatively high CaCO3 content (mean= 19.14%) and the broad variability (CV= 32.93%). In addition to indicating a high degree of soil alkalinity, the excessive CaCO3 also contributes to the fixation of P and the reduced availability of several micronutrients. These conditions collectively account for the general decrease in soil fertility and the prospective limitations on crop productivity in the study area. Figure 4.16 presents the spatial distribution of soil OM, pH, EC, CEC, and CaCO3 within the study area.

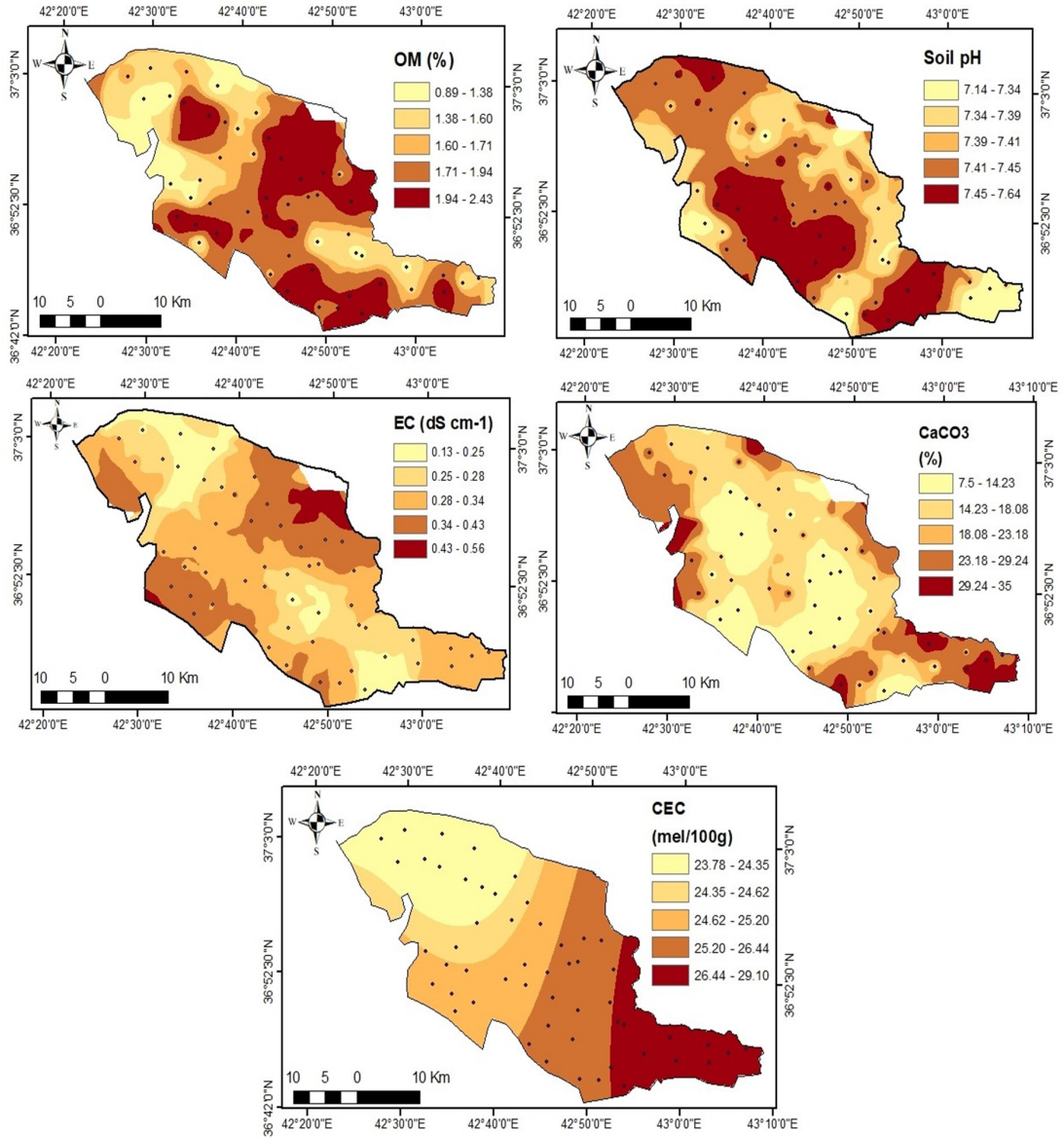

Figure 4.3. Spatial distribution of soil OM, pH, EC, CaCO3, and CEC in Semel district

Furthermore, the mean available N concentration was extremely low 30.00 mg/kg. Exch. Ca values in the studied soils ranged from 50.10 to 160.32 ppm, with an average of 92.82 ppm and a standard deviation of 19.86. The CV 21.40% indicates moderate variability among the samples. The distribution of Ca data showed a slight positive skewness 0.31 and kurtosis 1.37, suggesting that the data are nearly normally distributed. This is further supported by the P-value (0.09 > 0.05), confirming an approximately normal distribution pattern, while other macronutrients, including exchangeable K, and Mg, exhibited moderate variability with normal distributions.

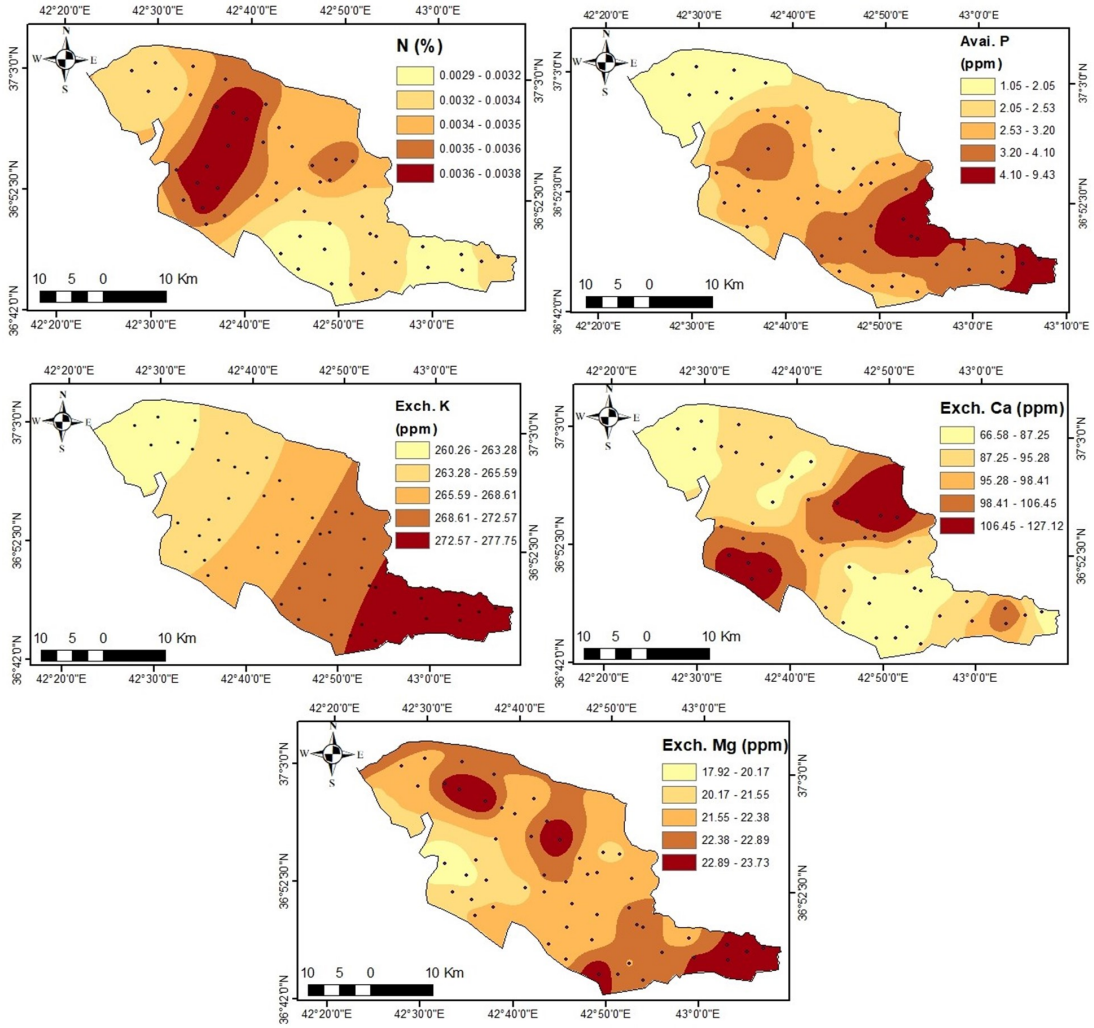

Figure 4.4. Spatial distribution of soil macronutrients in Semel district

The CV micronutrients, particularly Fe and Mn, were exceptionally high (81.06% and 68.67%, respectively), with Fe adhering to a non-normal distribution. This implies that there is a significant degree of spatial heterogeneity, which is likely to be influenced by the land management practices and progenitor material. The results of the study indicate that the soils under investigation are afflicted by a combination of low organic matter and phosphorus availability, as well as elevated calcium carbonate, which collectively serve as significant fertility constraints. These results underscore the necessity of integrated management practices, which include the application of phosphorus fertilizers and organic amendments, to increase soil productivity and surmount nutrient constraints. Figures 4.17 and 4.18 present the spatial distribution of macro- and micronutrients within the study area.

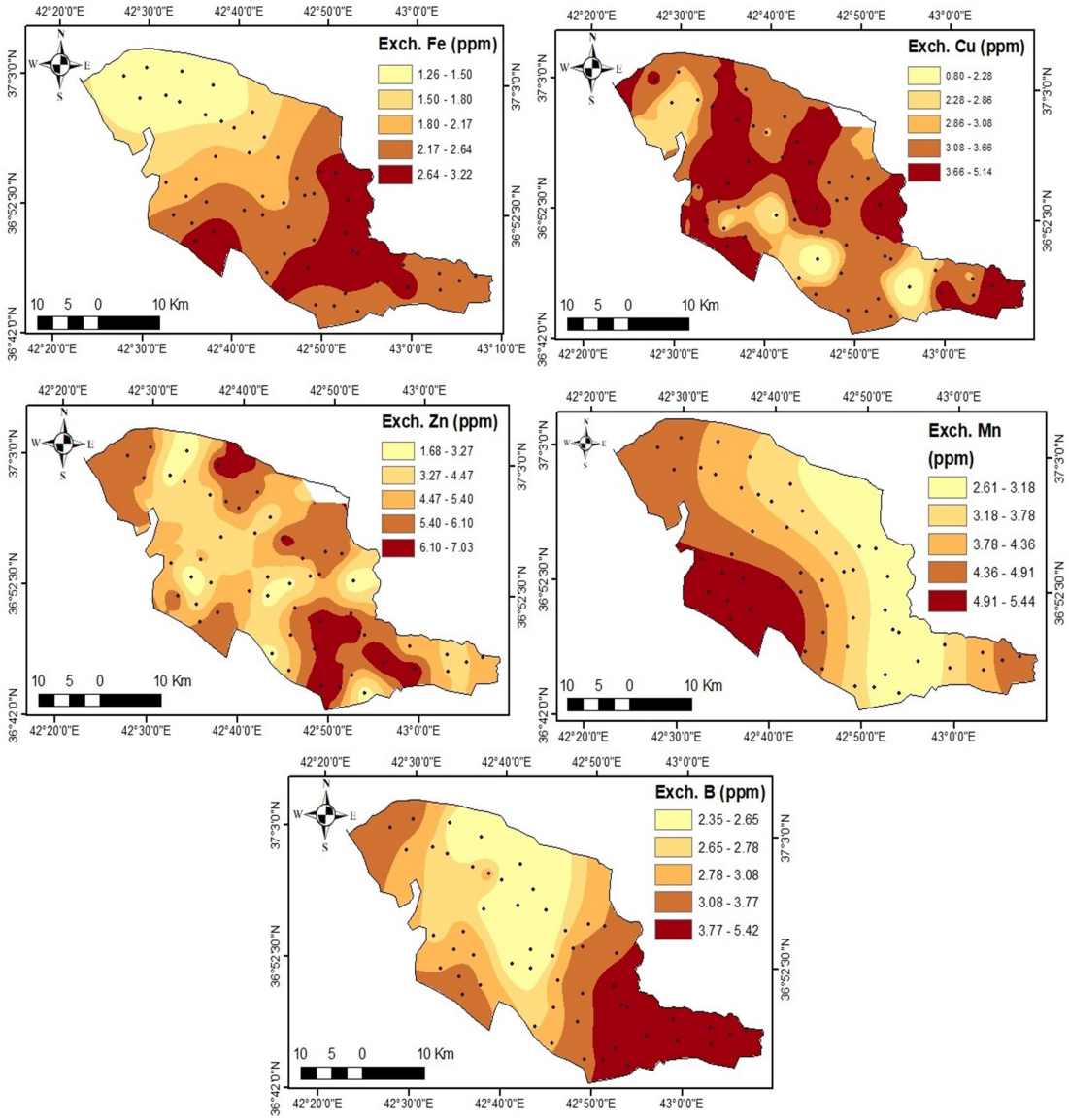

Figure 4.5. Spatial distribution of soil micronutrients in Semel district

4.1.3. AHP-Fuzzy weighted soil properties

The normalized weights of the eight spectrum indices and the seventeen soil physicochemical variables were systematically determined using the Analytic Hierarchy Process–Fuzzy (AHP-Fuzzy) framework. Through this approach, each characteristic was given a relative relevance for the final Soil Fertility Index (SFI) calculation based on expert judgment. The findings clearly rank the input variables according to their set weights, as seen in the bar chart (Figure 4.19).

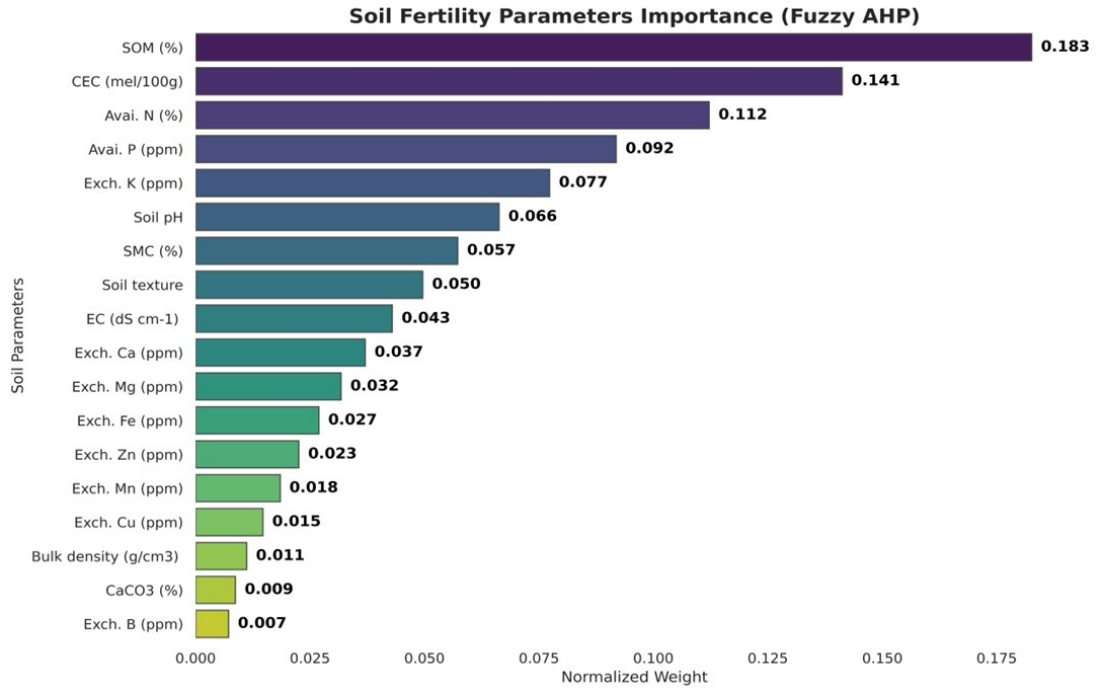

Figure 4.6. Normalized weights of soil properties and spectral indices as determined by the AHP-fuzzy method in Semel district

The study results showed that the largest weight 0.18 was assigned to OM%, which was followed by Available N 0.11 and CEC 0.14. The fact that these three factors together constituted a sizable amount of the overall weight highlights their paramount significance in the expert-based evaluation of soil fertility. B and CaCO3 were given the lowest weights among the remaining physicochemical characteristics and spectral indices (0.007 and 0.009, respectively).

4.1.4. SVM model performance

The best predicted performance for soil fertility classification was attained by methodically optimizing the SVM model. The hyperparameters that produced the greatest results were a linear kernel, a regularization parameter (C) of 0.5, and a gamma value set to scale. With a total classification accuracy of 0.9811 on the test set, the model showed remarkable performance. Table 4.9 displays each soil fertility class's specific performance metrics. All positive forecasts for the Very Low and Low fertility classes were accurate, as the model reached perfect accuracy 1.00 for both classes. The model's ability to accurately identify every occurrence of the Very Low and Medium classes was further demonstrated by the recall being perfect 1.00 for these classes (Table 4.9). The high F1-scores, all above 0.97, confirm a robust balance between precision and recall across all categories.

Table 4.3. SVM classification report for soil fertility classes in Semel district

Class	Precision	Recall	F1-Score	Support
Very Low	1.00	1.00	1.00	18
Low	1.00	0.94	0.97	17
Medium	0.95	1.00	0.97	18
Accuracy	-	-	0.98	53
Macro Avg	0.98	0.98	0.98	53
Weighted Avg	0.98	0.98	0.98	53

The confusion matrix (Figure 4.20), which displays the correct and incorrect predictions for every fertility class, provides further visual representation of the model's classification performance. The model correctly placed all 18 samples in the Very Low group and 18 out of 18 in the Medium category, as the matrix illustrates. 16 of the 17 samples in the Low class were properly recognized, while one sample was incorrectly categorized as Medium. The model's robustness is further validated by the Precision-Recall curve (Figure 4.21) and Receiver Operating Characteristic (ROC) curve (Figure 4.22).

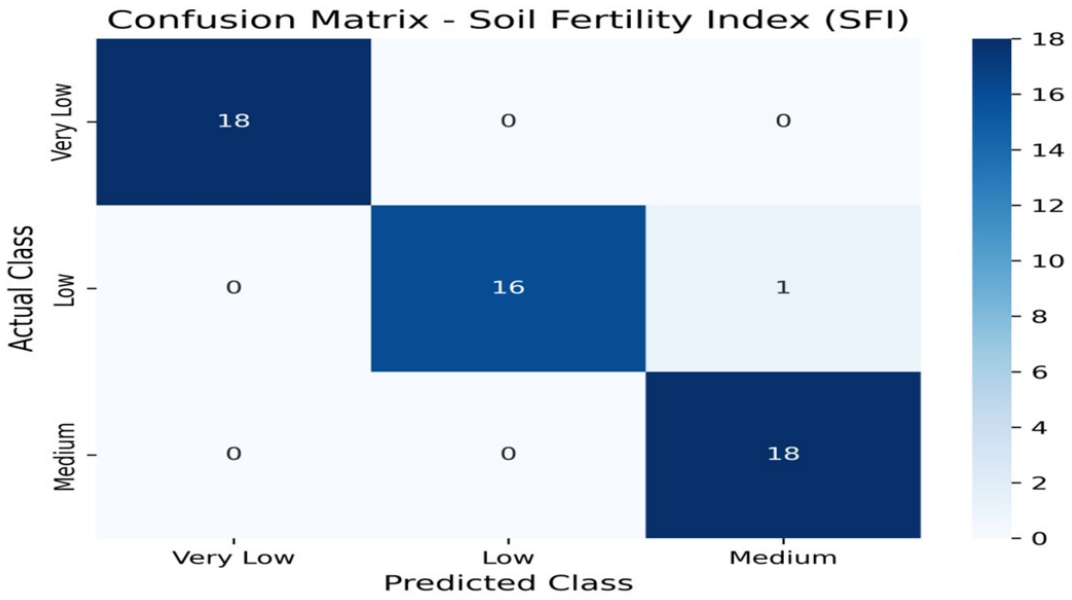

Figure 4.7. Confusion matrix of the SVM model for soil fertility classification in Semel district

The Area Under the Curve (AUC) values for the Very Low and Medium

fertility classes are 1.00 and 0.97, respectively, according to the ROC curves, demonstrating the model's exceptional discriminating capacity. A high average precision for all classes is further confirmed by the Precision-Recall curves, which show values of 1.00 for Very Low and Medium, and 0.96 for the Low class.

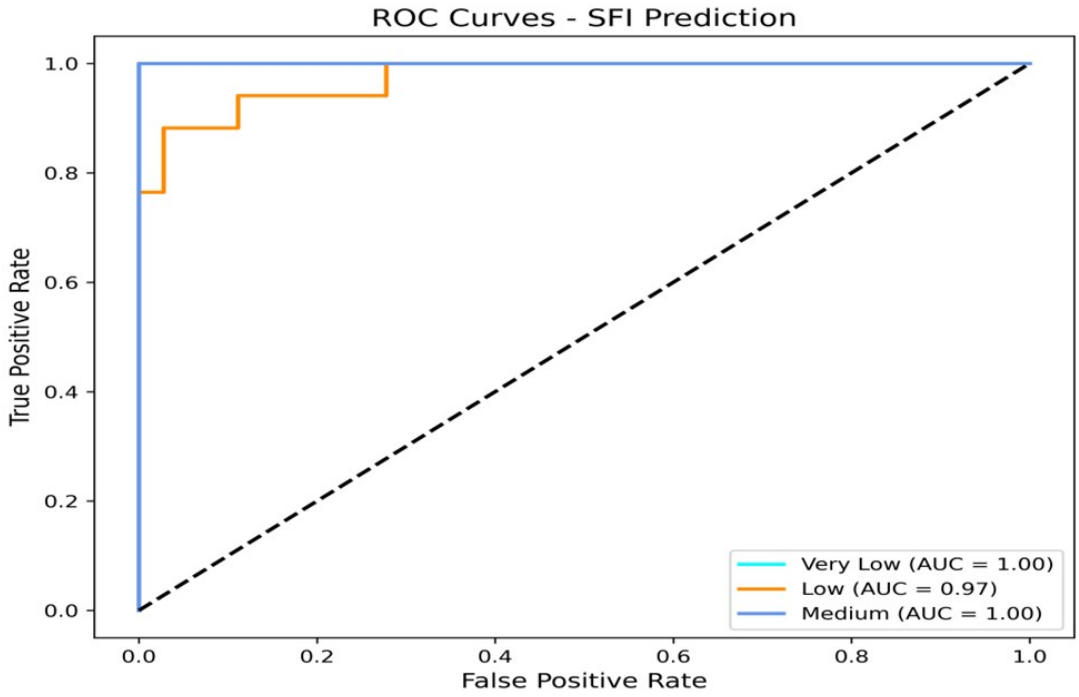

Figure 4.8. ROC curves for multi-Class SVM prediction of SFI in Semel district

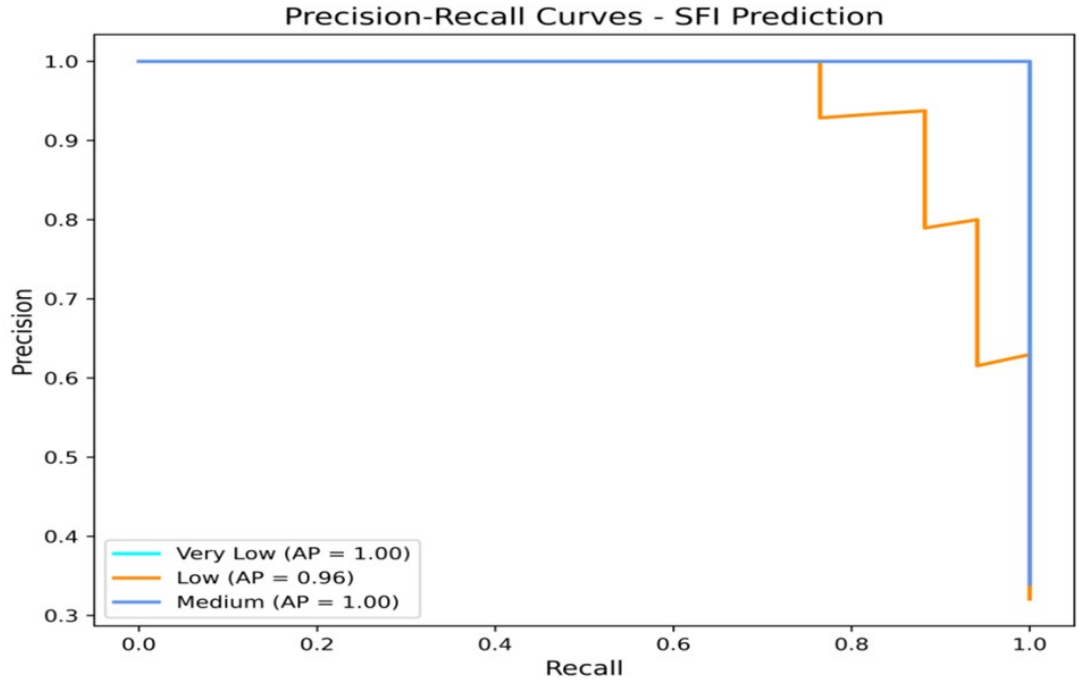

Figure 4.9. Precision-recall curves for the SVM-based SFI prediction in Semel district

4.1.5. Explainable AI insights

Although the SVM model has a high predicted accuracy, stakeholders who need clear, substantiated insights may find it difficult to use in practice due to its "black-box" character. In order to solve this, the study is the first to employ Explainable Artificial Intelligence (XAI), which converts the model's intricate predictions into understandable, useful conclusions. XAI offers a clear insight into the model's decision-making process by going beyond conventional performance indicators, which builds confidence and supports evidence-based land management. SHAP and LIME are the two main XAI techniques used in our investigation.

4.1.6. Shape

SHapley Additive exPlanations (SHAP) quantify the contribution of each input feature to the overall forecast, therefore offering a global interpretation of the model's behavior. In order to provide a consistent measure of feature relevance, SHAP values (Lundberg and Lee, 2017) are computed using cooperative game theory to fairly divide the "credit" for a prediction among all features. The bar plot (Figure 4.23) that displays the average absolute SHAP values reveals the most important spectral indices and soil characteristics that influence the model's classifications.

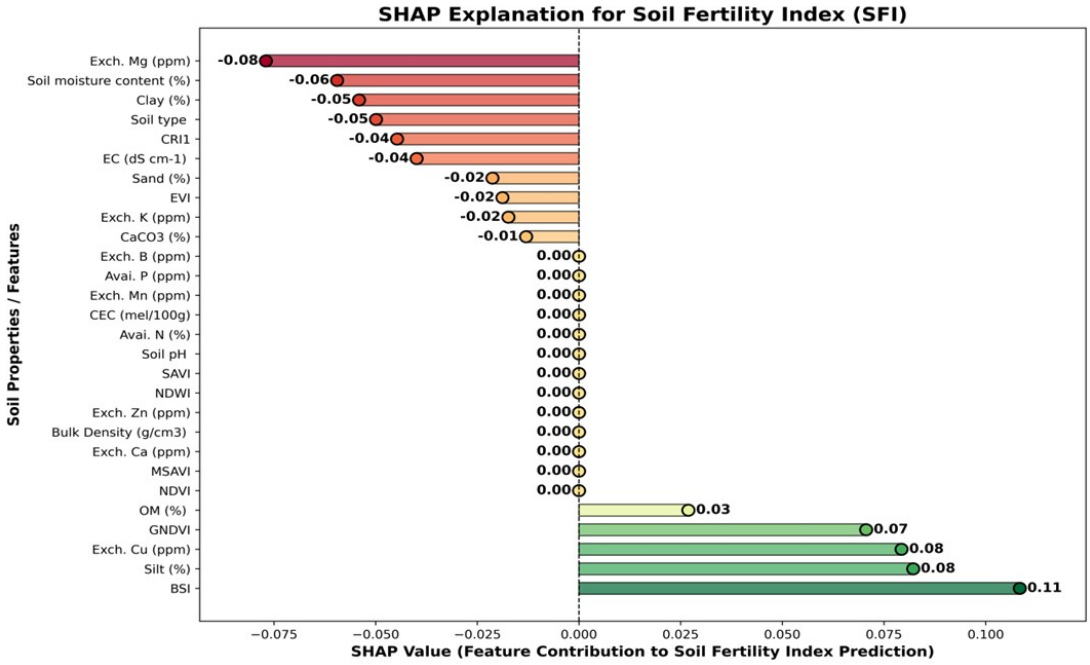

Figure 4.10. Global feature importance ranking of soil properties and spectral indices by SHAP values in Semel district

The SHAP study shows that the two most important factors in determining soil fertility are Silt (%) and the Bare Soil Index (BSI), which are closely followed by the Green Normalized Difference Vegetation Index (GNDVI) and Exch. Cu. In contrast, the SHAP values of characteristics like Bulk Density, Exch. Ca, and the Normalized Difference Vegetation Index (NDVI) were close to zero, indicating that they had little effect on the model's predictions.

4.1.7. Lime

Local Interpretable Model-agnostic Explanations (LIME) give a local interpretation, offering a condensed, human-understandable explanation for a single prediction, as opposed to the global viewpoint offered by SHAP (Ribeiro et al., 2016). LIME builds a locally linear model around the forecast for every individual soil sample or location, enabling us to see the precise characteristics that led to the sample's classification as Very Low, Low, or Medium. The factors that positively and adversely influenced the prediction are broken down sample-specifically by the LIME analysis, as shown in (Figure 4.24).

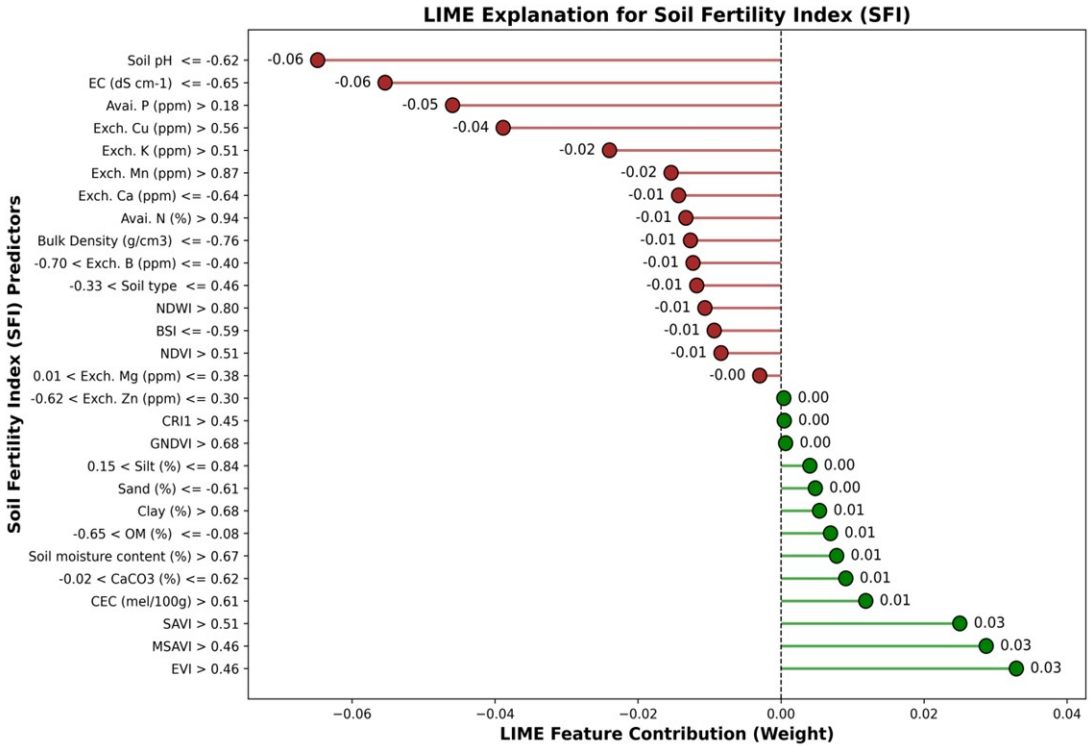

Figure 4.11. LIME explanation for an individual soil fertility prediction in Semel district

Relatively high EVI, MSAVI, and CEC values may have a beneficial impact on the model's choice for a given sample with "Medium" fertility, however high pH

and EC values (as shown by negative LIME weights) have a negative impact. Each of these characteristics gives a distinct fingerprint for a single prediction, as does their individual contribution.

4.1.8. Spatial distribution of soil fertility

A different distribution of soil fertility was found in the Semel region (Figure 4.25), with poor fertility found in most of the area, according to a geographical study. Based on the data presented, quantitative analysis reveals that the Low fertility class is the most prevalent, encompassing 443.07 km², or 47.71% of the entire research area (Table 4.10). Additionally, the Very low fertility class, which makes up 98.09 km² (10.56% of the area), is a substantial component. The large sections of the map that are tinted in light and dark brown visually demonstrate that low to extremely low fertility soils make up more than 58% of the research area overall.

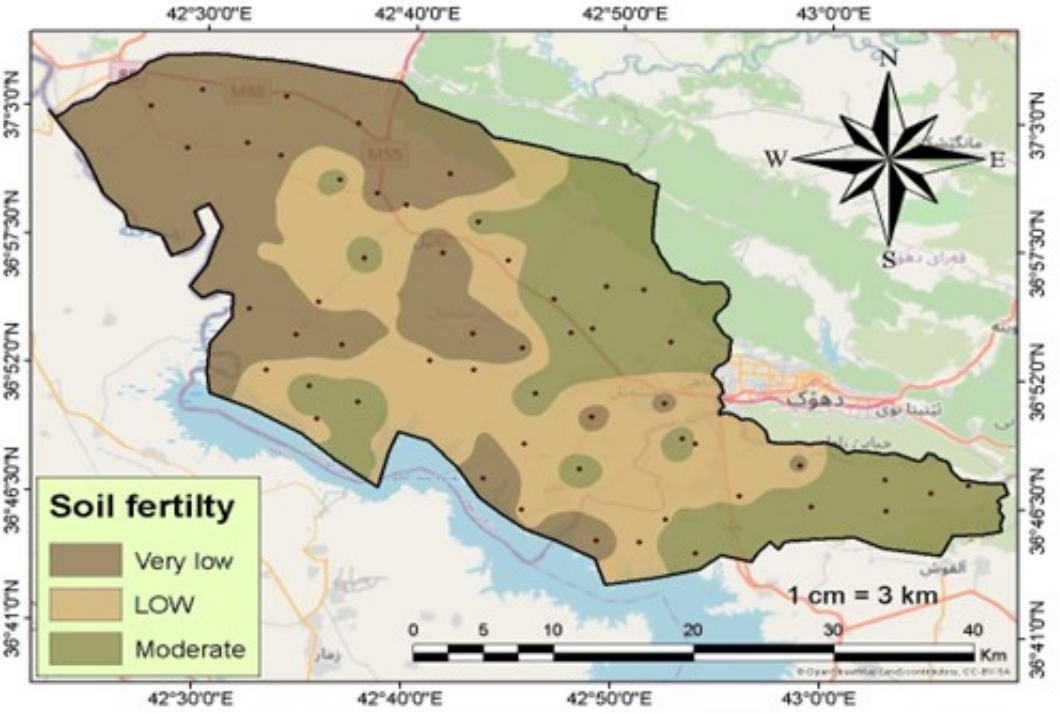

Figure 4.12. Spatial distribution of soil fertility in Semel district

Conversely, soil with Moderate fertility makes up a significant 41.72% of the area, or around 387.44 km² (Table 4.10). These moderate-fertility soils are not evenly dispersed geographically; instead, they show up as discrete, concentrated pockets, which are especially apparent in the map's north-central region. This variation implies that human and environmental causes have varying effects on soil health throughout the Semel area.

Table 4.4. Distribution of soil fertility classes in Semel district

Class of soil fertility	Area (km^2)	Percentage (%)
Very low	98.0888	10.56
Low	443.0673	47.71
Moderate	387.441	41.72

4.2. Bardarash district

4.2.1. Spatial distribution of environmental characteristics and their effects on soil fertility

Elevation, slope, and aspect are important environmental elements that have a significant impact on soil formation, hydrological processes, and land-use suitability. Figure 4.1 shows how these characteristics are distributed spatially.

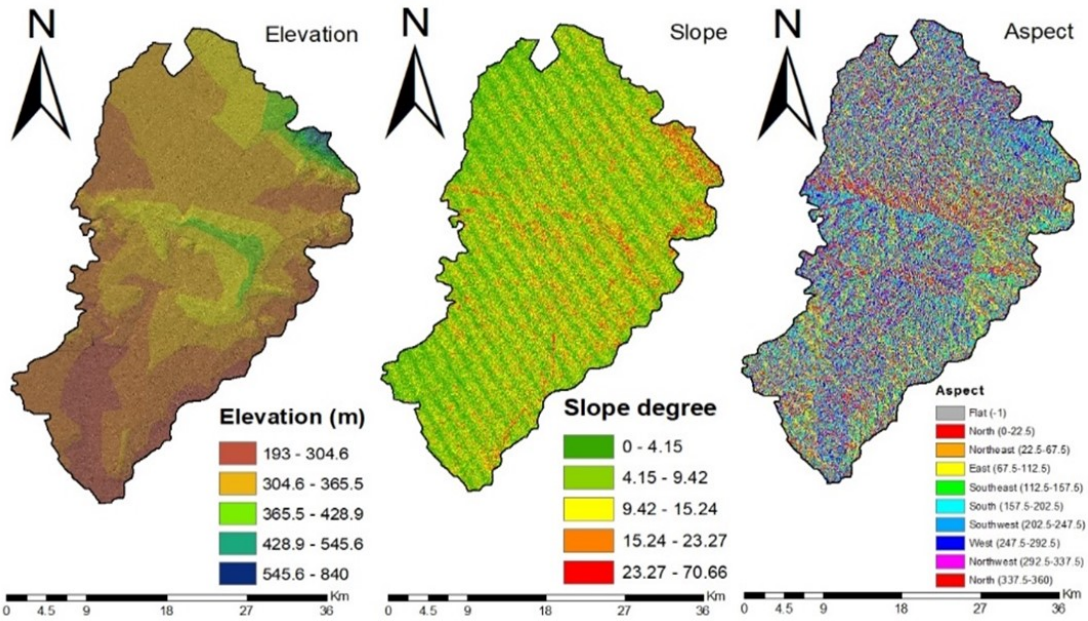

Figure 4.13. Environmental variable (Elevation, Slope, and aspect) of study region.

The research area's elevation varied from 193 to 840 meters, with the northern and central zones having the highest values. The local climate, drainage, and vegetation growth were all significantly impacted by these differences. Because of increased runoff and decreased soil stability, steep slopes (23.27° to 70.66°), which are concentrated in higher elevation areas, were shown to be more vulnerable

to rapid erosion. Slope values also varied significantly. The gentler slopes (0°-15°) that predominate in the southern zones, on the other hand, are less likely to experience erosion and are better suited for farming because of their easier access and stable soil.

Variability in the microclimate was also influenced by aspect. In contrast to south-facing slopes, which had drier soil conditions, faster evaporation, and more solar radiation, north-facing slopes held onto more soil moisture and supported unique vegetation patterns.

4.2.2. Laboratory and statistical evaluation of soil physical parameters

The laboratory analysis of soil physical properties revealed substantial variability in key parameters, including soil texture components (sand, silt, and clay), bulk density, and SMC, as presented in Table 4.1. The sand content ranged from 26.05 to 85.05%, with a mean result of 42.84%. Conversely, the silt concentration composition ranged from 2.00 to 45% (mean 26.16%), while the clay concentration ranged from 12.95 to 51.45% (mean 31.00%). The bulk density ranged from 1.22 to 1.72 Mg m-3, with a mean of 1.43 Mg m-3. The average SMC was 17.66%, with a range of 11.13% to 22.59%.

Table 4.5. Descriptive statistics of soil physical properties in the study area.

Soil Properties	Min	Max	Mean	StD	Skew	Kurt	CV (%)	P-value
Sand %	26.05	85.05	42.84	12.72	1.18	1.58	29.69	0.28
Silt %	2.00	45	26.16	9.01	-0.51	0.51	34.45	0.41
Clay %	12.95	51.45	31.00	8.59	0.17	-0.48	27.72	0.47
Bulk Density	1.22	1.72	1.43	0.11	0.29	-0.54	8.05	0.81
SMC (%)	11.13	22.59	17.66	2.88	-0.16	-0.93	16.32	0.25

Min= Minimum, Max= Maximum, StD= Standard Deviation, Skew= Skewness, Kurt= Kurtosis, CV= Coefficient of Variation

The CV data indicated substantial discrepancies in the variability of the analyzed parameters. The silt content had the greatest fluctuation at 34.45%, succeeded by sand at 29.69%, clay at 27.72%, soil moisture content at 16.32%, and bulk density at 8.05%. The Kolmogorov-Smirnov test P-values indicate that none of the soil parameters significantly deviated from normality; the minimum P-value for SMC was 0.25, implying that these characteristics can be considered normally distributed. Assessments of skewness, kurtosis, and coefficient of variation elucidated the distribution characteristics of diverse soil properties. Clay, silt, and sand possess skewness values of 0.17, -0.51, and 1.18, respectively. A right-tail distribution is suggested by Sand's positive skewness, with a few exceptionally high values interspersed with the bulk of observations. Silt's negative skewness indicates concentration towards higher levels, whereas clay's nearly zero skewness indicates a fairly symmetrical distribution.

Spatial Distribution of Soil Physical Parameters: Figures 4.2 and 4.3 illustrate the regional distribution of soil physical parameters, such as bulk density, SMC, and soil texture, particularly the percentages of sand, silt, and clay. These differences are indicative of topography. Sand in southern regions indicates soils that are well-drained but not as productive. These soils are more suitable for agricultural production because of the silt content, which shows a balance between water retention and appropriate drainage.

4.2.3. Spatial distribution of soil physical parameters

Figures 4.2 and 4.3 illustrate the regional distribution of soil physical parameters, such as bulk density, SMC, and soil texture, particularly the percentages of sand, silt, and clay. These differences are indicative of topography. Sand in southern regions indicates soils that are well-drained but not as productive. These soils are more suitable for agricultural production because of the silt content, which shows a balance between water retention and appropriate drainage.

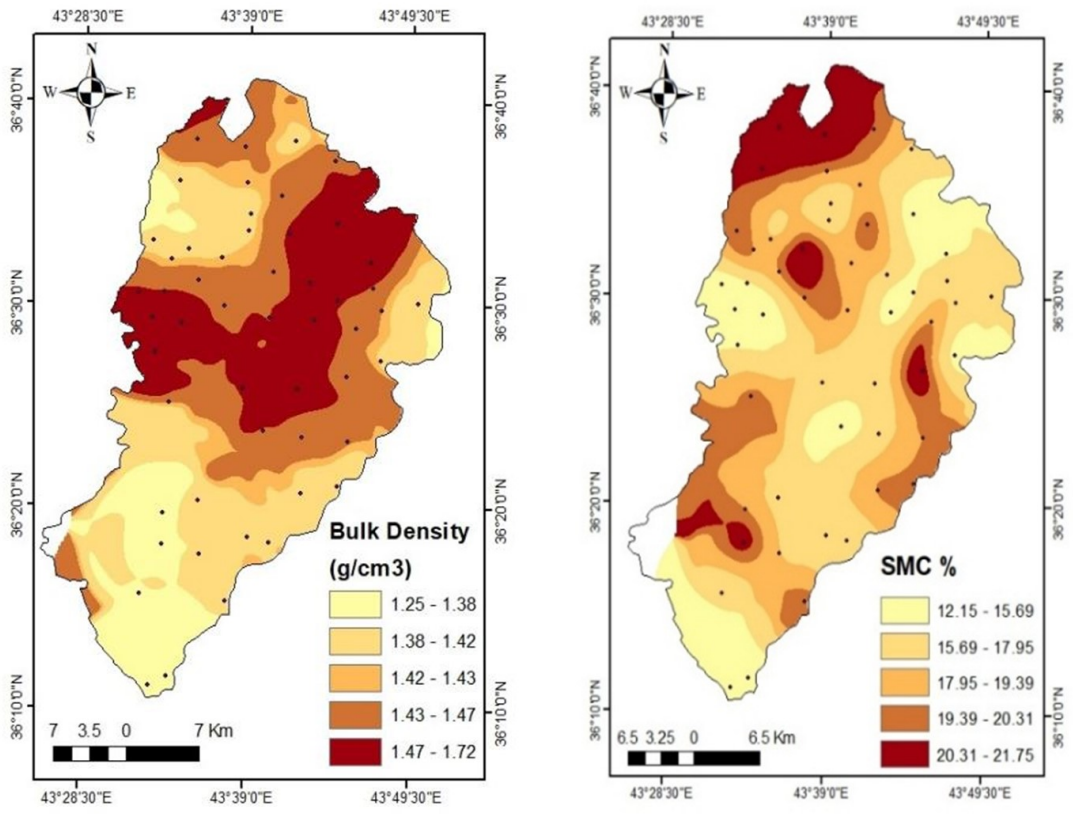

Figure 4.14. Spatial distribution of bulk density, and SMC in Bardarash district

Conversely, Figure 4.3 depicts higher levels of clay content that are found in the eastern and northern regions. Clay-rich soils have better cation exchange and water retention qualities, which can boost fertility.

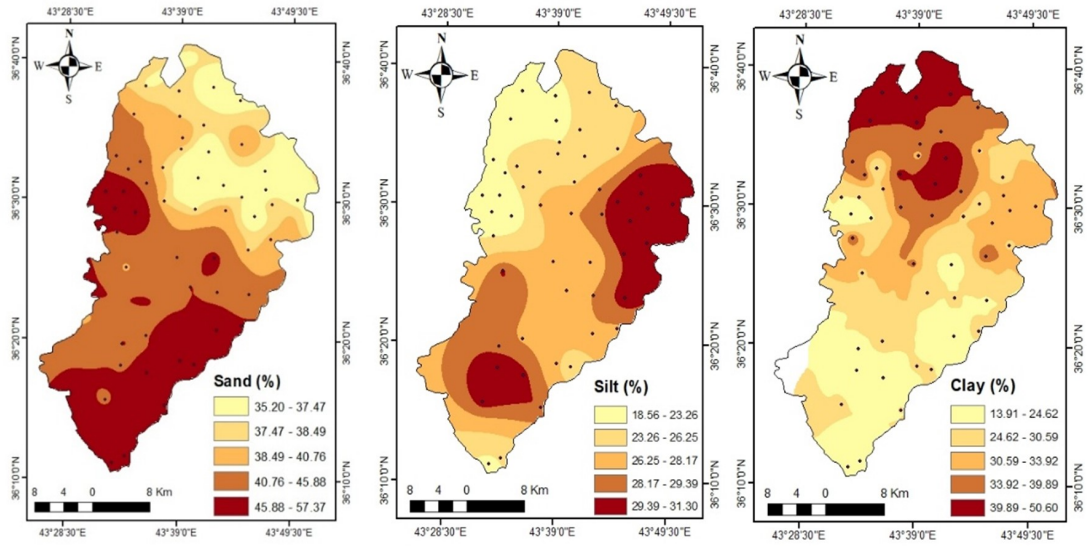

Figure 4.15. Spatial distribution of soil particles (sand, silt, and clay) in Bardarash district

Soil color is considered an indirect indicator of various critical soil

characteristics, including water drainage, aeration, mineral composition, and OM content (Foth, 1991). Black soils are typically rich in OM and thus highly fertile. In contrast, gray soils tend to have poor drainage and low organic content. Brown soils generally contain a moderate amount of OM, Fe, and other minerals, indicating good drainage. Red soils are characterized by high amounts of oxidized iron and usually have good drainage but low OM. Yellow soils often contain both oxidized and reduced iron, with limited OM and moderate drainage capacity.

In 29 samples, the predominant soil color was brown 10YR 5/4, which was observed under arid conditions. Other colors that were recorded included light brown 7.5YR 6/4 (6 samples), pinkish gray 7.5YR 6/2 (4 samples), strong brown 7.5YR 4/6 (3 samples), pink 7.5YR 7/4 (3 samples), pale brown 10YR 6/3 (2 samples), light brownish gray 10YR 6/2 (2 samples), very pale brown 10YR 7/4 (1 sample), very dark gray 7.5YR 3/1 (1 sample), and gray 7.5YR 6/2 (1 sample). Brown 10YR 5/4 was the most prevalent color under moist conditions (23 samples), with dark brown 7.5YR 3/4 (18 samples), strong brown 7.5YR 4/6 (3 samples), very dark gray (3 samples), dark yellowish brown (2 samples), yellowish brown (1 sample), very dark brown (1 sample), and dark grayish brown (1 sample) following in that order. as shown in (Figure 4.4).

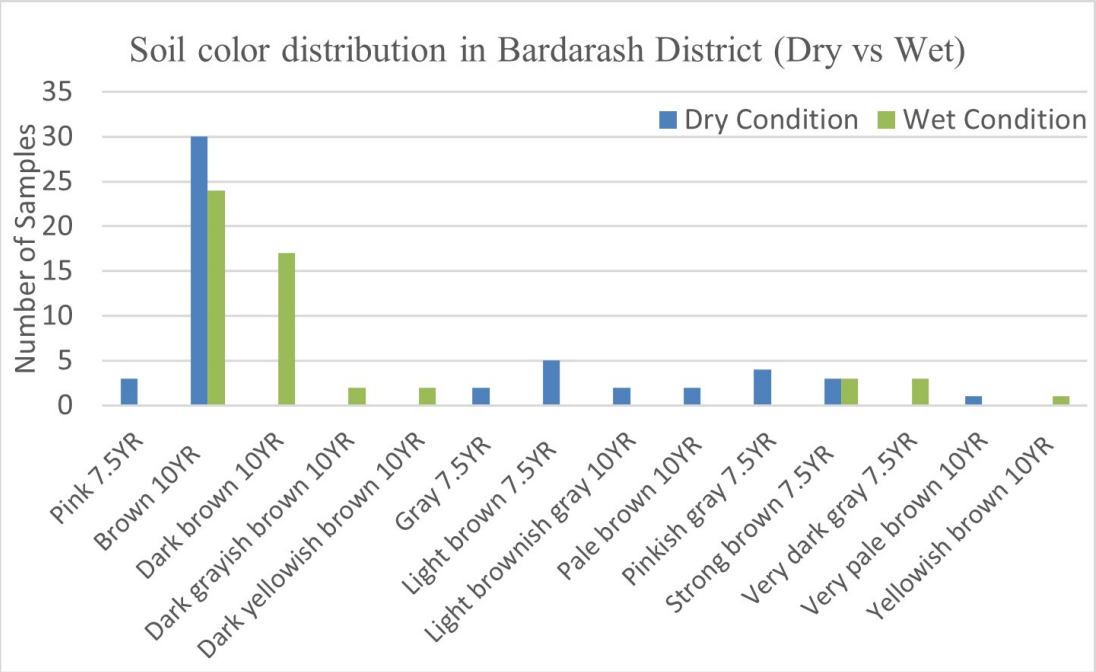

Figure 4.16. Soil color distribution under dry and moist conditions in Bardarash district.

4.2.4. Laboratory and statistical evaluation of soil chemical parameters

Descriptive statistics and laboratory analysis of soil chemical parameters: Lower, maximum, mean, StD, skewness, kurtosis, CV, and P-values were all included in the dataset (Table 4.2), suggesting that the soil's chemical properties varied significantly across a number of parameters.

Table 4.6. Descriptive statistics of soil chemical properties in Bardarash

Soil Properties	Min	Max	Mean	StD	Skewness	Kurtosis	CV (%)	P-value
OM (%)	0.2	2.79	1.42	0.69	0.18	-1.008	48.84	0.38
Soil pH	7.15	7.51	7.33	0.076	-0.17	0.11	1.04	0.92
EC (dS m^{-1})	0.12	0.585	0.32	0.089	0.39	0.710	27.67	0.76
CEC (Cmol kg^{-1})	12.22	31.7	24.50	4.88	-0.35	-0.78	19.91	0.00055
$CaCO_3$ (%))	9.00	45.00	28.14	9.23	-0.34	-0.64	32.82	0.81
Avail. N (mg/kg)	29.00	78.00	54.25	12.61	-0.15	-0.74	23.25	0.0034
Avail. P (ppm)	1.05	8.95	3.65	2.18	1.09	0.27	59.71	0.021
Exch. K (ppm)	28	288	138.76	56.18	0.38	0.81	40.48	0.32
Exch.Ca (ppm)	30.06	200.40	84.98	30.51	0.75	2.66	35.91	0.15
Exch.Mg (ppm)	12.9	22.4	18.14	2.05	-0.24	0.69	11.32	0.78
Exch. Fe (ppm)	2.72	97.5	36.05	30.80	0.79	-1.005	85.42	0.00027
Exch. B (ppm)	0.104	8.84	1.16	1.33	4.27	22.01	114.86	0.0015
Exch. Cu (ppm)	1.00	9.16	3.76	1.94	0.92	0.44	51.57	0.53
Exch. Zn (ppm)	10.00	99.7	59.44	25.06	-0.28	-0.84	42.17	0.78
Exch.Mn (ppm)	1.05	9.87	4.82	1.99	-0.0017	-0.46	41.27	0.47

A mean of 1.42% and a StD of 0.69% were found for the amount of OM. The range was from 0.2 to 2.79%. The skewness value of 0.18 shows that the distribution is almost symmetrical with a slight right tail. The kurtosis score of -1.008 suggests that the distribution is platykurtic, which means it is flatter than normal. The OM content seems to be very different, with a CV of 48.84%. There were three groups of soils according to the FAO's method from 1980: medium 23%, very low 35%, and low 42%. The P-value of 0.38 shows that the OM data follows a normal distribution.

The mean soil pH was 7.33±0.01, with a low StD of 0.076, and the range was from 7.15 to 7.51. The kurtosis is 0.11 and the skewness is -0.17, indicating that the distribution is nearly normal with a minor left tail. The CV is 1.04%, which indicates a low level of variability. No significant deviation from normality is further confirmed by the high P-value of 0.92. The soils were classified as neutral to mildly alkaline according to Jackson's (1973) classification, with 23% of them being neutral and 73% being mildly alkaline.

At 25°C, the EC of a 1:1 mixture of dirt and water in Bardarash ranged from 0.12 to 0.59 dS m-1, with 0.32 ± 0.012 dS m-1 being the average. With a skewness value of 0.39, the distribution was slightly skewed to the right. The kurtosis value of 0.71 shows that the distribution had a few more peaks than usual. The large P-value of 0.76 shows that the EC data are distributed normally. The CV was 27.67%, which means there was moderate fluctuation. Based on Duran's (1983) description, all of the soils in the area that was studied were not salty.

Spatial distribution of Soil OM, pH and EC across the study area is shown in Figure 4.5. Soils in Bardarash had a CEC that ranged from 12.22 to 31.70 Cmol kg-1, with 24.50 being the mean and 4.88 being the standard deviation. The distribution had a slight left skew -0.35 and a flat shape -0.78, which is called a platykurtic pattern. The P-value of 0.00055 shows that there is a big difference from normalcy. There was some difference, but not a lot. The coefficient of variation CV was 19.91%. Following Duran's (1983) classification, about 52% of the soils were found to have a high CEC, while 48% were found to have a middle CEC.

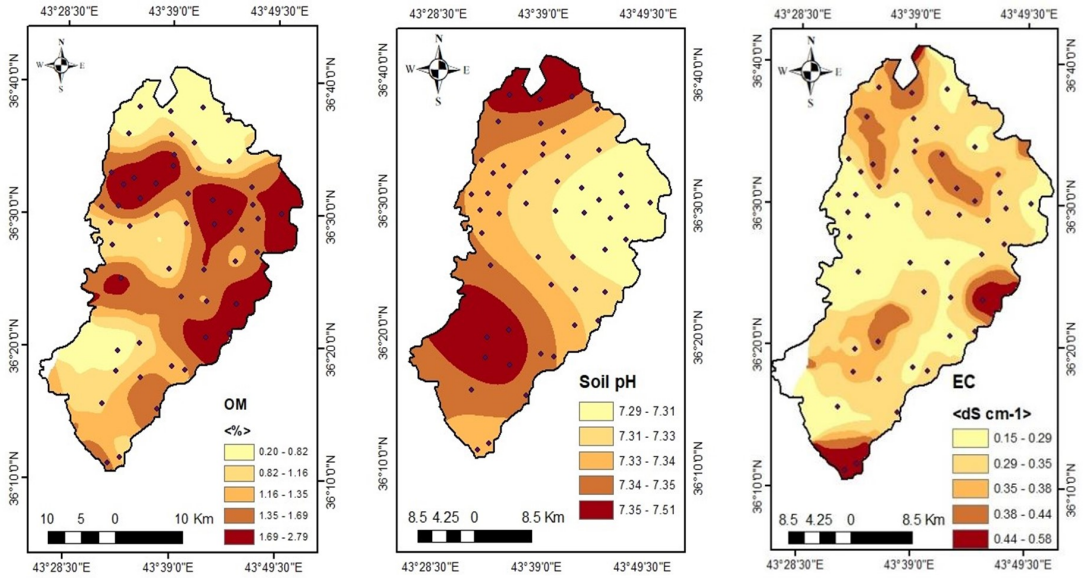

Figure 4.17. Spatial distribution of soil OM, pH, and EC in Bardarash district

CaCO3 levels in the Bardarash district ranged from 9 to 45%, with an average of 28.14%. As indicated by the skewness of -0.34 and kurtosis of -0.64, the distribution is platykurtic and slightly left-skewed. The estimated CV (32.82%) indicated a high degree of variability among the samples, whereas the P-value (0.81) was greater than 0.05, showing that the variation was not statistically significant. About 94% of the soils had a CaCO3 content that was categorized as high to very high, with the remaining 6% having a medium CaCO3 value (Belay et al., 2025). The spatial variability of CaCO3 and CEC is presented in Figure 4.6.

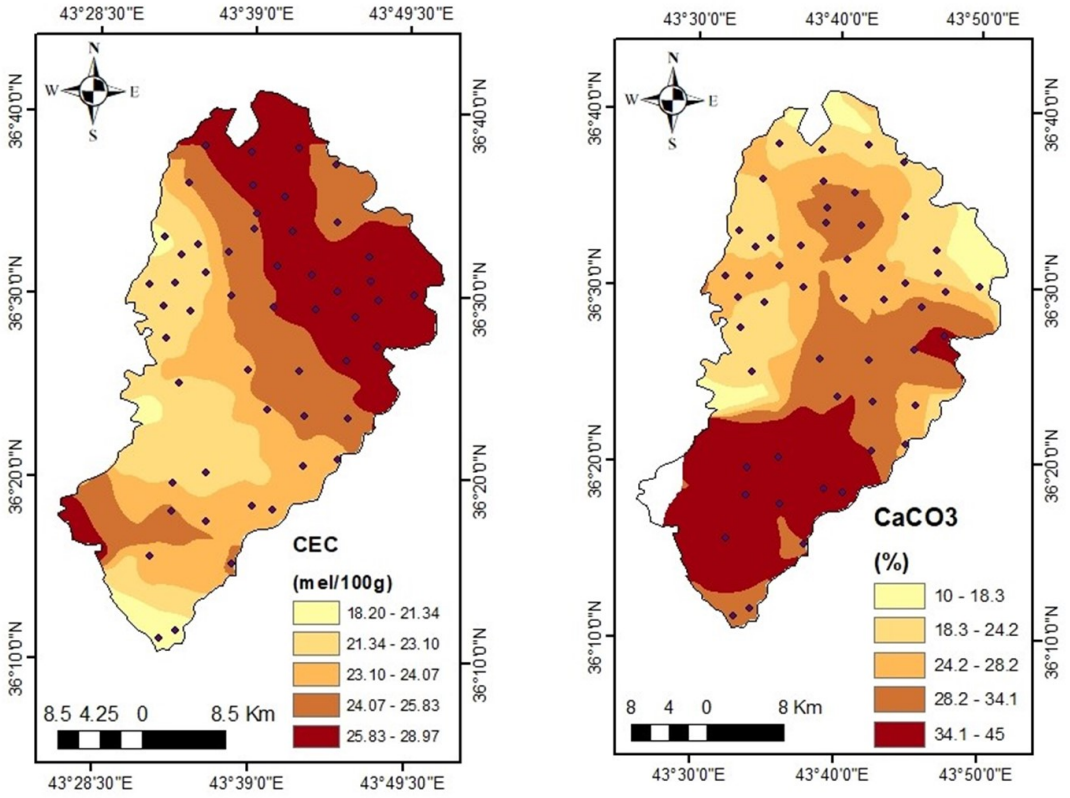

Figure 4.18. Spatial distribution of CEC and CaCO3 in Bardarash district

The available N in the soils of the Bardarash district varied from 29.00 to 78.00%, with an average of 54.25 ± 0.00017%. The distribution exhibited a minor left tail, evidenced by a skewness of -0.15, and a platykurtic characteristic, as indicated by a kurtosis of -0.74. A P-value of 0.034 suggests a tendency towards normality. Moderate variability was noted, with a CV of 23.25%. The available nitrogen (N) content in the studied soils ranged from 29 to 78 mg/kg, with an average value of 54 mg/kg. The amount of available P in the soils of the Bardarash area ranged from 1.05 to 8.95 ppm, with 3.65 ± 0.303 ppm being the mean and 2.18 ppm being the StD. The data was skewed to the right skewness 1.09, which means there were a lot of low numbers, and it had a slight peak kurtosis 0.27). A large departure from normalcy is shown by a P-value of 0.021. There is a lot of difference in the available P across the study area, as shown by the high CV of 59.71%. According to the classification of Matar (1992), 48% of the soils had very little P, 46% had low P, and only 6% had middle P. We found that the amount of K in the water was between 28 and 288 ppm, with 138.76 ppm as the mean and 56.18 ppm as the standard deviation. A small amount of skewness was seen to the right 0.38, and the distribution had more peaks than usual 0.81. The CV was found to be between 40.48 and 40.49 percent. However, the P-value of 0.32 showed that the distribution of available K did not deviate from normality in a big way. Exch. Ca ranged from 30.06

to 200.40 ppm, with a mean value of 84.98 ppm and a CV of 35.91%, indicating moderate-to-high spatial variability among the sampling sites. The distribution showed slight right skewness 0.75 and near-normal kurtosis 2.66, with P-value of 0.15, suggesting an approximately normal distribution of the data. The amount of Mg in the sample varied from 12.9 to 22.4 ppm, with 18.14 ppm as the mean 18.14 ± 0.29 ppm and 2.05 ppm as the StD. A high P-value of 0.78 meant that the distribution was normal, even though it was slightly skewed to the left skewness -0.24 and had a modest peak kurtosis 0.69. The CV of 11.32% indicates that there was little variation among the soil areas.

Micronutrients found in Bardarash soils were very different, with mean amounts going from lowest to highest in this order: Mn, Zn, Cu, Fe, and B. The Fe levels were very different, ranging from 2.7 to 97.5 ppm, with a mean of 36.05 ± 4.27 ppm and StD 30.80. The CV was 85.42%, and the distribution had a right skew skewness 0.79 and a flatter-than-normal curve kurtosis -1.01. A very low P-value of 0.00027 showed that there was a significant departure from normality. The B levels varied from 0.10 to 8.84 ppm, with a mean of 1.18 ± 0.19 ppm. The data had a very wide range of values CV 114.86%, a highly right-skewed distribution skewness 4.27, and very high peaks kurtosis 22.01. The P-value of 0.0015 showed that the data was not normally distributed. Cu levels varied from 1.0 to 9.16 ppm, with an average of 3.76 ± 0.27 ppm, 1.94 StD, and 51.57% CV. The data was skewed slightly to the right 0.92, had a mild kurtosis 0.44, and a P-value of 0.53 suggesting that it was mostly normal. Zn levels ranged from 10.0 to 99.7 ppm, with a mean of 59.44 ± 3.48 ppm and StD 25.06. The data had a moderate amount of variation CV 42.17%, a distribution that was flatter than normal kurtosis -0.84, and a small amount of left skew skewness -0.28. However, the high P-value 0.78 suggested that the data followed a normal distribution. Finally, Mn levels varied from 1.05 to 9.87 ppm, with a mean of 4.82 ± 0.28 ppm, an StD of 1.99, and a CV of 41.27%. Its distribution was almost symmetrical skewness -0.0017, slightly platykurtic kurtosis -0.46, and a P-value of 0.47 suggesting that it was normally distributed. For better visualization and interpretation, the spatial distribution maps of soil macronutrients (N, P, K, Mg) and micronutrients (Fe, Zn, Cu, Mn, B) were generated using geostatistical interpolation OK. These thematic maps (Figures 4.7 and 4.8) illustrate the variability and spatial patterns of these nutrients across the Bardarash district.

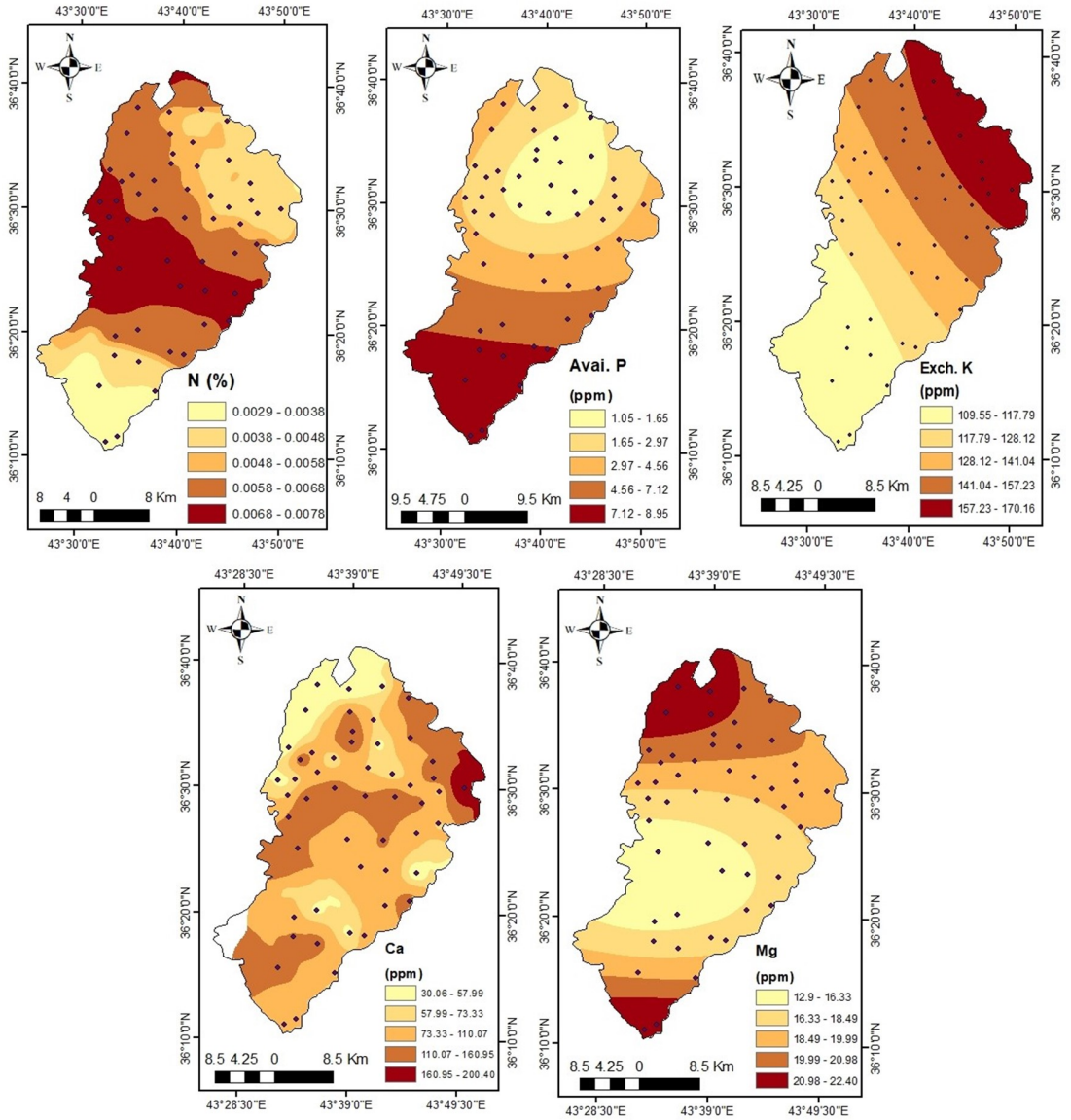

Figure 4.19. Spatial distribution of soil macronutrients (N, P, K, Ca and Mg) in Bardarash district

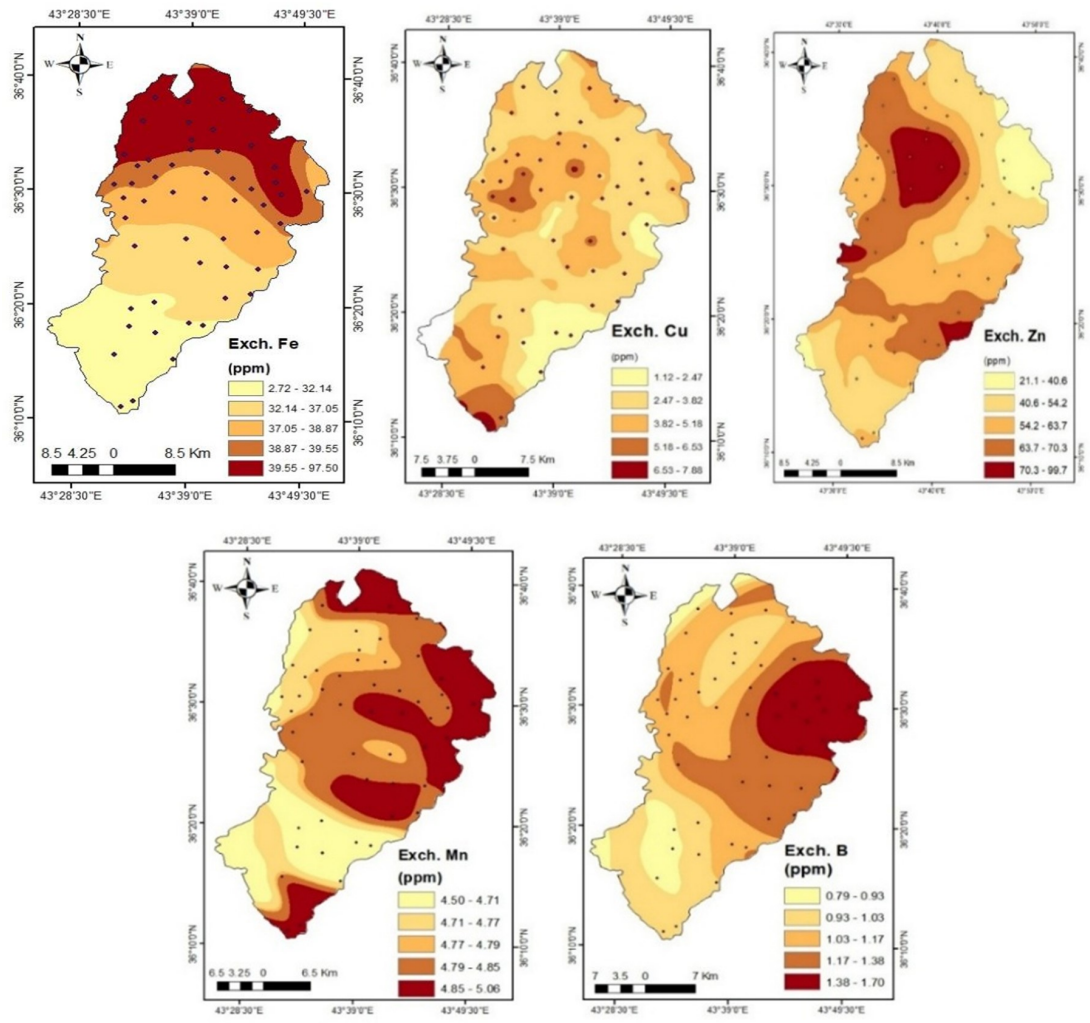

Figure 4.20. Spatial distribution of soil micronutrients (Fe, Cu, Zn, Mg and B) in Bardarash district

4.2.5. Semivariogram of soil properties

Before the models were selected, the semivariograms were fitted to spherical, exponential, Gaussian, or linear models, and the best fit with matching coefficients of determination (R2) was visually assessed. Nugget semivariance, range, and sill (total semivariance) were among the model parameters. The sill shows the lag distance beyond which values are no longer spatially connected, whereas nugget semivariance represents both field and experimental variability, displaying variance at zero distance.

The range is the distance at which there is no longer any spatial association between variables. Table 4.3 summarizes the model performance and spatial variability and presents the semivariogram parameters needed to produce OK interpolation for various soil attributes. Significant variance in geographical

interdependence among soil properties was revealed by statistical markers as Spatial Dependence (SD %), MAE, RMSE, and R2. For instance, there was a notable regional dependence in the low nugget-to-sill ratios of OM and accessible Fe.

Table 4.7. Semivariogram and error metric parameters of the soil properties in Bardarash district

Soil Properties	Model	Sill	Nugget	Range	SD (%)	MAE	RMSE	R^2
OM (%)	Spherical	0.518	0.183	8520	35.32	-0.00022	0.499	0.62
Soil pH	Exponential	0.00864	0.00419	40542	48.49	-0.00054	0.508	0.19
EC (dS m^{-1})	Gaussian	0.00822	0.00034	2010	4.13	0.001909	0.087	0.69
CEC (Cmol kg^{-1})	Linear	27.42	19.45	25304	70.93	0.115	4.791	0.14
$CaCO_3$ (%)	Spherical	83.08	20.06	1537	24.14	0.182	8.798	0.17
Avail. N (mg/kg)	Spherical	0.00003	0.00001	7720	33.33	1.13e-	0.001	0.69
Avail. P (ppm)	Gaussian	4.38	0.16	2226	3.65	-0.0083	2.193	0.68
Exch. K (ppm)	Spherical	2925	1053	4540	36	-0.016	55.74	0.51
Exch. Ca (ppm)	Spherical	0.072	0.032	2005	44.44	0.042	0.121	0.56
Exch. Mg (ppm)	Gaussian	3.76	0.7	1197	18.61	-0.020	2.124	0.51
Exch. Fe (ppm)	Gaussian	951	1.01	2100	0.106	0.688	30.66	0.81
Exch. B (ppm)	Gaussian	2.16	0.001	1391	0.046	0.0305	1.343	0.41
Exch. Cu (ppm)	Gaussian	3.86	0.01	2230	0.25	0.0082	1.980	0.66

Exch. Zn (ppm)	Gaussian	629.5	1.02	2300	0.16	0.615	25.42	0.68
Exch. Mn (ppm)	Linear	6.56	2.79	32551	42.53	0.0066	2.097	0.25
Bulk Density (Mg m^{-3})	Gaussian	0.012	0.00001	1920	0.083	0.0004	0.116	0.65
SMC (%)	Gaussian	8.91	0.01	2900	0.11	-0.011	2.747	0.78
Sand (%)	Exponential	174.36	65.9	6637	37.79	0.0065	12.20	0.33
Silt (%)	Linear	98.83	83.98	14603	84.97	0.099	9.084	0.19
Clay (%)	Exponential	68.38	15.8	4530	23.10	-0.077	6.681	0.61

SD (%) = Spatial Dependence

On the other hand, comparatively higher nugget values for soil pH and silt concentration indicated poorer spatial organization. Additionally, the ranges were quite large, ranging from localized values for accessible Mg (1,197 m) and CaCO3 (1,537 m) to widespread values for soil pH (40,542 m) and CEC (25,304 m). The model's performance also varied, with lower R2 values for soil pH (0.189) and silt content (0.186) reflecting weaker predictions and higher R2 values for available Fe (0.805) and SMC (0.774) suggesting great predictive accuracy.

4.2.6. Correlation matrix between soil properties

A dendrogram is presented in Figure 4.9, which also includes the clustered correlation matrix heatmap, to illustrate the relationships between soil and environmental properties. The dendrogram hierarchically groups variables based on their similarity, while the heatmap displays correlation coefficients that range from (-1 to 1), indicating the strength and direction of associations.

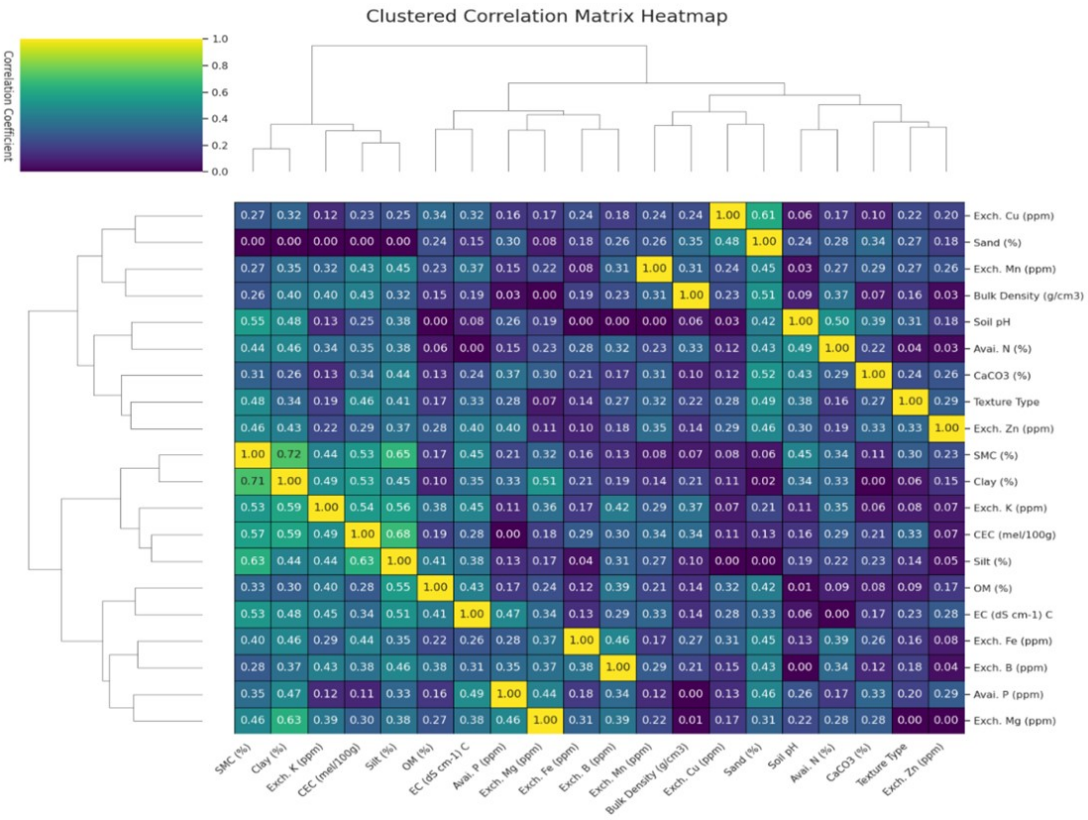

Figure 4.21. Correlation metric with dendrograms of soil properties in Bardarash district

The findings indicate that there are distinct clusters of variables that are significantly correlated. For example, the presence of a single cluster containing clay content, CEC, and OM suggests that a higher clay content is typically correlated with higher levels of CEC and OM. Another cluster was composed of nutrient-related variables, including available Mg, Ca, and K, which underscored their interconnection in nutrient availability. The inverse association between soil fertility indices and factors such as sand content and bulk density was confirmed by the negative correlations observed. The most robust positive correlations were observed between clay content and CEC, as well as between OM and CEC.

4.2.7. Principal component analysis (PCA) results

To determine the most important factors for calculating the SFI, PCA was used to examine the 19 soil characteristics in Bardarash. According to Figure 4.9, the first two main components (PC1 and PC2) combined accounted for XX% of the variation, with PC1 alone accounting for XX%. The first few components kept the majority of the information, as the cumulative variance plot verified. The loading results demonstrated that whereas CaCO3 and bulk density (BD) had a stronger effect on PC2, organic matter (OM), CEC, accessible phosphorus (P), available

nitrogen and pH were the main contributors to PC1 (Figure 4.10).

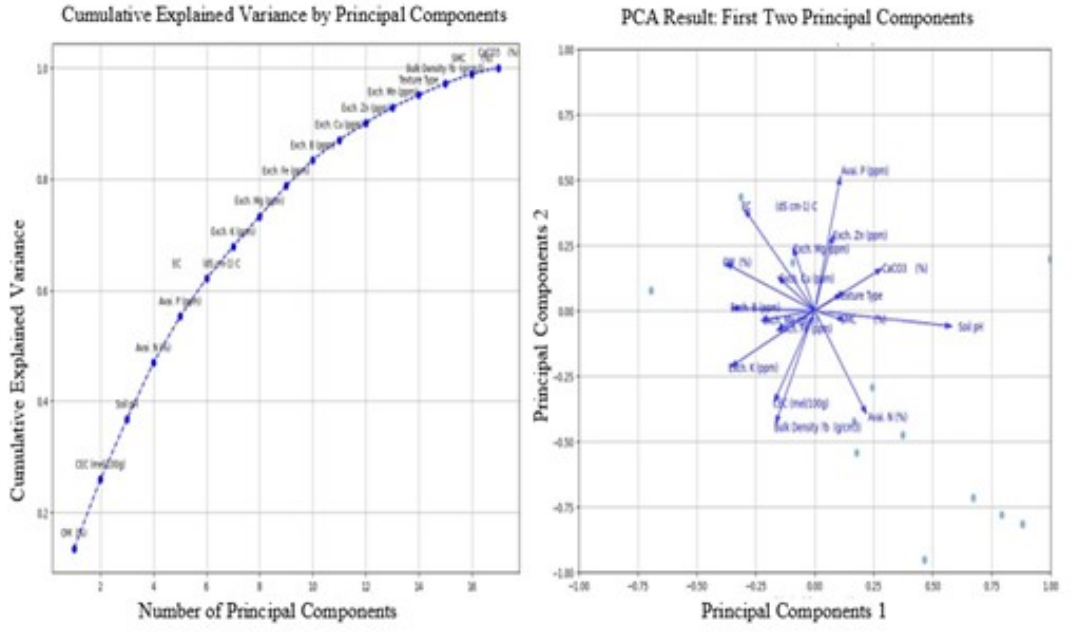

Figure 4.22. Assigning weight of soil properties by using PCA approach in Bardarash district

In determining soil variability in Bardarash, these findings emphasize the relative significance of chemical fertility attributes over physical properties. Thus, each parameter was given a weight generated from PCA, where the parameters that contributed more strongly to the first components were given greater weights. This made sure that the SFI represented the main factors influencing fertility in the area.

4.2.8. Spatial distribution of soil fertility

The semivariogram analysis of the SFI in Bardarash revealed that the spherical model offered the best fit, with a nugget value of 0.0043, a sill of 0.0072, and a range of 14,603 metres (Table 4.4). Cambardella et al. (1994) calculated a spatial dependence (SD) ratio of 59.72%, indicating a moderate degree of geographical reliance. These findings indicate that soil fertility variability in the district is impacted by both intrinsic soil qualities and extrinsic environmental influences, which supports the use of geostatistical interpolation for fertility mapping.

The spatial distribution patterns derived from these models are presented in Figure 4.11, which provides a comparative visualization of fertility status across the

study area. Understanding such regional variation is essential for effective land management and sustainable agricultural practices.

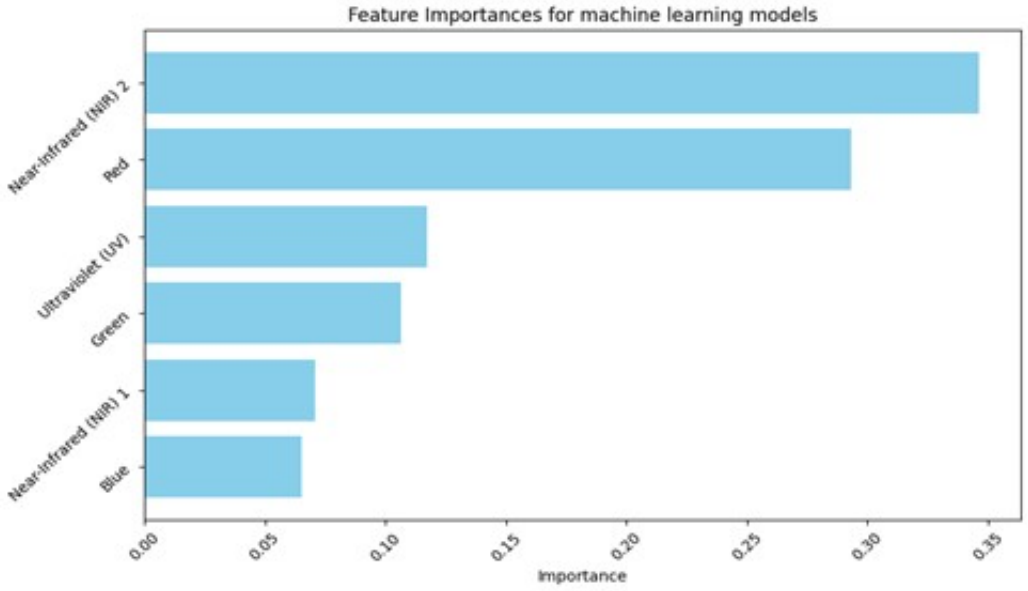

Figure 4.23. Feature importance of soil properties in predicting SFI using machine learning models (RF and GBR) in Bardarash district

Based on semivariogram modeling and geographic autocorrelation, OK generated fertility estimates using sill, nugget, and range parameters, as shown in Table 4.4.

Table 4.8. Semivariogram parameters of SFI in Bardarash district

Soil properties	Model	Nugget	Sill	Range	SD %
SFI	spherical	0.0043	0.0072	14603	59.72

Two important machine learning algorithms were uesd to predict SFI based on the spectroradiometers wavelength. The models consistently identified the Blue, Green, Ultralight, Red, NIR1, and NIR2 bands as the most important predictors of SFI. This suggests that both the visible and near-infrared parts of the spectrum include significant information about soil fertility fluctuations, allowing for the effective application of spectroradiometer and remote sensing indices in precision soil evaluation.

There are noticeable variations between models in the fertility categorization

results (Table 4.5). OK classified fertility as very low at 520 km2 (45.5%), low at 497 km² (43.5%), and moderate at 125 km2 (10.09%). 316 km2 (27.68%), 738 km2 (64.69%), and 87 km² (7.36%) were classified as moderate, low, and extremely low by RF. The GBR forecasted 285 km2 (24.97%) as moderate, 787 km2 (68.97%) as low, and 69 km2 (6.05%) as very low. The region is dominated by low fertility (68–70%) across all models, however GBR and RF showed more pockets of intermediate fertility than OK.

Table 4.9. Fertility classes resulted from geostatistical models used in Bardarash district

Model	**Very low fertility**		**Low fertility**		**Moderate fertility**	
	Area (km^2)	**%**	**Area (km^2)**	**%**	**Area (km^2)**	**%**
OK	520	45.5	497	43.5	125	10.09
RF	87	7.36	738	64.69	316	27.68
GBR	69	6.04	787	68.97	285	24.97

Additionally, there were differences in the spatial patterns: OK created smoother transitions between fertility zones, with low fertility in the southwest and moderate fertility in the north. GBR produced balanced maps that caught both subtle heterogeneity and seamless transitions, whereas RF produced more fragmented zones with clear borders and fine-scale detail as showed in Figure 4.12.

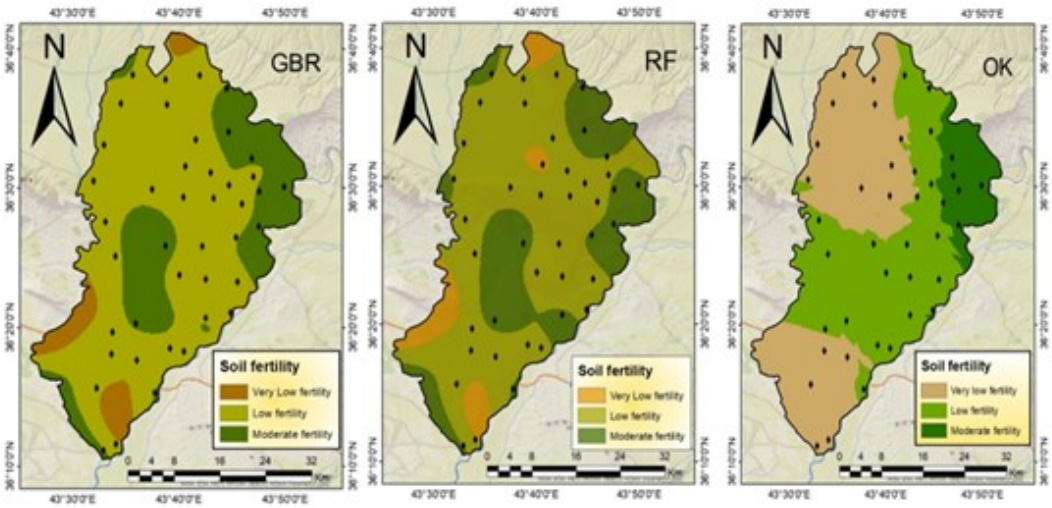

Figure 4.24. Spatial distribution of soil fertility in Bardarash district, predicted by GBR, RF, and OK in Bardarash district

4.2.9. Accuracy assessment of spatial distribution models of soil fertility

The predictive performance of Ordinary Kriging (OK), Random Forest (RF), and Gradient Boosting Regression (GBR) was compared using MAE, MSE, RMSE, and R2 (Table 4.6).

Table 4.10. Error metrics of OK, RF, and GBR in Bardarash district

Model	MAE	MSE	RMSE	R^2
Ordinary kriging (OK)	0.0428	0.0025	0.0505	0.22
Random forest (RF)	0.0184	0.0005	0.0228	0.83
Gradient boosting regression (GBR)	0.0075	0.0001	0.0087	0.97

With an R^2 value of 0.22, the OK model performed the worst, explaining only 22% of the variation in soil fertility (Isaaks and Srivastava, 1989). Greater differences between actual and anticipated values were corroborated by its higher RMSE (0.0505) and MAE (0.0428). In comparison, the RF model performed noticeably better. It explained 83% of the variation with an R^2 value of 0.83, although reduced prediction errors were suggested by MAE (0.0184) and RMSE (0.0228) values (Breiman, 2001). Both OK and RF performed worse than the GBR model. Its MAE (0.0075) and RMSE (0.0087) values showed exceptionally low prediction errors, and its R^2 value of 0.97 explained 97% of the dataset variation

(Friedman, 2001). According to these findings, GBR predicts soil fertility in the study area with the highest accuracy (Figure 4.13).

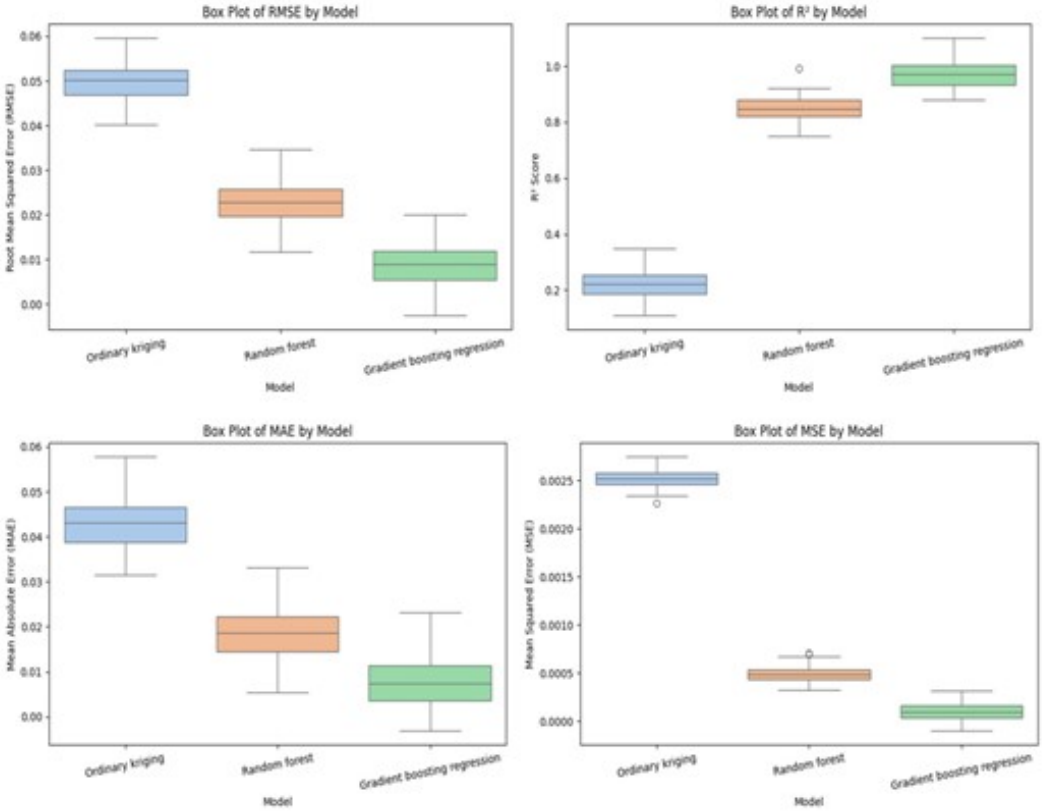

Figure 4.25. Error metrics (MAE, MSE, RMSE, and R2) for OK, RF, and GBR in Bardarash district

5. DISCUSSION

5.1. Bardarash district

5.1.1. Soil fertility status and key constraints

Soils in Bardarash have low OM, low Available P, high CaCO3 content, and moderate-to-poor CEC, according to laboratory tests. These constraints are common in semi-arid agroecosystems, where climate constraints and intense land use exacerbate soil deterioration. OM reduction is particularly distressing since OM is essential for nitrogen cycling, soil aggregation, and water retention (Lal, 2020). Continuous farming in Iraq without enough organic amendments has been shown to increase OM loss, lowering soil fertility and resilience (Al-Ansari et al., 2014). High $CaCO_3$ in calcareous soils stimulates P fixation, making it inaccessible to plants (Frossard et al., 2000; Havlin et al., 2010). Furthermore, poor CEC limits the soil's ability to absorb and exchange nutrients, reducing fertilizer efficiency (Brady and Weil, 2017). Collectively, these limits underscore the study region's precarious reproductive state and are consistent with studies from other dry locations, such as North Africa (Noumi et al., 2011) and South Asia (Khadka et al., 2018).

According to the classification proposed by Ryan et al. (2001) and Havlin et al. (2014), the N status in the study area varied from low to moderate, with a few locations showing relatively higher values. The mean concentration indicates a moderate level of nitrogen availability, suggesting that while the soils can generally support crop growth, supplemental nitrogen fertilization may still be required to maintain optimal productivity, especially in areas with lower N content.

According to general soil fertility classifications, all samples fall within the Low category of exchangeable calcium, which reflects a clear deficiency in available Ca for plant uptake. Such low levels may negatively affect the Ca/Mg and Ca/K ratios, leading to imbalances in nutrient uptake and possible physiological disorders in crops. The deficiency may result from leaching of Ca, low CEC, or dominance of Na^+ or H^+ ions in the exchange complex.

5.1.2. Weighting approaches for soil fertility index (SFI)

Assigning suitable weights to soil factors was crucial in developing a reliable SFI. In Bardarash, Principal Component Analysis (PCA) was used to objectively identify factors with the highest variance contribution, such as OM, CEC, and available N. This is consistent with previous research in which PCA was successfully

utilized to eliminate redundancy among linked soil parameters and emphasize fertility determinants (Andrews et al, 2004; Qi et al., 2009). The PCA technique guarantees that statistically dominating characteristics have a greater effect in the composite score, improving objectivity.

5.1.3. Spatial dependence and geostatistical analysis

The results of the semivariogram study showed a considerable geographical dependency (SD = 59.72%), indicating that both extrinsic (management techniques, fertilization, irrigation) and intrinsic (parent material, topography) elements influence the variability in soil parameters. In accordance with the agricultural history of the research area, where natural variability is layered on top of intensive farming, Cambardella et al. (1994) categorized moderate reliance as suggestive of mixed management.

The degree of unexplained variability is further reflected by the nugget-to-sill ratio, which may result from human influences, small-scale variation, or sample mistakes (Goovaerts, 1997). These results demonstrate how difficult it is to accurately represent variations in soil fertility in semi-arid environments using straightforward linear models.

5.1.4. Model performance: geostatistics vs machine learning

The performance of the prediction models was inconsistent. OK had poor predictive value (R2 = 0.22), despite being commonly employed in soil mapping. This subpar performance is probably due to its dependence on stationarity and linear assumptions, which are ineffective in heterogeneous soils affected by nonlinear interactions (Li and Heap, 2014).

On the other hand, RF used its capacity to manage complicated interactions and nonlinear correlations between variables to achieve outstanding accuracy (R2 = 0.83). When it comes to mapping soil properties, RF has been praised for outperforming linear models (Taghizadeh-Mehrjardi et al., 2016; Wiesmeier et al., 2011). But when there are too many irrelevant characteristics, RF can occasionally overfit.

GBR performed the best (R2 = 0.97, RMSE = 0.0087). GBR has an advantage in capturing fine-scale variability because of its iterative error-correction and residual optimization capabilities. Boosting algorithms often beat RF and conventional

geostatistics in digital soil mapping investigations, according to similar findings (Heung et al., 2016; Bhunia et al., 2022). Thus, the results confirm that machine learning, particularly boosting models, is more suitable for predicting SFI in heterogeneous soils than geostatistical methods alone.

5.1.5. Feature importance of spectral and soil data

The most important characteristics in predicting SFI were consistently found to be the Blue, Green, Red, Ultralight, NIR1, and NIR2 spectral bands by both RF and GBR. This is consistent with data showing that soil OM, texture, and moisture have a significant impact on visible and near-infrared wavelengths (Stenberg et al., 2010; Guerrero et al., 2016).

In particular, soil color and organic matter affect the visible bands (blue, green, and red), whereas NIR bands record vegetation indices, moisture content, and soil mineralogy (Mulder et al., 2011). The significant contribution of NIR1 and NIR2 implies that vegetation indices (e.g., NDVI) and VNIR spectroscopy offer vital information for evaluating fertility, facilitating the combination of field and lab data with remote sensing in precision soil management.

5.1.6. Spatial distribution of environmental characteristics and their effects on soil fertility

Through their effects on erosion, microclimate, and soil–water dynamics, the results validate that topographic factors—elevation, slope, and aspect—play a crucial role in determining soil fertility. While gentler slopes improve soil stability and agricultural compatibility, steeper slopes are more likely to experience erosion and nutrient losses. This supports new research by Amare et al. (2024) and Zhou et al. (2024), which showed that land use and slope location work together to regulate soil nutrient variability. In line with Duan et al. (2025), who found that slope exposure has a major impact on nutrient heterogeneity and vegetation regeneration, aspect also affects soil fertility, with north-facing slopes holding onto more moisture and nutrients. Similarly, convexity and elevation are important indicators of fine-scale soil fertility in forest ecosystems, as demonstrated by Rodrigues et al. (2021). All of these findings point to the necessity of including topographic characteristics into soil fertility mapping and management plans in order to produce more precise forecasts and sustainable land-use planning.

5.2. Semel disctrict

5.2.1. Soil fertility status and key constraints

The statistical investigation of soil attributes in the Semel region lays a solid foundation for understanding the geographical distribution of soil fertility. As a starting point, the statistical characteristics indicated high diversity among the major soil qualities. For example, the CV for Avail. P, Fe, and B was quite high, showing that the concentrations of these critical nutrients are not uniform and exhibit significant regional variation. This conclusion is congruent with the geostatistical concepts laid forth by Goovaerts (1997), who underlined that the spatial variability of soil nutrients frequently determines the necessity for precision agriculture. Similarly, the positive skewness for Avail. P and Exch. B indicate a leptokurtic distribution, with most samples having low amounts of these nutrients but a few isolated hot spots with high levels. This supports the visual patterns on the soil fertility map, which reveal a predominance of low-fertility areas interspersed with a few pockets of intermediate fertility. This sort of distribution is frequently caused by localized variables like as focused fertilizer application or specialized micro-environmental conditions that promote nutrient retention.

5.2.2. Spatial distribution of soil fertility

The geographical distribution of soil fertility, as illustrated in the map and backed by quantitative data, identifies a key problem for regional agricultural output. The Low and Very low fertility classes account for almost 58% of the research area (443.07 km2 and 98.09 km2, respectively). The widespread presence of nutrient-deficient soils shows that factors contributing to soil deterioration, such as geological limits, unsustainable land use practices, and erosion, have a dominant effect. The substantial proportion of low-fertility soils needs a thorough and focused strategy to soil management and conservation to prevent further deterioration and improve long-term production.

5.2.3. Weighting approaches for soil fertility index (SFI)

To simulate this complicated system, the researchers used a strong, integrated framework. The weighting of soil factors using the AHP-Fuzzy model, for example, prioritized OM, CEC, and N. This hierarchical weighting is based on recognized soil research, which identifies these measures as key markers of soil health (Brady and Weil, 2008). This method ensures that the next machine learning model is trained on a scientifically weighted representation of soil health, rather than a simple arithmetic average. The effectiveness of AHP-Fuzzy models in resolving the inherent ambiguity

of expert opinion in environmental decision-making is demonstrated in literature, which supports the successful implementation of this technique (Mikhailov and Tsvetinov, 2004). Multi-criteria decision analysis (MCDA), a critical component of contemporary pedometric research, is made apparent and defensible by this method's methodical conversion of qualitative expert opinions into a quantitative, hierarchical structure.

5.2.4. Super vector machine performace in Semel region

The SVM model's excellent predictive capacity, as demonstrated by an amazing accuracy of 0.9811, is a major result that is consistent with recent advances in digital soil mapping. This performance is similar with the findings of Taghizadeh-Mehrjardi et al. (2020), who showed that when machine learning algorithms are applied to a mix of environmental variables and soil data, they may achieve exceptional success in soil property mapping. Our SVM model's improved performance can be ascribed to the integrated study's methodological rigor. The model was able to make use of a large, complex dataset by mixing in-situ physicochemical soil parameters with broad-scale Sentinel 2 derived spectral indices. The spectral indices, which reflect the geographical variability of plant cover and soil conditions, offered important contextual information to supplement the discrete point data from the soil samples. This synergy enabled the model to successfully understand the complicated, nonlinear interactions that influence soil fertility across the terrain.

5.2.5. Explainable artificial intelligence (XAI)

The ensuing SHAP analysis gave critical insights into the model's decision-making process, revealing that silt content and remote sensing indices such as BSI and GNDVI were the most influential predictors of soil fertility. This conclusion emphasizes the importance of physical soil composition and remote sensing in capturing the geographical variability of fertility, as evidenced by research linking these indices to soil deterioration and plant health (Gitelson et al., 1996; Al-Ghobari and Mohammad, 2021). Conversely, the low effect of parameters such as bulk density and NDVI, which are routinely employed in soil research, implies that their significance in this specific SVM model is less relevant given the study area's unique characteristics.This finding highlights the value of Explainable AI in moving beyond a generic understanding of soil science and toward a site-specific, data-driven identification of the most dominant predictors.

A significant percentage of the land (41.72% or 387.44 km2) has Moderate fertility, providing a crucial possibility for sustained agricultural growth. These places may benefit from favorable local conditions, implying that focused actions based on the models projections might result in large productivity gains. For example, the substantial contribution of Exch. Cu to the SHAP analysis shows a particular environmental stressor, presumably caused by anthropogenic activities, necessitating site-specific mitigating measures. The LIME study improves on this by offering granular-level interpretability, allowing land managers to grasp the specific mix of elements (e.g., high EC and low OM) causing poor fertility at a given place, allowing for precise, data-driven remedial measures. This capability converts the abstract prediction model into a usable decision-support tool. By providing a clear justification for each forecast, LIME builds stakeholder trust and encourages the adoption of precision agricultural methods, bridging the gap between complicated computer models and on-the-ground decisions.

Finally, this study's integrated method, which combines statistical analysis, an AHP-Fuzzy weighting model, and an SVM-based classification with explainable AI, provides a reliable and scientifically sound framework for measuring soil fertility. The findings highlight the crucial need to address widespread low fertility while also proactively managing and safeguarding communities with intermediate fertility. This technique provides a strong, accurate, and cost-effective decision-support tool to guide sustainable land management, promote food security, and assure long-term agricultural sustainability in the Semel region.

6. CONCLUSION

The exhaustive evaluation of soil fertility in the Bardarash and Semel districts indicates that the majority of the examined regions are marked by a deplorable fertility status, with over half of the land classified as low to extremely low fertility. The availability of nutrients and the productivity of crops are collectively restricted by critical limiting factors, which include high calcium carbonate (CaCO3) content and low levels of available phosphorus (P) and organic matter (OM). The comprehension of soil fertility dynamics was substantially improved by the implementation of advanced modeling techniques. In Bardarash, the superiority of machine learning in capturing intricate spatial variability was demonstrated by Gradient Boosting Regression ($R2 = 0.91$) and Random Forest ($R2 = 0.83$), which outperformed traditional Ordinary Kriging ($R2 = 0.22$). The integration of Sentinel-2 indicators, Fuzzy-AHP weighting, and explainable AI tools (SHAP and LIME) in Semel resulted in high predictive accuracy (98%) and interpretability, with sediment content, BSI, GNDVI, and exchangeable copper (Cu) being the most influential factors.

While simultaneously emphasizing the potential of precision agriculture in moderately fertile zones, these results underscore the pressing necessity for targeted soil management interventions, including phosphorus fertilization, erosion control, and organic matter enrichment. The study is significant in that it establishes a data-driven, robust framework that integrates sophisticated geospatial and machine learning techniques with traditional soil analysis. This paradigm not only enhances the scientific integrity of digital soil fertility mapping but also provides practical advice for sustainable land management and agricultural decision-making in semi-arid regional areas. In order to improve fertility mapping and guarantee food security in the face of evolving environmental conditions, future research should expand this framework to encompass broader landscapes and integrate emerging datasets (e.g., hyperspectral and LiDAR).

7. RECOMMENDATIONS

The following scientific and practical recommendations are suggested to improve soil fertility and guarantee sustainable land management in semi-arid regions, as supported by the results of the Bardarash and Semel districts studies:

Soil Organic Matter (OM) Improvement: Encourage the incorporation of crop residues, as well as the use of organic amendments such as farmyard manure, compost, and cover crops, to increase soil organic carbon, improve soil structure, and improve water-holding capacity.

Microbial Activity Stimulation: In order to preserve soil integrity and encourage beneficial microbial populations, implement conservation tillage practices. Furthermore, to enhance soil health and nutrient cycling, implement biofertilizers and microbial inoculants, including Rhizobium and mycorrhizal fungi.

Optimized Nutrient Management: Use organic and slow-release fertilizers to reduce nutrient losses and enhance nutrient-use efficiency. Frequent soil testing programs should be implemented to ensure that fertilizer applications are calibrated to the actual soil need.

Fertilization Strategies Specific to the Site: Utilize precision fertilization methods that are informed by detailed soil fertility zoning maps to optimize crop productivity and ensure efficient nutrient allocation.

Sustainable Land Management Practices: Promote the use of rotational grazing, intercropping, and agroforestry systems to promote biodiversity, reduce erosion, and improve nutrient recycling. Apply contour cultivation and terracing in sloping areas to reduce soil erosion.

Precision Agriculture Technologies Adoption: Adopt user-friendly decision support systems (DSS) that integrate remote sensing, GIS, and machine learning tools. Encourage the development of mobile platforms that enable producers to access soil fertility maps and make data-driven management decisions.

Institutional Support and Capacity Building: Offer financial assistance and incentives from the government to promote the implementation of sustainable practices and contemporary technologies. Organize specialized training programs to

enhance the capabilities of agricultural stakeholders and producers.

Foster partnerships among agricultural extension services, research institutions, and producers in order to enhance collaboration and knowledge exchange. Establish farmer field schools (FFS) as practical platforms for the transmission of technology and the exchange of knowledge.

Monitoring and Evaluation Framework: Establish continuous monitoring systems that utilize remote sensing and field surveys to assess the efficacy of land management and soil fertility practices, thereby guaranteeing adaptive management over time.

Macronutrients and Micronutrients: Integrated nutrient management strategies are strongly advised for both macronutrients and micronutrients in order to address the nutrient deficiencies identified in the soils under investigation. Macronutrients; The insufficient levels of avail. N and P necessitate balanced fertilization that incorporates both organic and inorganic sources. Depending on the crops needs, the application of triple superphosphate or DAP (100-150 kg P2O5 ha-1) and urea or ammonium nitrate (150-200 kg N ha-1) is recommended. K and Mg were determined to be within acceptable limits; consequently, maintenance dosages are required. Gypsum (CaSO4·2H2O) or agricultural lime should be applied at a rate of 1-2 t ha-1 to improve the Ca2+ exchange pool and preserve ionic balance (Ca:Mg and Ca:K ratios) due to the low exchangeable calcium content despite the high $CaCO_3$ levels. Micronutrients; The correction of Fe deficiencies and marginal levels of Mn and Zn can be achieved by applying Fe-EDDHA, MnSO4, and ZnSO4 through foliar application during the early growth stages. The levels of Cu and B were satisfactory; however, they should be periodically monitored to prevent imbalances or toxicity. The integration of micronutrient foliar coatings, biofertilizers, and organic matter will enhance plant uptake efficiency, improve nutrient availability, and sustain soil fertility in the semi-arid conditions of the Bardarash and Semel districts.

Land Use and Crop Suitability Suggestions: According to the comprehensive soil fertility assessment, which includes moderate organic matter, slightly alkaline pH, nonsaline conditions, and moderate cation exchange capacity, the soils of Bardarash and Semel are moderately fruitful and suitable for a variety of agricultural endeavors. Wheat and barley are cereal crops that are extremely suitable for cultivation due to their ability to tolerate slightly alkaline and calcareous conditions. Fruit trees, such as the apple, grape, and pomegranate, can thrive; however, they

necessitate appropriate management of Ca, Fe, and Zn to prevent nutrient-related disorders, including fruit shattering and chlorosis. N and P fertilizers, in conjunction with calcium supplementation, can be used to cultivate vegetable crops (eggplant, onion, and tomato). The current fertility status renders legume crops (lentil, chickpea, and faba bean) less appropriate due to their low phosphorus and organic matter contents. However, their insertion into the rotation is advised to enhance nitrogen fixation and soil structure over time. The semi-arid agro-ecosystems of Duhok Province will be optimized in terms of productivity, nutrient efficiency, and sustainable land use by aligning crop selection with soil fertility classes and instituting site-specific fertilization.

Summary of General Soil Recommendations

Effective soil fertility management requires an integrated approach that combines physical, chemical, and biological interventions. Key practices include enriching the soil with OM, alleviating compaction through gypsum application, and addressing macro- and micronutrient deficiencies using tailored fertilization strategies. Managing high soil pH through sulfur amendments and organic acids further enhances nutrient availability.

Additionally, implementing efficient irrigation systems helps maintain soil moisture balance and supports optimal plant performance. These practices are essential for sustaining long-term soil productivity and ensuring the success of diverse cropping systems across various soil types.

REFERENCES

Adhikari, K., Kheir, R. B., Greve, M. B., Bocher, P. K., Malone, B. P., Minasny, B., ... and Greve, M. H., 2013. High-resolution 3-D mapping of soil texture in Denmark. Soil Science Society of America Journal, 77(3), 860-876.

Akpa, S. I., Odeh, I. O., Bishop, T. F., and Hartemink, A. E., 2014. Digital mapping of soil particle-size fractions for Nigeria. Soil Science Society of America Journal, 78(6), 1953-1966.

Al Alwani, A. A. M. and Al-Shaye, O. N. A., 2019. Studying the fertility status of the soil in some areas of agricultural expansion within western desert from Iraq. Plant Arch, 19, 2343-2350.

Al-Ghobari, H., and Mohammad, A., 2021. Developing a remote sensing-based index for the assessment of land degradation. Sustainability, 13(15), 8443.

Al-Kaysi, S., 1989. Effect of wetting-drying cycles of soils on carbonate and phosphorus adsorption. Physical and Chemical Properties of Carbonate. In 5th Scientific Conference Research Council (Baghdad, Iraq) (Vol. 1, No. 2, pp. 29-36).

Allison, L., 1965. Organic carbon. Methods of soil analysis: Part 2 Chemical and microbiological properties, 9, pp.1367-1378.

Alloway, B. J., 2008. Micronutrients and crop production: An introduction. In Micronutrient deficiencies in global crop production (pp. 1-39). Dordrecht: Springer Netherlands.

Alsafran, M., Usman, K., Ahmed, B., Rizwan, M., Saleem, M. H. and Al Jabri, H., 2022. Understanding the phytoremediation mechanisms of potentially toxic elements: A proteomic overview of recent advances. Frontiers in Plant Science, 13, 881242.

Alwis, L., Sun, T. and Grattan, K. T. V., 2013. Optical fibre-based sensor technology for humidity and moisture measurement: Review of recent progress. Measurement, 46(10), pp.4052-4074.

Amara, D. M. K., Patil, P. L., Kamara, A. M. and Saidu, D. H., 2017. Assessment of soil fertility status using nutrient index approach. Academia Journal of Agricultural Research, 5(2), 28-38.

Amare, H., Admase, H. and Ewunetu, T., 2024. Influence of land-use types and topographic slopes on the physico-chemical characteristics of soils in Northwestern Ethiopia. Frontiers in Soil Science, 4, 1463315.

Andrews, S. S., Karlen, D. L. and Cambardella, C. A., 2004. The soil management assessment framework: a quantitative soil quality evaluation method. Soil Science Society of America Journal, 68(6), 1945-1962.

Arshad, M. A., Lowery, B. and Grossman, B., 1997. Physical tests for monitoring soil quality. Methods for assessing soil quality, 49, 123-141.

Arvidsson, J., 1999. Nutrient uptake and growth of barley as affected by soil

compaction. Plant and Soil, 208, 9-19.

Askari, M. S. and Holden, N. M., 2015. Quantitative soil quality indexing of temperate arable management systems. Soil and Tillage Research, 150, 57-67.

Bao, H., Lann, T., Ao, X., Yang, L., Lan, H. and Peng, J., 2024. Evolution characteristic of soil water in loess slopes with different slope angles. Geoenvironmental Disasters, 11(1), 43.

Bationo, A., Kihara, J., Vanlauwe, B., Waswa, B. and Kimetu, J., 2007. Soil organic carbon dynamics, functions and management in West African agro-ecosystems. Agricultural Systems, 94(1), 13-25.

Bear, F. E., 1977. Soil in relation to crop growth. Robert E Krieger. 2nd ed. Oxford and IHB Publishing Corporation. New Delhi. 514 pp.

Bekele, A. and Hudnall, W. H., 2006. Spatial variability of soil chemical properties of a prairie–forest transition in Louisiana. Plant and Soil, 280, 7-21.

Belay, A. M., Selassie, Y. G., Tsegaye, E. A. and Meshesha, D. T., 2025. Comparison of laboratory methods for predicting soil lime requirements of Luvisol in Dera district, the Northwestern highlands of Ethiopia. Tropical Agriculture, 102(1), 105-123.

Bewket, W. and Stroosnijder, L., 2003. Effects of agroecological land use succession on soil properties in Chemoga watershed, Blue Nile basin, Ethiopia. Geoderma, 111(1-2), 85-98.

Bharat, S., Singh, S., Ak, S., Shrivas, N. T. R. and Pawar, S., 2017. Study of wheat crop growth and productivity monitoring for Hoshangabad district in MP using geospatial technology. Bull. Env. Pharmacol. Life Sci, 3153-3157.

Bishop, C. M., 2006. Pattern recognition and machine learning. Springer.

Black, C. A., 1965. Methods of soil analysis. Madison, Wisconsin, USA: Part I, American Society of Agronomy. 157 p.

Bockheim, J. G. and Hartemink, A. E., 2013. Distribution and classification of soils with clay-enriched horizons in the USA. Geoderma, 209, 153-160.

Bolt, G. H., Bruggenwert, M. G. M. and Kamphorst, A., 1976. Adsorption of cations by soil. In Developments in Soil Science (Vol. 5, pp. 54-90). Elsevier.

Bould, C. and Hewitt, E. J., 1963. Mineral nutrition of plants in soils and in culture media. In Inorganic Nutrition of Plants (pp. 15-133). Academic Press.

Bouyoucos, G. J., 1962. Hydrometer method improved for making particle size analyses of soils. Agronomy Journal, 54(5), 464–465.

Brady, N. C., and Weil, R. R., 2017. The nature and properties of soils, 15th edition (eBook).

Brady, N. C., 1984. The nature and properties of soils. 9th Edition. Macmillan Publishing Company New York. 750 p.

Brady, N. C. and Weil, R. R., 2008. The nature and properties of soils (Vol. 13, pp.

662-710). Upper Saddle River, NJ: Prentice Hall.

Bremner, J. M., 1965. Total nitrogen. Methods of soil analysis: Part 2 Chemical and microbiological properties, 9, pp.1149-1178.

Bundy, L. G., and Meisinger, J. J., 1994. Nitrogen availability indices. Methods of soil analysis: Part 2 Microbiological and biochemical properties, 5, 951-984.

Burgess, T. M. and Webster, R., 1980. Optimal criterion for intermediate point prediction of a regionalized variable. Geoderma, 24(1), 1-14.

Burstrom, H. G., 1968. Calcium and plant growth. Biological Reviews, 43(3), 287-316.

Cambardella, C. A. and Karlen, D. L., 1999. Spatial analysis of soil fertility parameters. Precision Agriculture, 1(1), pp.5-14.

Chang, D. Y., 1996. Applications of the extent analysis method on fuzzy AHP. European Journal of Operational Research, 95(3), 649-655.

Chaudhari, P. R., Ahire, D. V., Ahire, V. D., Chkravarty, M., and Maity, S., 2013. Soil bulk density as related to soil texture, organic matter content and available total nutrients of Coimbatore soil. International Journal of Scientific and Research Publications, 3(2), 1-8.

Clevers, J. G., Kooistra, L. and Schaepman, M. E., 2008. Using spectral information from the NIR water absorption features for the retrieval of canopy water content. International Journal of Applied Earth Observation and Geoinformation, 10(3), pp.388-397.

Cohen, J., 1960. A coefficient of agreement for nominal scales. Educational and Psychological Measurement, 20(1), 37-46.

Cortes, C., and Vapnik, V., 1995. Support-vector networks. Machine Learning, 20(3), 273-297.

Corwin, D. L. and Lesch, S. M., 2005a. Apparent soil electrical conductivity measurements in agriculture. Computers and Electronics in Agriculture, 46(1-3), 11-43.

Corwin, D. L., Kaffka, S. R., Hopmans, J. W., Mori, Y., Lesch, S. M. and Oster, J. D., 2003. Assessment and field-scale mapping of soil quality properties of a saline-sodic soil. Geoderma, 114(3–4), 231–259.

Corwin, D. L. and Lesch, S. M., 2003. Application of soil electrical conductivity to precision agriculture: theory, principles, and guidelines. Agronomy Journal, 95(3), 455-471.

Corwin, D. L. and Lesch, S. M., 2005b. Characterizing soil spatial variability with apparent soil electrical conductivity: I. Survey protocols. Computers and Electronics in Agriculture, 46(1-3), 103-133.

Counties, S., 2010. Primary plant nutrients: Nitrogen, phosphorus and potassium. Ucanr.edu, 3, 4-6.

Craig, R. F., 2004. Craig's soil mechanics. Craig's soil mechanics (7th ed.). CRC Press.

Cressie, N., 2015. Statistics for spatial data. John Wiley & Sons.

Cui, S., Zhu, P., Liu, P. and Geng, X., 2023. Effects of soil particle structure on the distribution and transport of soil water and salt. Water, 15(15), 2842.

Das, B. M. and Sobhan, K., 1990. Principles of geotechnical engineering.

Day, P. R., 1965. Particle fractionation and particle-size analysis. Methods of Soil Analysis: Part 1 Physical and Mineralogical Properties, Including Statistics of Measurement and Sampling, 9, pp.545-567.

Demšar, U., Harris, P., Brunsdon, C., Fotheringham, A. S. and McLoone, S., 2013. Principal component analysis on spatial data: an overview. Annals of the Association of American Geographers, 103(1), 106-128.

Desalegn Eshetu, M., 2021. Soil fertility status and nutrients content in maize (Zea mays L.) tissue at Migna Kura in Wayu Tuka district, East Wollega, Ethiopia (Doctoral dissertation, Haramaya University).

Dhanve, S. S., Mane, S. S. and Deshmukh, G. B., 2018. Assessment of soil fertility status of Agricultural Research Station, Badnapur, India. International Journal of Current Microbiology and Applied Sciences, Special Issue-6, pp.2424-2429.

Diaz-Zorita, M., Grove, J. H. and Munoz, A., 2002. Soil properties and crop yield relationships in a Typic Argiudoll of the Rolling Pampas. Soil Science Society of America Journal, 66(2), 525-531.

Dijkstra, F. A., Van Breemen, N., Jongmans, A. G., Davies, G. R., and Likens, G. E., 2003. Calcium weathering in forested soils and the effect of different tree species. Biogeochemistry, 62(3), 253-275.

Dobermann, A., Bruulsema, T., Cakmak, I., Gerard, B., Majumdar, K., McLaughlin, M., ... and Zhang, X., 2022. Responsible plant nutrition: A new paradigm to support food system transformation. Global Food Security, 33, 100636.

Dor, E. B., Chabrillat, S., Karyotis, K., and Schmid, T., 2024. P4005 Standards and protocols for soil spectroscopy in laboratory and field conditions [Technical committees]. IEEE Geoscience and Remote Sensing Magazine, 12(4), 358-363.

Duan, W., Duan, J., Qu, M., Wang, Y., Zhu, S., Wang, H. and Mu, M., 2025. The influence of slope aspect on the spatial heterogeneity of soil nutrients and seedling regeneration in Pinus sylvestris var. mongolica plantation forests. Forests, 16(7), 1100.

Enakiev, Y. I., Bahitova, A. R., and Lapushkin, V. M., 2018. Microelements (Cu, Mo, Zn, Mn, Fe) in corn grain according to their availability in the fallow sod-podzolic soil profile.

FAO, 1980. Soil testing and plant analysis. Bull. No. 38/1, Food and Agriculture

Organization, Rome, Italy.

FAO, 2017. The state of food security and nutrition in the world 2017. http://www.fao.org/3/a-I7695e.pdf

Fattah, S. A. and Fayyadh, M. A., 2019. Comparison of some soil quality indicators of forest soils under two different tree species. Journal of Duhok University, 22(2), pp.133-146.

Fayyadh, M. A., and Ismail, H. K., 2021. Genesis, development, and classification for some selected soils at Kurdistan Region, north of Iraq. Iraqi Journal of Agricultural Sciences, 52(6), 1498-1507.

Fayyadh, M. A., and Rekani, S. A. F., 2022. Distribution path of total and active carbonates, and iron oxides under two different forest tree species. In IOP Conference Series: Earth and Environmental Science (Vol. 1120, No. 1, p. 012038). IOP Publishing.

Flores-Magdaleno, H., Mancilla-Villa, O. R., Mejia-Saenz, E., Olmedo-Bolanos, M. C. and Bautista-Olivas, A. L., 2011. Heavy metals in agricultural soils and irrigation wastewater of Mixquiahuala, Hidalgo, Mexico. African Journal of Agricultural Research, 6(24), 5505-5511.

Follett, R. H. and Lindsay, W. L., 1971. Changes in DTPA-extractable zinc, iron, manganese, and copper in soils following fertilization. Soil Science Society of America Journal, 35(4), 600-602.

Foth, H. D., 1991. Fundamentals of soil science (No. Ed. 8). New York: John Wiley and Sons, Inc., 360 pp.

Foth, H. D. and Ellis, B. G., 1997. Soil fertility. 2nd Ed. CRC Press, Boca Raton, Florida. 290 p.

Friedman, S. P., 2005. Soil properties influencing apparent electrical conductivity: a review. Computers and Electronics in Agriculture, 46(1-3), 45-70.

Gardner, W. H., 1986. Water content. Methods of soil analysis: Part 1 Physical and mineralogical methods, 5, 493-544.

Gaskin, G. J. and Miller, J. D., 1996. Measurement of soil water content using a simplified impedance measuring technique. Journal of Agricultural Engineering Research, 63(2), pp.153-159.

Gessler, P. E., McKenzie, N. J. and Hutchinson, M. F., 1996. Progress in soil-landscape modeling and spatial prediction of soil attributes for environmental models. In Proceedings of the Third International Conference/Workshop on Integrating GIS and Environmental Modeling, Santa Barbara, CA (pp. 21-26). January. National Center for Geographic Information and Analysis Sante Fe, NM.

Gitelson, A. A., Kaufman, Y. J., and Merzlyak, M. N., 1996. Use of a new vegetation index for remote sensing of terrestrial vegetation from satellite observations. Remote Sensing of Environment, 58(3), 289-299.

Gokmen, V., Surucu, A., Budak, M. and Bilgili, A. V., 2023. Modeling and mapping the spatial variability of soil micronutrients in the Tigris basin. Journal of King Saud University-Science, 35(6), 102724.

Goovaerts, P., 1998. Geostatistical tools for characterizing the spatial variability of microbiological and physico-chemical soil properties. Biology and Fertility of Soils, 27, 315-334.

Goovaerts, P., 1997. Geostatistics for natural resources evaluation. Oxford University Press.

Gransee, A. and Fuhrs, H., 2013. Magnesium mobility in soils as a challenge for soil and plant analysis, magnesium fertilization and root uptake under adverse growth conditions. Plant and Soil, 368, 5-21.

Greenland, D. J. and Mott, C. J. B., 1978. Surfaces of soil particles. In The Chemistry of Soil Constituents (eds D. J. Greenland and M. H. B. Hayes), pp. 321-353. Chichester: John Wiley and Sons.

Grimme, H., 1991. Magnesium in landwirtschaftlichen und forstlichen Ökosystemen. KALI Briefe, 20.

Grossl, P. R. and Inskeep, W. P., 1991. Precipitation of dicalcium phosphate dihydrate in the presence of organic acids. Soil Science Society of America Journal, 55(3), 670-675.

Gurav, P. P., Datta, S. C., Ray, S. K., Choudhari, P. L. and Ahmed, N., 2018. Assessment of potassium release threshold levels of Vertisols (shrink-swell soils) in different agro-ecological regions of India. Applied Clay Science, 165, 155-163.

Habib, H., 2006. Pedological study of soil topsequence in Jabal Alarab Sowaida Governorate. Damascus University Journal of the Agricultural Sciences (Syria), (1).

Hao, Y., Yang, Y., Liu, B., Liu, Y., Gao, X. and Guo, Q., 2016. Size characteristics of sediments eroded from three soils in China under natural rainfall. Journal of Soils and Sediments, 16(8), 2153-2160.

Hasanuzzaman, M., Bhuyan, M. B., Nahar, K., Hossain, M. S., Mahmud, J. A., Hossen, M. S. and Fujita, M., 2018. Potassium: A vital regulator of plant responses and tolerance to abiotic stresses. Agronomy, 8(3), 31.

Hassan, H. A., and Al-Barzinji, Y. M., 2022. Genesis and development of Vertisols in Selivany plain at Duhok Governorate, Kurdistan Region, Iraq. ResearchGate.

Hassink, J., 1997. The capacity of soils to preserve organic C and N by their association with clay and silt particles. Plant and Soil, 191, 77-87.

Havlin, J. L., Beaton, J. D., Tisdale, S. L. and Nelson, W. L., 2010. Soil fertility and fertilizers - An introduction to nutrient management. 7th edition. PHI Learning Private Limited, New Delhi, India. 516 p.

Heung, B., Zhang, J., Ho, H. C., and Zhang, J., 2016. Machine learning approaches for predicting soil nutrient contents based on satellite imagery. Geoderma, 266, 16-27.

Hillel, D., 2012. Soil and water: physical principles and processes. Elsevier.

Hillel, D. and Hatfield, J. L., 2005. Encyclopedia of soils in the environment (Vol. 3). Amsterdam, The Netherlands: Elsevier.

Hudson, B. D., 1994. Soil organic matter and available water capacity. Journal of Soil and Water Conservation, 49(2), 189-194.

Hunt, N. and Gilkes, R., 1992. Farm monitoring handbook – a practical down-to-earth manual for farmers and other land users. University of Western Australia: Nedlands, WA, and Land Management Society: Como, WA.

Isaboke, J., Osano, O., Humphrey, O. S., Dowell, S. M., Njoroge, R. and Watts, M. J., 2025. Influence of agricultural land use management on soil particle size distribution and nutrient adsorption in Western Kenya. Chemistry Africa, 8(4), 1599-1610.

Jackson, M. L., 1973. Soil chemical analysis. Prentice Hall of India Pvt. Ltd., New Delhi, India, 498, pp.151-154.

Jackson, T., Mansfield, K., Saafi, M., Colman, T. and Romine, P., 2008. Measuring soil temperature and moisture using wireless MEMS sensors. Measurement, 41(4), pp.381-390.

Jensen, H. L. and Lamm, C. G., 1961. On the zinc content of Danish soils. Acta Agriculturae Scandinavica, 11(1), 63-71.

Johan, P. D., Ahmed, O. H., Omar, L. and Hasbullah, N. A., 2021. Phosphorus transformation in soils following co-application of charcoal and wood ash. Agronomy, 11(10), 2010.

Johnson, G. V., and Fixen, P. E., 1990. Testing soils for sulfur, boron, molybdenum, and chlorine. Soil testing and plant analysis, 3, 265-273.

Jolliffe, I., 2011. Principal component analysis. In International Encyclopedia of Statistical Science (pp. 1094-1096). Springer, Berlin, Heidelberg.

Jones, C. and Jacobsen, J., 2009. Micronutrients: cycling, testing and fertilizer recommendations. Nutrient Management Module, 7, 2-4.

Jones, C. and Jacobsen, J., 2005. Plant nutrition and soil fertility. Nutrient Management Module, 2(11), 1-11.

Joshi, V. D., Palei, N. N. and Rachh, P. R., 2009. Physico-chemical properties of four farm site soils in area surrounding Rajkot, Gujarat, India. International Journal of ChemTech Research, 1(3), 709-713.

Kahraman, C., Cebeci, U., and Ulukan, Z., 2003. Multi-criteria supplier selection using fuzzy AHP. Logistics Information Management, 16(6), 382-394.

Kanwar, J. S., 2000. Soil and water resource management for sustainable agriculture

imperatives for India. In International Conference on Managing Natural Resources for Sustainable Agricultural Production in the 21st Century, invited papers (pp. 14-18).

Karlen, D. L., Mausbach, M. J., Doran, J. W., and Franzluebbers, R. M., 2003. Soil quality: A concept, a framework, and an example. In Soil and water conservation for productivity and environmental protection (pp. 391-412). CRC Press.

Kavitha, C. and Sujatha, M. P., 2015. Evaluation of soil fertility status in various agro ecosystems of Thrissur District, Kerala, India. International Journal of Agriculture and Crop Sciences (IJACS), 8(3), 328-338.

Keeney, D. R., 1982. Nitrogen—availability indices. Methods of soil analysis: Part 2 Chemical and Microbiological Properties, 9, pp.711-733.

Kerry, R. and Oliver, M. A., 2007. The analysis of ranked observations of soil structure using indicator geostatistics. Geoderma, 140(4), 397-416.

Khadka, D., Lamichhane, S., Bhantana, P., Ansari, A. R., Joshi, S. and Baruwal, P., 2018b. Soil fertility assessment and mapping of Chungbang farm, Pakhribas, Dhankuta, Nepal. Advances in Plants & Agriculture Research, 8(3), 219-227.

Khadka, D., Lamichhane, S., Bhurer, K. P., Chaudhary, J. N., Ali, M. F. and Lakhe, L., 2018a. Soil fertility assessment and mapping of regional agricultural research station, Parwanipur, Bara, Nepal. Journal of Nepal Agricultural Research Council, 4, 33-47.

Khudher, S. A., and Alkhaled, K. A., 2024. Study of some fertility characteristics of soils with different agricultural uses in the Aqra Region/Duhok. World Journal of Advanced Research and Reviews, 21(2), 301-312.

Kiekens, L., 1995. Zinc. In Alloway, B. J. (ed.) Heavy Metals in Soils (2nd edn.). Blackie Academic and Professional, London, pp. 284-305.

Kokaly, R. F., Clark, R. N., Swayze, G. A., Livo, K. E., Hoefen, T. M., Pearson, N. C., ... and Klein, A. J., 2017. USGS spectral library version 7 (No. 1035). US Geological Survey.

Krauskopf, K. B., 1972. Geochemistry of micronutrients. In Micronutrients in Agriculture.

Kumar, K., Dasgupta, C. N., and Das, D., 2014. Cell growth kinetics of Chlorella sorokiniana and nutritional values of its biomass. Bioresource Technology, 167, 358-366.

Kumawat, R. and Gehlot, Y., 2020. GIS based mapping of soil fertility status of Tehsil Jobat, District Alirajpur, Madhya Pradesh, India. International Journal of Current Microbiology and Applied Sciences, 9(10), 60-69.

Lakudzala, D. D., 2013. Potassium response in some Malawi soils. International Letters of Chemistry, Physics and Astronomy, 8, 175-181.

Lal, R., 2004. Soil carbon sequestration impacts on global climate change and food

security. Science, 304(5677), 1623-1627.

Lal, R., 2020. Soil organic matter and water retention. Agronomy Journal, 112(5), 3265–3277.

Lamb, J. A., Fernandez, F. G., and Kaiser, D. E., 2014. Understanding nitrogen in soils. University of Minnesota Extension, (Revised), 1-5.

Landon, J. R., 2014. Booker tropical soil manual: A handbook for soil survey and agricultural land evaluation in the tropics and subtropics. Routledge.

Legge, R. L., Thompson, J. E., Baker, J. E. and Lieberman, M., 1982. The effect of calcium on the fluidity and phase properties of microsomal membranes isolated from postclimacteric Golden Delicious apples. Plant and Cell Physiology, 23(2), 161-169.

Lindsay, W. L. and Norvell, W., 1978. Development of a DTPA soil test for zinc, iron, manganese, and copper. Soil Science Society of America Journal, 42(3), pp.421-428.

Liu, X., He, P., Chen, W., and Gao, J., 2019. Improving multi-task deep neural networks via knowledge distillation for natural language understanding. arXiv preprint arXiv:1904.09482.

Lukas, V., Neudert, L. and Kren, J., 2009. Mapping of soil conditions in precision agriculture. Acta Agrophysica, 13(2 [167]).

Lundberg, S. M., and Lee, S. I., 2017. A unified approach to interpreting model predictions. In Proceedings of the 31st International Conference on Neural Information Processing Systems (pp. 4765–4774).

Luo, W., Taylor, M. C. and Parker, S. R., 2016. A comparison of spatial interpolation methods to predict continuous soil properties using limited data. Ecological Informatics, 35, 16–24.

Magdic, I., Safner, T., Rubinic, V., Rutic, F., Husnjak, S. and Filipović, V., 2022. Effect of slope position on soil properties and soil moisture regime of Stagnosol in the vineyard. Journal of Hydrology and Hydromechanics, 70(1), 62-73.

Maguire, M. E. and Cowan, J. A., 2002. Magnesium chemistry and biochemistry. Biometals, 15, 203-210.

Marschner, H., 2011. Marschner's mineral nutrition of higher plants. Academic Press.

Matar, A. E., 1992. Soil testing as a guide to fertilization in West Asia and North African (WANA) region. Communications in Soil Science and Plant Analysis, 23(17-20), 2075-2085.

Mayland, H. F. and Wilkinson, S. R., 1989. Soil factors affecting magnesium availability in plant-animal systems: a review. Journal of Animal Science, 67(12), pp.3437-3445.

McBratney, A. B., Mendonça Santos, M. L., and Minasny, B., 2003. On digital soil

mapping. Geoderma, 117(1-2), 3–52.

McCauley, A. and Jacobsen, J., 2009. Soil pH and organic matter. Nutrient Management Module, 8(2), 1-12.

McKenzie, N. N., Jacquier, D. D., Isbell, R. R., and Brown, K. K., 2004. Australian soils and landscapes: An illustrated compendium. CSIRO Publishing.

McLaren, R. G. and Crawford, D. V., 1973. Studies on soil copper. I. The fractionation of copper in soils. Soil Science, 24, 172-181.

Meena, H. B., Sharma, R. P. and Rawat, U. S., 2006. Status of macro-and micronutrients in some soils of Tonk district of Rajasthan. Journal of the Indian Society of Soil Science, 54(4), 508-512.

Meisinger, J. J., 1984. Evaluating plant-available nitrogen in soil-crop systems. Nitrogen in Crop Production, pp.389-416.

Mengel, K. and Kirkby, E. A., 2001. Principles of plant nutrition. 5th ed., Kluwer Academic Publishers, Dordrecht.

Mengel, K. and Kirkby, E. A., 1987. Principles of plant nutrition. International Potash Institute, Worblaufen-Bern, Switzerland, pp. 481–492.

Mikhailov, L., and Tsvetinov, P., 2004. Evaluation of services using a fuzzy analytic hierarchy process. Applied Soft Computing, 5(1), 23-33.

Mikkelsen, R. L., and Bruulsema, T. W., 2005. Fertilizer use for horticultural crops in the US during the 20th century. HortTechnology, 15(1), 24.

Minasny, B. and Hartemink, A. E., 2011. Predicting soil properties in the tropics. Earth-Science Reviews, 106(1-2), 52-62.

Mittelbach, H., Lehner, I. and Seneviratne, S. I., 2012. Comparison of four soil moisture sensor types under field conditions in Switzerland. Journal of Hydrology, 430, pp.39-49.

Mohammed, I. J., Hassan, H. K., Mohammed, H. A. and Hamed, A., 1997. Study of the Shafi Irrigation Project (Basra Governorate). Water Resources Research Center, Soil Investigations Department, Ministry of Irrigation.

Mohammed, S. H., Ahmad, H. M., and Yousif, H. A., 2020. Soil physico-chemical properties as influenced by slope position under different vegetation covers in Duhok Governorate. Scientific Journal of University of Zakho, 8(4), 25–35.

Morgan, R. P. C., 2009. Soil erosion and conservation. John Wiley & Sons.

Mulugeta, T., Melese, A. and Wondwosen, T., 2019. Effects of land use types on selected soil physical and chemical properties: The case of Kuyu District, Ethiopia. Eurasian Journal of Soil Science, 8(2), 94-109.

Munsell, A. H., 1975. Munsell soil color charts. Munsell Color.

Murashkina, M. A., Southard, R. J. and Pettygrove, G. S., 2007. Silt and fine sand fractions dominate K fixation in soils derived from granitic alluvium of the San Joaquin Valley, California. Geoderma, 141(3-4), pp.283-293.

Murdoch, W. J., Singh, C., Kumbier, R. R., and Mou, H., 2019. Explainable AI for environmental and Earth system sciences: a review. Environmental and Earth System Sciences, 5(2), 1-23.

Musarhad, A. H., Farhan, M. J. and Khalaf, A. A., 2023. Evaluation of the fertility status of some soil series of the North Tikrit Agricultural Project using geospatial technologies. In IOP Conference Series: Earth and Environmental Science (Vol. 1158, No. 2, p. 022032).

Nganga, W. B., Ng'etich, K. O., Macharia, M. J., Kiboi, N. M., Adamtey, N., and Ngetich, K. F., 2020. Multi-influencing-factors' evaluation for organic-based soil fertility technologies out-scaling in Upper Tana Catchment in Kenya. Scientific African, 7, e00231.

Nguemezi, C., Tematio, P., Yemefack, M., Tsozue, D. and Silatsa, T. B. F., 2020. Soil quality and soil fertility status in major soil groups at the Tombel area, South-West Cameroon. Heliyon, 6(2).

Nigussie, A., Ambaw, G. and Kissi, E., 2013. Fertility status of eutric nitisol and fertilizer recommendation using NuMaSS in the selected areas of Jimma Zone, southwestern Ethiopia. Tropical and Subtropical Agroecosystems, 16(3).

Olsen, S. R., 1954. Estimation of available phosphorus in soils by extraction with sodium bicarbonate (No. 939). US Department of Agriculture.

Owens, P. R. and Rutledge, E. M., 2005. Soil morphology. Encyclopedia of Soil Science in the Environment, 2.

Panda, S. C., 2006. Soil management and organic farming. Agrobios.

Pawar, S., Singh, B., Thakur, N. S., Sharma, A. K. and Shrivas, R., 2020. Integrated nutrient management – a remedy for enhancing the lives of microbes in soil. International Journal of Current Microbiology and Applied Sciences, Special Issue (10).

Pedregosa, F., Varoquaux, G., Gramfort, A., Michel, V., Thirion, B., Grisel, O., ... and Duchesnay, É., 2011. Scikit-learn: machine learning in Python. The Journal of Machine Learning Research, 12, 2825-2830.

Pierce, C., 1994. Importance of classroom climate for at-risk learners. The Journal of Educational Research, 88(1), 37-42.

Portal, F. S., 2016. Management of calcareous soils. Food and Agriculture Organization of United Nations: Rome, Italy.

Prasad, R. P. and Power, J. F., 1997. Soil fertility management for sustainable agriculture. Boca Raton, FL: CRC Press LLC. 356 p.

Rasheed, A. and Ryan, J., 2004. Micronutrient constraints to crop production in soils with Mediterranean-type characteristics: a review. Journal of Plant Nutrition, 27(6), 959-975.

Rawal, N., Acharya, K. K., Bam, C. R. and Acharya, K., 2018. Soil fertility mapping

of different VDCs of Sunsari District, Nepal using GIS. International Journal of Applied Sciences and Biotechnology, 6(2), 142-151.

Razvanchy, H. A. S., and Fayyadh, M. A., 2022. Application of geospatial techniques in analyst distribution pattern of some soil properties in Erbil Province, Kurdistan Region- Iraq. Journal of Duhok University, 25(1), 26-37.

Reed, S. T. and Martens, D. C., 1996. Copper and zinc. Methods of Soil Analysis: Part 3 Chemical Methods, 5, 703-722.

Rekani, S. I., Al-Qazili, M. S. and Al-Obaidi, M. J., 2022. The inclusive in soil, plant, water and fertilizer analysis, text books. Dar Dijla, Amman, Jordan. (In Arabic).

Rhoades, J. D., Chanduvi, F. and Lesch, S. M., 1999. Soil salinity assessment: methods and interpretation of electrical conductivity measurements (No. 57). Food & Agriculture Organization.

Rhoades, J. D. and Miyamoto, S., 1990. Testing soils for salinity and sodicity. Soil testing and plant analysis, 3, 299-336.

Ribeiro, M. T., Singh, S., and Guestrin, C., 2016. "Why should I trust you?": Explaining the predictions of any classifier. In Proceedings of the 22nd ACM SIGKDD International Conference on Knowledge Discovery and Data Mining (pp. 1135–1144).

Rodriguez-Galiano, V., 2012. Machine learning tools for environmental feature selection and modeling. Environmental Modelling & Software, 37, 1-6.

Rowell, D. L., 2014. Soil science: methods & applications. Routledge.

Roy, R. N., Finck, A., Blair, G. J., and Tandon, H. L. S., 2006. Plant nutrition for food security. A guide for integrated nutrient management. FAO Fertilizer and Plant Nutrition Bulletin, 16(368), 201-214.

Ryan, J., Estefan, G., and Rashid, A., 2001. Soil and plant analysis laboratory manual. ICARDA.

Saaty, T. L., 1980. The analytic hierarchy process. McGraw-Hill.

Salmon, R. C., 1963. Magnesium relationships in soils and plants. Journal of the Science of Food and Agriculture, 14(9), 605-610.

Samadi, A., 2006. Potassium exchange isotherms as a plant availability index in selected calcareous soils of Western Azarbaijan Province, Iran. Turkish Journal of Agriculture and Forestry, 30(3), 213-222.

Sanchez, P. A., 1977. Properties and management of soils in the tropics. Soil Science, 124(3), 187.

Savci, S., 2012. An agricultural pollutant: chemical fertilizer. International Journal of Environmental Science and Development, 3(1), 73.

Schroeder, D., 1984. Soils–facts and concepts. Bern, International Potash Institute, pp.140.

Schulte, E. E., and Kelling, K. A., 1996. Understanding plant nutrients: soil and applied phosphorus. University of Wisconsin-System Board of Regents and University of Wisconsin-Extension Cooperative Extension.

Schulte, E. E., 1992. Soil and applied magnesium (Vol. 2524). University of Wisconsin–Extension.

Schulte, E. E., 2004a. Understanding plant nutrients A2524: Soil and applied magnesium. University of Wisconsin-Extension, Cooperative Extension. RP, 8.

Schulte, E. E., 2004b. Understanding plant nutrients A3554: Soil and applied iron. University of Wisconsin-Extension, Cooperative Extension, RP, 08 (I 09/92).

Schulte, E. E. and Kelling, K. A., 2004a. Understanding plant nutrients: soil and applied copper. A2527. University of Wisconsin-Extension.

Schulte, E. E. and Kelling, K. A., 2004b. Understanding plant nutrients: soil and applied Zn. Understanding plant nutrients: soil and applied soil. University of Wisconsin-Extension. A2528.

Schwartz, B. F., Schreiber, M. E. and Yan, T., 2008. Quantifying field-scale soil moisture using electrical resistivity imaging. Journal of Hydrology, 362(3-4), pp.234-246.

Schwertmann, U., 1979. Non-crystalline and accessory minerals. In Developments in Sedimentology (Vol. 27, pp. 491-499). Elsevier.

Scull, P., Okin, G., Chadwick, O. A. and Franklin, J., 2005. A comparison of methods to predict soil surface texture in an alluvial basin. The Professional Geographer, 57(3), 423-437.

Shahabi, H., Shirzadi, A., Ghaderi, K., Omidvar, E., Al-Ansari, N., Clague, J. J., Geertsema, M., Khosravi, K., Amini, A., Bahrami, S. and Rahmati, O., 2020. Flood detection and susceptibility mapping using Sentinel-1 remote sensing data and a machine learning approach: hybrid intelligence of bagging ensemble based on k-nearest neighbor classifier. Remote Sensing, 12(266), 1-30.

Shand, C., 2007. Plant nutrition for food security. A guide for integrated nutrient management. By R. N. Roy, A. Finck, G. J. Blair and H. L. S. Tandon. Rome: Food and Agriculture Organization of the United Nations (2006), pp. 348, US $70.00. ISBN 92-5-105490-8. Experimental Agriculture, 43(1), 132-132.

Sharma, V. and Mathpal, B., 2020. Iron deficiency: a global issue and its possible remedies. Journal of Pharmacognosy and Phytochemistry, 9(5S), 811-816.

Shelp, B. J., 1993. Physiology and biochemistry of boron in plants. In Boron and its role in crop production (Gupta, U. C., ed.). pp. 53–85. CRC Press, Boca Raton, FL, USA.

Shi, C., Luo, S., Xu, M., and Tang, J., 2021. Learning gradient fields for molecular conformation generation. In International Conference on Machine Learning

(pp. 9558-9568). PMLR.

Shields, J. A., St. Arnaud, R. J., Paul, E. A. and Clayton, J. S., 1966. Measurement of soil color. Canadian Journal of Soil Science, 46(1), 83-90.

Shorrocks, V. M., 1997. The occurrence and correction of boron deficiency. Plant and Soil, 193(1), pp.121-148.

Simonsson, M., Andersson, S., Andrist-Rangel, Y., Hillier, S., Mattsson, L. and Oborn, I., 2007. Potassium release and fixation as a function of fertilizer application rate and soil parent material. Geoderma, 140(1-2), 188-198.

Singh, A., Agrawal, M., and Marshall, F. M., 2010. The role of organic vs. inorganic fertilizers in reducing phytoavailability of heavy metals in a wastewater-irrigated area. Ecological Engineering, 36(12), 1733-1740.

Singh, K. N., Rathore, A., Tripathi, A. K., Subba Rao, A., and Khan, S., 2010. Soil fertility manning and its validation using spatial prediction techniques. Journal of the Indian Society of Agricultural Statistics, 64, 359-365.

Soane, B. D., 1990. The role of organic matter in soil compactibility: a review of some practical aspects. Soil and Tillage Research, 16(1-2), 179-201.

Soil Survey Staff, 2010. Keys to soil taxonomy. 11th Edition. USDA, Natural Resources Conservation Service, Washington, D.C.

Soltanpour, P. N., 1985. Use of ammonium bicarbonate DTPA soil test to evaluate elemental availability and toxicity. Communications in Soil Science and Plant Analysis, 16(3), 323-338.

Sparks, D. L., 2000. Bioavailability of soil potassium. Handbook of Soil. CRC Press, New York.

Sparks, D. L., and Huang, P. M., 1985. Physical chemistry of soil potassium. Potassium in Agriculture, 201-276.

Stenberg, B., Rossel, R. A. V., Mouazen, A. M., and Wetterlind, J., 2010. Visible and near infrared spectroscopy in soil science. Advances in Agronomy, 107, 163-215.

Swaine, D. J. and Mitchell, R. L., 1960. Trace-element distribution in soil profiles. Journal of Soil Science, 11(2), 347-368.

Taghizadeh-Mehrjardi, R., Minasny, B., and Malone, B. P., 2020. A global review of digital soil mapping using machine learning and deep learning. Soil Science Society of America Journal, 84(4), 935-949.

Tematio, P., Tsafack, E. I. and Kengni, L., 2011. Effects of tillage, fallow and burning on selected properties and fertility status of Andosols in the Mounts Bambouto, West Cameroon. Agricultural Sciences, 2(03), 334.

Thompson, J. A., Roecker, S., Grunwald, S. and Owens, P. R., 2012. Digital soil mapping: interactions with and applications for hydropedology. In H. Lin (ed.), Hydopedology. 1st ed. Academic Press, Amsterdam. pp. 665–709.

Tisdale, S. L. and Nelson, W. L., 1966. Soil fertility and fertilizers. Soil Science, 101(4), 346.

Tisdale, S. L., Nelson, W. L., and Beaton, J. D., 1985. Soil fertility and fertilizers. Collier Macmillan Publishers.

Torrent, J. and Barron, V., 1993. Laboratory measurement of soil color: theory and practice. Soil Color, 31, 21-33.

Troeh, F. R. and Thompson, L. M., 2005. Soils and soil fertility (Vol. 489). Iowa: Blackwell.

Tsozue, D., Nghonda, J. P., Tematio, P. and Basga, S. D., 2019. Changes in soil properties and soil organic carbon stocks along an elevation gradient at Mount Bambouto, Central Africa. Catena, 175, 251-262.

Umer, M. I., Rajab, S. M., and Ismail, H. K., 2020. Effect of CaCO3 form on soil inherent quality properties of calcareous soils. In Materials Science Forum (Vol. 1002, pp. 459-467). Trans Tech Publications Ltd.

Van Laarhoven, P. J. M., and Pedrycz, W., 1983. A fuzzy extension of Saaty's priority theory. Fuzzy Sets and Systems, 11(1-3), 229-241.

Van Zonneveld, M., Turmel, M. S., and Hellin, J., 2020. Decision-making to diversify farm systems for climate change adaptation. Frontiers in Sustainable Food Systems, 4, 32.

Vaysse, K., Heuvelink, G. B. and Lagacherie, P., 2017. Spatial aggregation of soil property predictions in support of local land management. Soil Use and Management, 33(2), 299-310.

Verchot, L. V., Van Noordwijk, M., Kandji, S., Tomich, T., Ong, C., Albrecht, A. ... and Palm, C., 2007. Climate change: linking adaptation and mitigation through agroforestry. Mitigation and Adaptation Strategies for Global Change, 12, 901-918.

Viscarra Rossel, R. A., 2011. Fine-resolution multiscale mapping of clay minerals in Australian soils measured with near infrared spectra. Journal of Geophysical Research: Earth Surface, 116(F4).

Viscarra Rossel, R. A., Bui, E. N., De Caritat, P. and McKenzie, N. J., 2010. Mapping iron oxides and the color of Australian soil using visible–near-infrared reflectance spectra. Journal of Geophysical Research: Earth Surface, 115(F4).

Warington, K., 1923. The effect of boric acid and borax on the broad bean and certain other plants. Annals of Botany, 37(148), 629-672.

Webster, R., and Oliver, M. A., 2007. Geostatistics for environmental scientists (2nd ed.). Wiley.

Worku, R. and Hunduma, T., 2020. Soil fertility assessment and mapping at Adami Tulu Jidoo Kombolcha District, East Shewa Zone, Oromia Region, Ethiopia.

Yang, M., Li, Y., Liu, Z., Tian, J., Liang, L., Qiu, Y. and Lian, X., 2020. A high

activity zinc transporter OsZIP9 mediates zinc uptake in rice. The Plant Journal, 103(5), 1695-1709.

Zhang, L., Liang, T., Wei, X., and Wang, H., 2024. An improved indicator standardization method for multi-indicator composite evaluation: A case study in the evaluation of ecological civilization construction in China. Environmental Impact Assessment Review, 108, 107600.

Zhou, W., Peng, J., Li, H. and Wang, Y., 2024. Effects of land use and slope position on the spatial distribution of soil nutrients. Geoderma Regional, 32, e00654.

Zorb, C., Senbayram, M. and Peiter, E., 2014. Potassium in agriculture–status and perspectives. Journal of Plant Physiology, 171(9), 656-669.